

Titre: Cinétique de corrosion des réfractaires par l'aluminium liquide
Title:

Auteur: Jingguo Gao
Author:

Date: 2003

Type: Mémoire ou thèse / Dissertation or Thesis

Référence: Gao, J. (2003). Cinétique de corrosion des réfractaires par l'aluminium liquide
[Mémoire de maîtrise, École Polytechnique de Montréal]. PolyPublie.
Citation: <https://publications.polymtl.ca/7183/>

Document en libre accès dans PolyPublie

Open Access document in PolyPublie

URL de PolyPublie: <https://publications.polymtl.ca/7183/>
PolyPublie URL:

Directeurs de recherche: Claude Allaire
Advisors:

Programme: Non spécifié
Program:

UNIVERSITÉ DE MONTRÉAL
ÉCOLE POLYTECHNIQUE DE MONTRÉAL

**CINÉTIQUE DE CORROSION DES RÉFRACTAIRES PAR L'ALUMINUM
LIQUIDE**

JINGGUO GAO
DÉPARTEMENT DE GÉNIE PHYSIQUE
ÉCOLE POLYTECHNIQUE DE MONTRÉAL

MÉMOIRE PRÉSENTÉ VUE DE L'OBTENTION DU DIPLÔME DE MAÎTRISE ÉS
SCIENCES APPLIQUÉES (GÉNIE MÉTALLURGIQUE)
DÉCEMBRE 2003



National Library
of Canada

Bibliothèque nationale
du Canada

Acquisitions and
Bibliographic Services

Acquisitions et
services bibliographiques

395 Wellington Street
Ottawa ON K1A 0N4
Canada

395, rue Wellington
Ottawa ON K1A 0N4
Canada

Your file *Votre référence*

ISBN: 0-612-91941-2

Our file *Notre référence*

ISBN: 0-612-91941-2

The author has granted a non-exclusive licence allowing the National Library of Canada to reproduce, loan, distribute or sell copies of this thesis in microform, paper or electronic formats.

L'auteur a accordé une licence non exclusive permettant à la Bibliothèque nationale du Canada de reproduire, prêter, distribuer ou vendre des copies de cette thèse sous la forme de microfiche/film, de reproduction sur papier ou sur format électronique.

The author retains ownership of the copyright in this thesis. Neither the thesis nor substantial extracts from it may be printed or otherwise reproduced without the author's permission.

L'auteur conserve la propriété du droit d'auteur qui protège cette thèse. Ni la thèse ni des extraits substantiels de celle-ci ne doivent être imprimés ou autrement reproduits sans son autorisation.

In compliance with the Canadian Privacy Act some supporting forms may have been removed from this dissertation.

Conformément à la loi canadienne sur la protection de la vie privée, quelques formulaires secondaires ont été enlevés de ce manuscrit.

While these forms may be included in the document page count, their removal does not represent any loss of content from the dissertation.

Bien que ces formulaires aient inclus dans la pagination, il n'y aura aucun contenu manquant.

Canada

UNIVERSITÉ DE MONTRÉAL
ÉCOLE POLYTECHNIQUE DE MONTRÉAL

Ce mémoire intitulé:

**CINÉTIQUE DE CORROSION DES RÉFRACTAIRES PAR L'ALUMINUM
LIQUIDE**

Présenté par: GAO Jingguo

En vue de l'obtention du diplôme de: Maîtrise és sciences appliquées

A été dûment accepté par le jury d'examen constitué de:

Pr. RIGAUD Michel, président

Pr. ALLAIRE Claude, membre et directeur de recherche

Dr. PARANSKY Eugéne, membre

ACKNOWLEDGEMENTS

I would like to express my sincere gratitude to my supervisor, Prof. C. Allaire, for this expert guidance, valuable advice and constant support and encouragement.

I sincerely thank Prof. M. Rigaud who has accepted to act as chairman of the jury, Dr. E. Paransky for accepting to be the other member of the jury.

In no particular order, grateful acknowledgements are also made to my friends and colleagues in CIREP and REFRAL, Dr. S. Afsar, Dr. K. Sankaranarayanan, Dr. H. He, Dr. S. Palco, Dr. R. Pelletier, Dr. E. Divry, Mr. F. Ye, Mr. M. Zhang, Mr. X. Zhou, Mr. Y. Douche, Mr. V. Ébacher, Mr. R. Metageli.

I am also sincerely thankful to Mr. Jean-Philippe Bouchard for his great help with some experimental works, and Dr. N. Ntakaburimvo for his valuable advices.

RESUMÉ

Les réfractaires alumino-siliceux sont largement utilisés dans l'industrie d'aluminium. En service, ils sont confrontés à des conditions sévères, telles que les températures élevées, les réactions chimiques avec les composés liquide ainsi que les conditions dynamiques etc. puisque la corrosion ne peut pas être évitée, la cinétique de corrosion présente un outil important d'évaluation et d'amélioration des matériaux utilisés dans l'industrie d'aluminium.

La cinétique de corrosion des matériaux alumino-siliceux par Al-5wt%Mg liquide a été traitée dans le présent travail. L'aspect majeur qui a été couvert durant cette étude est : l'influence de la silice sur le temps d'incubation, l'influence de la silice sur la cinétique de corrosion, profondeur de la corrosion vs. Temps, et l'influence des conditions dynamiques sur la cinétique de corrosion.

L'influence de la silice sur le temps d'incubation avant l'apparition de la corrosion chimique est étudiée en utilisant des échantillons pressés à sec. Dans le chapitre 3, la procédure expérimentale et la mesure du temps d'incubation sont décrits en détails. L'influence de la quantité de silice sur le temps d'incubation est aussi discutée. Cette étude montre que le temps d'incubation avant l'apparition de la corrosion chimique diminue avec la diminution de la quantité de silice dans l'échantillon.

L'influence de la quantité de silice sur la cinétique de la corrosion est vérifiée en utilisant des échantillons alumino-siliceux coulés dans un test à immersion à 850 C. Après la même période de test, la profondeur de corrosion des échantillons contenant

différentes quantités de silice est mesurée. La surface irrégulière de corrosion ainsi que la profondeur de corrosion ont été décrits en détails dans le chapitre 4, la variation de la vitesse de corrosion avec l'augmentation de la quantité de silice dans les matériaux a été aussi remarquée. Ces études ont montré que la profondeur affectée et la profondeur de la corrosion augmentent linéairement avec l'augmentation de la quantité de silice dans les matériaux réfractaires alumino-siliceux durant le test d'immersion dans Al5wt%Mg liquide. Comparer avec son influence sur le temps d'incubation, la quantité de silice contenue dans les réfractaires a plus d'influence sur les réactions chimiques ou sur la corrosion chimique.

Deux types de matériaux alumino-siliceux sont utilisés pour vérifier la différence de profondeur de pénétration au cours du temps, par l'intermédiaire d'essais statiques d'immersion dans l'alliage Al-5wt%Mg sous un atmosphère d'air à 850°C. Les résultats ont démontré que la profondeur de la zone corrodée et celle de la zone pénétrée augmentent linéairement avec la racine carrée du temps, indiquant que la corrosion des réfractaires par l'alliage Al-5wt%Mg est régie par un processus de diffusion.

Pour accomplir les tests de corrosion dynamique, la mise en place d'un montage expérimental a été réalisée en laboratoire. Les conditions dynamiques sont générées par la rotation des échantillons à différentes vitesses. La croissance de corindon est limitée par un balayage de gaz protecteur directement au-dessus de la surface du métal liquide. La description détaillée du montage expérimental est montrée au chapitre 6. Durant les tests de corrosion dynamique, les échantillons de dimensions particulières doivent être utilisés. Les détails de ces dimensions et la procédure d'usinage figurent également dans ce chapitre. Il a été prouvé que ce montage permet de réaliser des tests de corrosion avec succès, en toute sécurité et sans croissance de corindon en surface de l'alliage Al-5wt%Mg fondu.

Deux sorte de matériaux, soient le NA et le SP, ont été utilisés lors des tests de corrosion en conditions statique ou dynamique dans le but de vérifier l'influence des conditions

dynamiques sur la cinétique de corrosion des réfractaires. Ces tests ont, évidemment, été accomplis à l'aide du montage décrit au chapitre 6. Après des tests de corrosion sous les mêmes conditions, la corrosion dynamique a produit différents effets sur divers matériaux. Dans les matériaux NA, une corrosion plus sévère a été observée en conditions dynamiques par rapport aux conditions statiques. Pour les matériaux SP, aucune différence significative entre les deux conditions n'a été notée. Différentes explications possibles quant aux causes de ce phénomène ont été discutées au chapitre 6. D'un autre côté, les résultats d'autres tests de corrosion ont montré que la corrosion était plus sévère sous une atmosphère d'azote que sous une atmosphère d'argon à une température de 850°C.

Lors des tests de corrosion dynamique, des changements ont été notés au niveau de la cinétique de corrosion sous différentes conditions dynamiques. Ceci est dû soit à la bonne résistance à la corrosion des matériaux sélectionnés, soit à un temps de test trop court, soit à une température moins élevée. Une solution possible serait la sélection de matériaux facilement corrodés ou la réalisation de tests dans des conditions plus sévères.

Les objectifs, tels que l'influence de la silice sur la cinétique de corrosion ou sur des échantillons contenant des proportions élevées de silice, les mécanismes engendrant la corrosion des matériaux réfractaires par l'alliage Al-5wt%Mg et la différence entre la corrosion en conditions statique et dynamique, ont été atteints.

ABSTRACT

Alumino-silicate refractories are widely used refractory materials in aluminum industry. In service, they are subjected to severe conditions, such as high temperature, chemical reactions with molten alloy, dynamic conditions etc. Since the corrosion cannot be avoided, the corrosion kinetics is important for evaluation or improvement of refractory material serving in the aluminum industry.

The corrosion kinetics of alumino-silicate material by molten Al-5wt%Mg has been conducted in the present study. The major aspects which have been covered during this study are: silica influence on incubation time, silica influence on corrosion kinetics, corrosion depth .vs. time, dynamic condition influence on corrosion kinetics.

Influence of silica content on the incubation time prior to visible chemical corrosion is studied by using dry-pressed alumino-silicate samples, through immersion test at 850°C. In chapter 3, the test procedures and measurement of the "incubation time" is described in detail, and the influence of silica content on incubation time is also discussed. This study has shown that the incubation time prior to visible chemical corrosion decreases with increasing the amount of silica in the samples

Influence of silica content on the corrosion kinetics is verified by using cast alumino-silicate samples, through immersion test at 850°C. After same test period, the corrosion depth of different silica content samples is measured. The irregular corrosion area and corrosion depth have been described in detail in chapter 4, the changes of corrosion rate with the increase of silica content inside materials are also found. The studies have shown that both affected depth and corrosion depth increase linearly with increasing of

silica content in alumino-silicate refractory material during immersion test in molten Al-5wt%Mg. As compared with its influence on incubation time, the silica content inside refractories has more significant influence on the chemical reactions or chemical corrosion.

Two kinds of alumino-silicate material are used to verify the changes of corrosion depth with time, through static immersion test in molten Al-5wt%Mg, at 850°C, under air. The results have shown that the corrosion depth and affected depth increase linearly with the square root of time, indicating the corrosion of refractory material by molten Al-5wt%Mg is governed by a diffusion process.

To conduct the dynamic corrosion test, an experimental set-up has been built in the lab. Dynamic condition is generated by rotating the samples at different speed. The corundum growth is prevented by purging protective gas onto the surface of molten alloy directly. The detailed description of the experiment set-up has been shown in chapter 6. During the dynamic corrosion test, sample with a special dimension has to be used. The details about the dimensions and making method of the sample were also given in the same chapter. It has been proven through corrosion tests that the experiment set-up can make dynamic corrosion test process safely and successfully, and no corundum growth took place on the surface of the molten Al-5wt%Mg.

Two kinds of alumino-silicate material, NA and SP, had been used in corrosion test under static or dynamic conditions, to verify the influence of dynamic condition on corrosion kinetics of refractory material, by using the experiment set-up in chapter 6. After corrosion test under same conditions, different effect of dynamic condition on different material has been found. As compared to static condition, more severe corrosion is observed under dynamic condition in NA material. For SP material, no significant difference was found between static corrosion and dynamic corrosion. Possible explanations for this phenomenon have been discussed in chapter 6. On the

other hand, the corrosion test results also show that the corrosion under nitrogen gas is more severe than under argon gas at the temperature of 850°C.

In dynamic corrosion test, changes of corrosion kinetics with different dynamic conditions have not been found, this is due to the good corrosion resistance of the selected material, test period not long enough or lower test temperature. The possible foreseen solution will be selection of some easily corroded material or processing the test under more severe conditions.

The objectives such as silica influence on the higher silica content samples, silica influence on corrosion kinetics, governing mechanism of corrosion of refractory material by molten Al-5wt%Mg, difference between dynamic corrosion and static corrosion, have been achieved.

TABLE OF CONTENTS

ACKNOWLEDGEMENTS.....	v
RÉSUMÉ.....	vi
ABSTRACT.....	ix
TABLE OF CONTENTS.....	xii
LIST OF TABLES.....	xv
LIST OF FIGURES.....	xvi
CHAPTER 1: INTRODUCTION.....	1
CHAPTER 2: LITERATURE REVIEW ON CORROSION MECHANISM OF REFRACTORIES BY MOLTEN ALUMINUM.....	5
2.1 CORROSION TEST ON REFRACTORY FOR ALUMINIUM TREATMENT FURNACE	5
2.2 UNDERSTANDING CORROSION BEHAVIOUR OF REFRACTORIES BY MOLTEN ALUMINUM FROM A THERMODYNAMICS POINT OF VIEW	8
2.3 UNDERSTANDING CORROSION OF REFRACTORIES FROM A KINETICS POINT OF VIEW....	17
2.3.1 <i>Basic principles of wetting</i>	17
2.3.2 <i>Basic principle of penetration</i>	18
2.3.3 <i>Wetting and penetration of aluminum into refractories</i>	20
2.3.4 <i>Incubation time existence prior to chemical reaction</i>	21
2.3.5 <i>Porosity effect on the corrosion of refractories</i>	22
2.4 CONTROLLING MECHANISM OF CORROSION OF REFRACTORIES BY MOLTEN ALUMINUM	22

2.5 CORROSION PROCESS OF REFRACTORIES BY MOLTEN ALUMINUM UNDER DYNAMIC CONDITION	30
2.5.1 <i>Experimental set-ups to create different dynamic conditions</i>	30
2.5.2 <i>Effect of dynamic condition on the corrosion process of refractory material by molten aluminum</i>	32
2.6 INFLUENCE PARAMETER OF CORROSION PROCESS OF REFRACTORY MATERIAL BY MOLTEN ALUMINUM CONTAINING Mg	33
2.6.1 <i>Effect of Mg on the corrosion process of molten aluminum</i>	33
2.6.2 <i>Effect of Si on the corrosion process</i>	33
2.6.3 <i>Influence of partial oxygen pressure on the corrosion process</i>	34
2.6.4 <i>Effect of temperature on the penetration process</i>	36
2.7 SUMMARIES OF LITERATURE REVIEW	38
 CHAPTER 3: INFLUENCE OF SILICA ON THE INCUBATION TIME PRIOR TO CHEMICAL REACTION.....	 41
3.1 INTRODUCTION	41
3.2 EXPERIMENTAL PROCEDURE	41
3.2.1 <i>Preparation of samples</i>	41
3.2.2 <i>Description of the experiment process</i> :	44
3.3 RESULTS AND DISCUSSION	48
3.3.1 <i>Criteria to verify corrosion</i>	48
3.3.2 <i>Results and discussion</i>	48
3.4 CONCLUSION OF CHAPTER 3	53
 CHAPTER 4: SILICA INFLUENCE ON THE CORROSION PROCESS OF REFRACTORIES BY MOLTEN ALUMINUM	 54
4.1. INTRODUCTION	54
4.2 EXPERIMENTAL PROCEDURES	54

4.2.1 <i>Sample preparation</i>	55
4.2.2 <i>Corrosion test experimental set-up</i>	59
4.3 RESULTS AND DISCUSSION	61
4.4 CONCLUSION OF THE CHAPTER 4.....	66
CHAPTER 5: CONTROLLING MECHANISM OF CORROSION OF REFRACTORIES BY MOLTEN ALUMINUM----CORROSION DEPTH VS. TIME.....	67
5.1 INTRODUCTION	67
5.2 EXPERIMENTAL PROCEDURES	68
5.2.1 <i>Sample preparation</i>	68
5.2.2 <i>Experimental set-up</i>	71
5.2.3 <i>Corrosion Test Procedure</i>	71
5.3 DISCUSSION OF THE TEST RESULTS.....	72
5.3.1 <i>Test results</i>	72
5.3.2 <i>Discussion of test result</i>	77
5.4 CONCLUSION OF CHAPTER 5.....	80
CHAPTER 6: INFLUENCE OF DYNAMIC CONDITION ON CORROSION PROCESS OF REFRACTORY MATERIAL BY MOLTEN ALUMINUM.....	81
6.1 INTRODUCTION	81
6.2 PRINCIPLE AND METHOD OF THE DYNAMIC TEST	82
6.3.1 <i>Sample preparation</i>	85
6.3.2 <i>Test process procedure</i>	86
6.3 TEST RESULTS AND DISCUSSION	87
6.4 CONCLUSION OF CHAPTER 6	95
CHPTER 7: GENERAL CONCLUSIONS	97

LIST OF TABLES

TABLE 2.1	Wetting angles of aluminum alloys to alumino-silicate material-----	20
TABLE 4-1	The composition for the 15% silica content samples-----	55
TABLE 4-2	The composition for the 20% silica content sample-----	56
TABLE 4-3	The composition for the 34% silica content samples-----	56
TABLE 5-1	Typical test data of SP material-----	69
TABLE 5-2	Physical properties of the SP material-----	69
TABLE 5-3	Chemical composition analysis of SP material-----	70
TABLE 5-4	Chemical composition of the SF material-----	71
TABLE 6-1	Chemical analysis of the NA castable-----	85
TABLE 6-2	Physical properties of the samples-----	86

LIST OF FIGURES

Fig.1-1 Work plan of the project -----	4
Fig.2-1 Full immersion test -----	6
Fig.2-2 Partial immersion test-----	6
Fig.2-3 Schematic of the different experimental set up used to reproduce: a) circulated air; b) entrapped air; c) argon gas atmosphere-----	7
Fig.2-4 CIREP- Bellyband Test Set-Up -----	8
Fig.2-5 The Ellingham diagrams for free enthalpy of formation of single oxides ---	9
Fig.2-6 Outward corundum growth according to the DIMOX TM process -----	13
Fig.2-7 Design of the calculation of the diagram Al-Mg-SiO ₂ -----	14
Fig.2-8 Depletion process of Mg in the corrosion process-----	15
Fig.2-9 Schematic of a refractory subjected to an inward corundum growth -----	16
Fig.2-10 Wetting between melt and Ceramic material -----	18
Fig.2-11 Capillary Tube -----	19
Fig.2-12 Time until first observation of reaction product as a function of the temperature, for reaction in vacuum and in air, compared with results of Standage and Gani. Left ends of horizontal bars indicate no reaction products observed; right ends indicate first observation of Si -----	22
Fig.2-13 A reaction model for penetration process in molten aluminum-----	23
Fig.2-14 Aluminum penetration depth, as a function of time, for the reaction of aluminum and Ceraten mullite at 1000°C, 1050°C, 1100°C -----	26
Fig.2-15 Si production /transportation rate as function of temperature-----	27
Fig.2-16 Penetration vs. time for Al-----	27
Fig.2-17 Depth of penetration vs. time for bulk reaction at 800°C-----	28

Fig.2-18 Effect of time on Si pick up(A: 35% <chem>SiO2</chem> , 64% <chem>Al2O3</chem> , B: 54% <chem>SiO2</chem> , 45% <chem>Al2O3</chem>)-----	29
Fig.2-19 Growth of the composite reaction layer from Al penetration at 1000°C into mullite and sillimanite-----	29
Fig.2-20 Principle of the test furnace -----	30
Fig.2-21 Schematic layout of the rotating cylinder apparatus -----	31
Fig.2-22 Main methods to create different dynamic condition-----	31
Fig.2-23 Difference between dynamic corrosion and static corrosion-----	32
Fig.2-24 Stability diagram for the Al-Mg-O at 1100°C-----	34
Fig.2-25 Effect of oxygen partial pressure on the relative stability of alumina and silica -----	35
Fig.2-26 Effect of oxygen partial pressure on extend of corrosion of refractory material during inward corundum growth-----	36
Fig.3-1 Particle size distribution of powders used in the test-----	42
Fig.3-2 Presser used in the test / Fig.3-3 Die used for pressing -----	43
Fig.3-4 Samples after pressed -----	43
Fig.3-5 Operating profile of the furnace during firing -----	44
Fig.3-6 CIREP-standard immersion test -----	45
Fig.3-7 CIREP-standard immersion test set-up-----	45
Fig.3-8 Samples and crucibles inside the furnace-----	46
Fig.3-9 Operating curve of the furnace during test-----	47
Fig.3-10 Sample containing 10% silica after different immersion periods -----	49
Fig.3-11 Sample containing 20% silica after different immersion periods -----	49
Fig.3-12 Sample containing 30% silica content after immersion different periods	50
Fig.3-13 Sample containing 40% silica after different immersion periods -----	50
Fig.3-14 Effect of silica content influence on the incubation time prior to chemical reaction -----	51
Fig.4-1 Mixing machine used in the test -----	57

Fig.4-2 Vibration table used for casting samples -----	57
Fig.4-3 Operation profile for the furnace during corrosion test-----	58
Fig.4-4 Arrangement of samples and crucibles in the furnace in the corrosion test	59
Fig.4-5 Operation profile of the furnace for corrosion test -----	60
Fig.4-6 Measurement of irregular area in computer-----	61
Fig.4-7 Samples with a) 34% silica, b) 20% silica, c) 15% silica after corrosion test in molten Al-5%Mg alloy at 850°C-----	62
Fig.4-8 Influence of silica content inside the refractories on corrosion -----	63
Fig.4-9 Effect of silica content on the corrosion of silica content refractories -----	64
Fig.4-10 Relation of volume change and silica content inside the refractories at 850 °C -----	65
Fig.5-1 Operation profile of furnace firing the SF precast samples-----	70
Fig.5-2 Corroded SP samples after different test period corrosion -----	73
Fig.5-3 Corroded SF samples after different test period corrosion -----	74
Fig.5-4 Relationship between affected depth, corroded depth of SP material and square root of time-----	75
Fig.5-5 The relation between the corrosion depth of SF samples and square root of time-----	75
Fig.5-6 Affected depth .vs. time for SP samples-----	76
Fig.5-7 Affected depth .vs. time for SF samples-----	76
Fig.5-8 Schematic of the sample with penetrated/corroded area -----	78
Fig.5-9 Discoloration depth .vs. time (SF material) -----	79
Fig.5-10 Discoloration depth .vs. time (SP material) -----	79
Fig.6-1 Experimental setup for dynamic corrosion test -----	83
Fig.6-2 Dimension of sample used in the dynamic /static corrosion test -----	84
Fig.6-3 Corroded NA sample under static condition-----	88
Fig.6-4 Corroded NA sample under dynamic condition-----	88
Fig.6-5 SP sample after Dynamic corrosion test under Ar-----	89

Fig.6-6 SP sample after Dynamic corrosion test under Ar-----	89
Fig.6-7 Dynamic corrosion under N ₂ (850° C, 3.34 r.p.s.) -----	89
Fig.6-8 SP material after Static corrosion test under N ₂ (850° C) -----	90
Fig.6-9 SP samples after Dynamic corrosion under Ar (850°C, 3.34r.p.s.)-----	90
Fig.6-10 SP material after Dynamic corrosion under N ₂ (850°C, 3.34r.p.s.)-----	90
Fig.6-11 Schematic of silicon diffusion from reaction front to bulk metal-----	92

CHAPTER 1: INTRODUCTION

Aluminum industry has been developed since 1950s [1]. The unique combination of properties found in aluminum makes it useful for applications in many aspects, such as aircraft, beverage cans and electrical transmission lines, and this stimulated the development of the aluminum industry. This resulted in the increase of refractories consumptions in the aluminum industry [2]. Refractories used in the manufacture of non-ferrous metals represented less than 8% of all refractories sold in 1985. Refractories for aluminium represented slightly over one-half of this amount. Today, aluminum industry is still growing and becoming more and more efficient. This put high demands on the refractories used in this industry, in order to reduce the operation costs.

Refractory materials are heterogeneous and porous in nature, having a very high melting temperature (up to 1800°C and more). This particular property indicates refractories offer a certain mechanical resistance at high temperature. They are also used to confine molten glass, cement and for many metallurgical sectors such as aluminium, copper, etc.

Refractory material used in the aluminium industry often serves three purposes described as the following:

- To preserve energy during operation;
- To protect the underlying insulation materials from percolating molten aluminum;
- To protect the steel casing from high temperature and liquid metal.

In aluminium industry, aluminosilicate material are widely used, especially in melting and holding furnaces, and this kind of material will continue to play a major role due to its lower cost and flexibility.

In spite of a relatively low melting and pouring temperature, (Aluminium melts at 650°C, and is generally tapped from the furnace between 700°C and 900°C [3]) liquid aluminium is still a redoubtable corrosive agent for the refractories used for the lining of melting and holding furnaces. In fact, the refractory materials used in melting and holding furnaces are subjected to severe corrosion conditions, and will be degraded by reactions with the molten aluminium below the metal line and by reaction with the corundum that grows along the wall above the metal line [4].

The upkeep of refractories in melting and holding equipments and in transport crucibles is a constant preoccupation for the foundrymen. In fact, it is important to an operator that the working tool does not fail unexpectedly and cause an abrupt stoppage of production. Refractory wear is inevitable. It is therefore normal to carry out repairs from time to time and occasionally a total replacement. It is essential that these interventions come within a maintenance programme established in advance and that they do not upset manufacturing processes that are more and more operated on a tight schedule, and hence, it is important to know when the refractories should be replaced or repaired, in order to avoid fatal damage of the furnace. So it means corrosion process .vs. time should be verified.

To predict or improve the service life of refractories and to know how the corrosion is taking place, the real mechanism and controlling mechanism of the corrosion process of refractory materials must be better understood.

There have been many research results about corrosion mechanism and corrosion kinetics under static condition. Unfortunately, the studies on the influence of dynamic

condition and silica content on corrosion kinetics are scanty. Moreover, the available data on controlling mechanism are confusing with disagreement on each other.

In most of cases, the refractories under use for aluminum application in industries are subjected to the corrosion of aluminum melt containing 5wt% Mg. Based on this, the current investigation also employs molten aluminum with 5wt% Mg as source of corrosion of aluminosilicate based refractory system.

The prime goal of this investigation is to understand and explore the corrosion kinetics of aluminosilicate refractories by molten aluminum at 850°C. The influence of silica on incubation time prior to chemical reaction, the influence of silica content on corrosion rate and the effect of dynamic condition on the corrosion kinetics are studied. The relationship between corrosion/penetration depth and time is also studied.

To fulfill the objectives of the study, the following works have been carried out.

- Literature review on corrosion mechanism of refractories by molten aluminum containing 5 wt% Mg;
- Influence of silica content on the corrosion rate;
- Influence of silica content on the incubation time prior the chemical reactions;
- The relationship between the corrosion depth and time;
- Influence of dynamic condition on corrosion.

The work plan for the current investigation is shown in Fig.1-1.

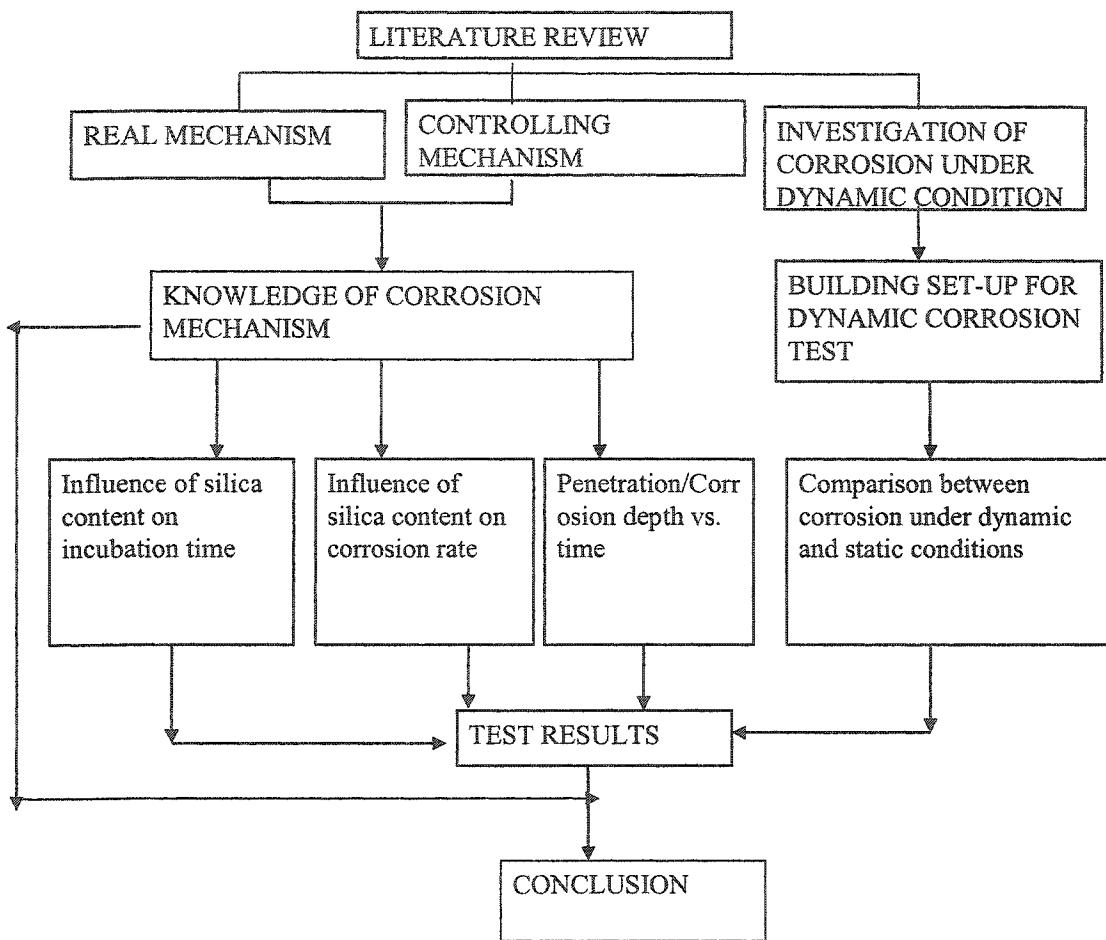


Fig.1-1 Work plan of the project

CHAPTER 2: LITERATURE REVIEW ON CORROSION MECHANISM OF REFRactories BY MOLTEN ALUMINUM

2.1 Corrosion Test on Refractory for Aluminium Treatment furnace

In aluminium confinement units, refractories are corroded by molten aluminium often containing Mg. In most corrosion tests, molten aluminium containing 5% Mg is often used as the corrosion source to simulate the circumstance of refractory in real industry [5-8]. There are four main conventional types of test referred to in previous research works [7-8,10].

- Full immersion test

In this test, as shown in Fig.2-1, the samples are immersed completely in the molten aluminium containing 5wt% Mg. This kind of test can simulate the conditions that take place below the metal line of the aluminium treatment furnaces.

- Partial immersion test (finger immersion test)

In this test, as shown in Fig. 2-2, the samples are partially immersed in the molten alloy with a part exposed above the metal line. The corrosion of the samples can simulate the

corrosion of the refractories serving as the furnace wall in the aluminium treatment furnaces.

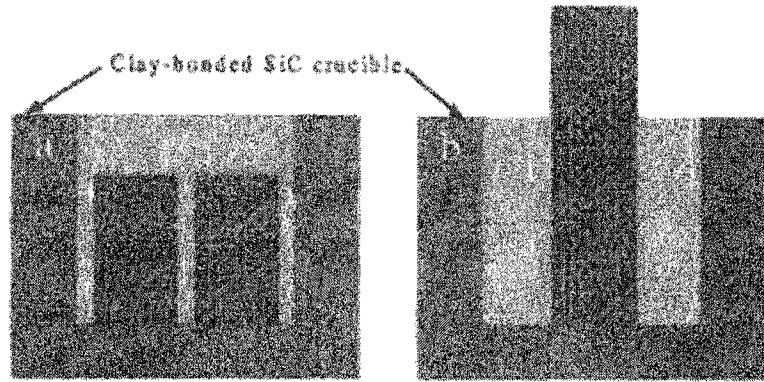


Fig.2-1 Full immersion test [10]

Fig.2-2 Partial immersion test [10]

- **Crucible test at uniform temperature**

The crucible samples are cylinders with a cavity, as shown in Fig.2-3, which contain the molten alloy during the test. The temperature of the crucible is uniform. The set-up can simulate the conditions at the bellyband area and the conditions below the metal line by purging the furnace chamber with air and argon gas separately.

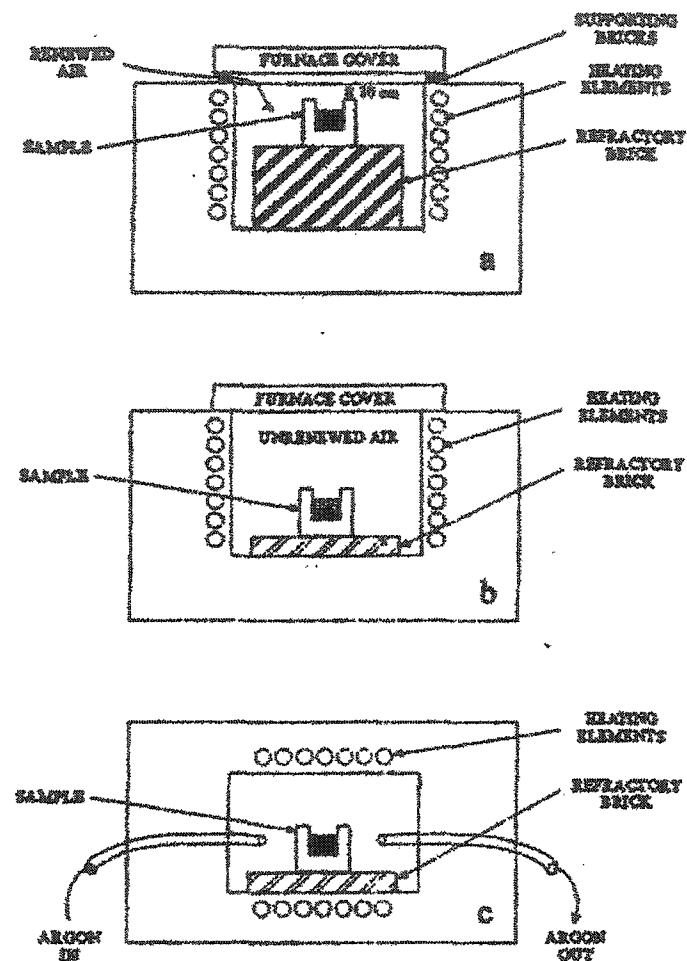


Fig.2-3 Schematic of the different experimental set up used to reproduce: a) circulated air; b) entrapped air; c) argon gas atmosphere [7]

- Crucible test under thermal gradient (CIREP-Bellyband test):

In this kind of test, as shown in Fig.2-4 [10], a bottom loading furnace is used to achieve a temperature drop from 1150—950°C across the air (atmosphere) interface and the molten aluminium alloy. The crucible sample is cubic with a cavity inside it.

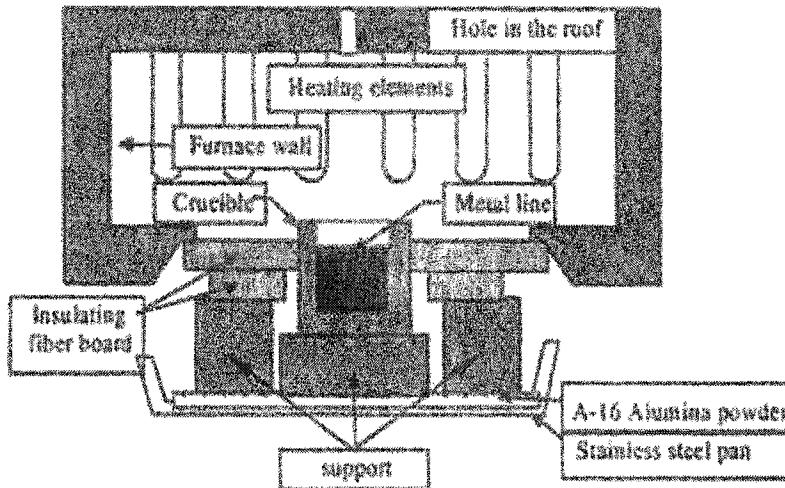
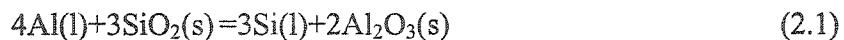


Fig.2-4 CIREP- Bellyband Test Set-Up [10]

This test is used to evaluate the resistance of refractories at the metal line. CIREP-CRNF has developed some standard test known as CIREP-Corrosion Test, Alcan-Immersion Test and Modified Alcan-Immersion Test for this kind of research. The detailed description about these tests has been reported in previous works [8,10].

2.2 Understanding corrosion behaviour of refractories by molten aluminum from a thermodynamics point of view

According to the Ellingham diagram, as shown in Fig.2-5 [9], after wetting or penetration, reactions between molten aluminum and refractories may take place. In this reaction, SiO_2 or silicates in refractories are reduced, giving rise to metallic Si and oxidation product of Al_2O_3 , according to the following equation.



Owing to the formation of metallic Si, infiltration of molten aluminum is enhanced, resulting in the formation of corundum and more Si.

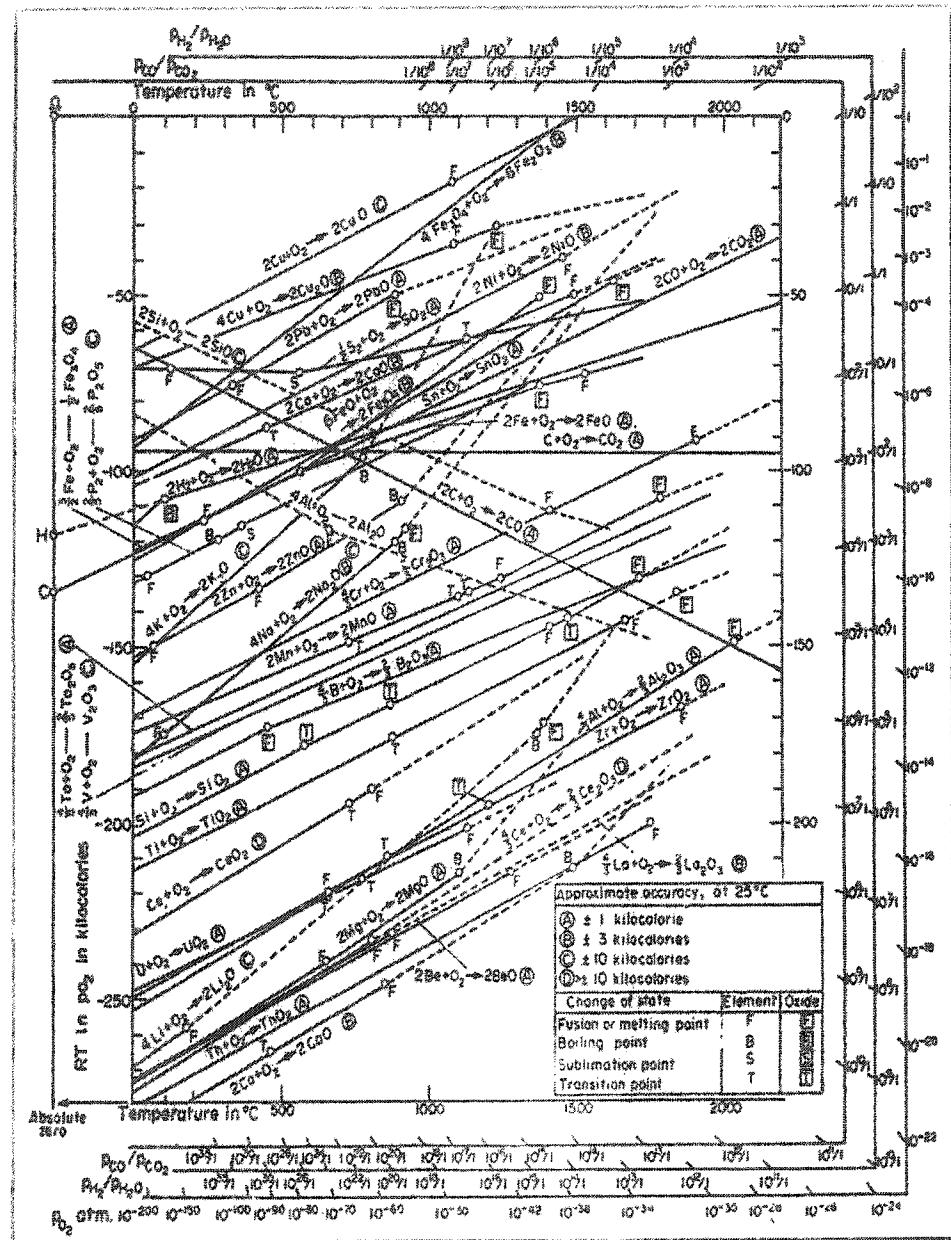


Fig.2-5 The Ellingham diagrams for free enthalpy of formation of single oxides [9]

According to the Ellingham diagram, the Mg contained in the molten aluminum can also react with the silica inside the refractories.

On the other hand, at the interface of molten aluminum and air, the oxidation of aluminum and Mg can also happen. This kind of oxidation process is called Direct Metal Oxidation process (**DIMOX™**).

So, at the metal line, outward corundum growth can happen because of direct-oxidation process. Inward corundum growth can happen below the metal line because of oxidation-reduction reaction. These two corundum growth mechanisms or their combination are the main degradation causes for the refractories when they are in contact with the molten aluminum containing Mg.

- **Outward corundum growth**

In the presence of oxygen, often at the metal line of aluminium treatment furnaces, **outward corundum growth** takes place, and this is attributed to the **DIMOX™** process [10].

At the initial stage, the crystal form is γ -Al₂O₃, but with the passage of the time, it can be converted into α - Al₂O₃ (corundum) due to exposure to a high temperature atmosphere near the heat source. As a result of volume shrinkage during the conversion, a number of micro-cracks are formed [11]. This leads to the formation of Al/Al₂O₃, which is a composite material containing molten metal channels. As it grows, the composite may contact with the furnace wall above the metal line. In this way, liquid alloy is brought in contact with the furnace wall above the metal line through the metal channels. At higher temperatures above the metal line combined with the wicking action of the corundum growth, favourable conditions are created for penetration. In addition, the composition of the alloy in the channels of the composite may be quite different and perhaps even more aggressive than in the bulk metal [5].

The corundum can grow to a large extent and then become a build-up on the furnace wall, and it must be removed by stopping the furnace operation. It can be removed easily in the early stage because it is soft at that time. The build-up can become a dense and hard mass, which sticks tightly to the refractory and appears to be an integral part of the furnace wall, removal of this build-up becomes extremely difficult, and may destroy the furnace wall. [12].

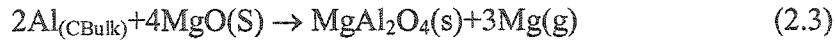
Outward corundum growth was considered to originate from the surface of the molten aluminium. There is some evidence showing that the micro-channels underneath the corundum are not connected with the refractory sample, but only to the metal [13]. This strongly suggested that corundum grows straight from the surface of the melt alloy.

According to the DIMOX theory, this involves the following steps: [10]

- 1) Mg evaporation followed by its oxidation promoting the formation of a thin and continuous magnesia layer at the molten metal /atmosphere interface.

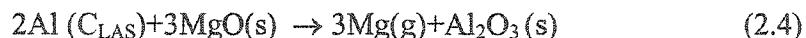


- 2) Reaction of the magnesia layer in contact with the Al-Mg bulk metal (C_{bulk}) leading to the formation of a porous primary spinel layer. This primary spinel layer contains microchannels because of its higher molar volume as compared to the magnesia layer:

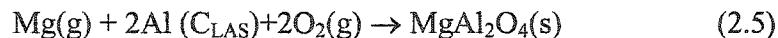


- 3) Infiltration of the bulk metal through the spinel microchannels leading to a reduction of its Mg content up to the three phase equilibrium Liquid-Alumina–spinel concentration (C_{LAS}).

- 4) Reaction of the magnesia layer with the Al-Mg molten metal having the C_{LAS} , leads to the formation of an Al_2O_3/Al composite made of columnar alumina crystals growing on top of the primary spinel layer.



- 5) Formation of a dense secondary spinel underneath the magnesia layer, which prevents the establishment of reaction that take place in step 4), and reduces the alumina crystals growing rate. This secondary spinel is formed from the Mg vapour released from reaction that take place in step 2), where it cannot escape through micro cracks into the magnesia layer. The higher density of the secondary spinel, as compared to the primary spinel, could be explained by the fact that only fluid phase participate in its formation.



- 6) Decomposition of the secondary spinel layer by the action of the molten Al-Mg metal having the C_{LAS} concentration. The rate of the corundum growth in this reaction is slow, as compared with the reaction in step 4).



Outward corundum growth process, according to DIMOXTM theory, is shown schematically in Fig.2-6.

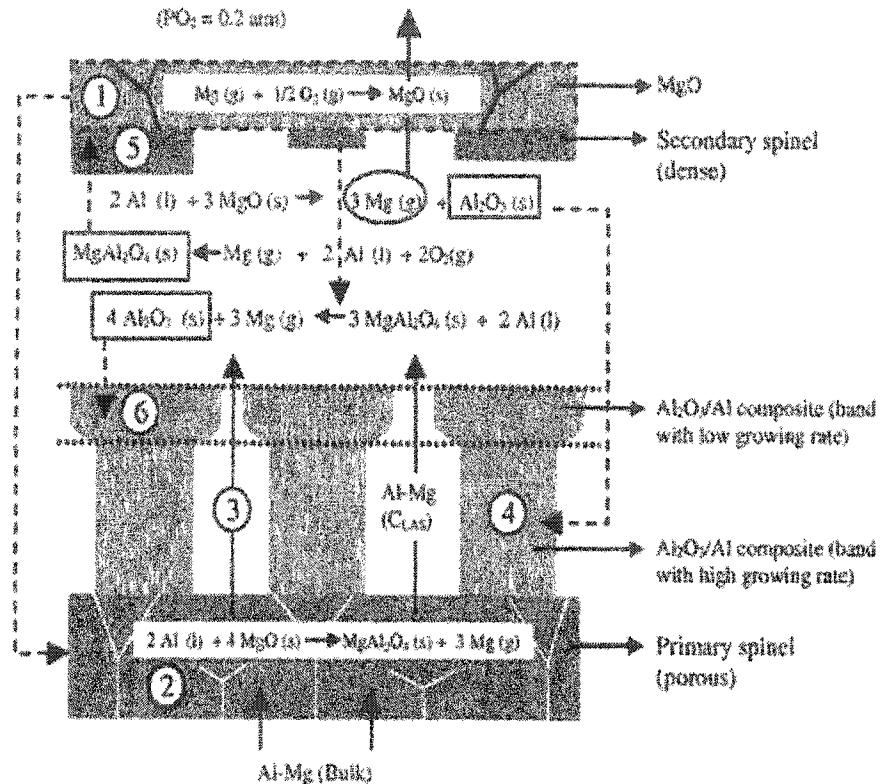


Fig.2-6 Outward corundum growth according to the DIMOX™ process [10]

- Inward corundum growth

According to the Ellingham diagram, the Mg and aluminum can react with the silica inside the refractory material, and this is called a redox process, which causes inward corundum growth during corrosion process of refractories by molten Al-Mg alloy.

In order to understand the formation mechanism of inward corundum here, one must have knowledge of reactions and phase involved during this process. The phase diagram and reaction program of F*A*C*T software has been used here

The mechanism of the inward corundum growth can be clarified by analysis of the depletion process of Mg contained in the molten aluminum. This can be carried out by F*A*C*T program [14], and a calculation model is shown in Fig.2-7.

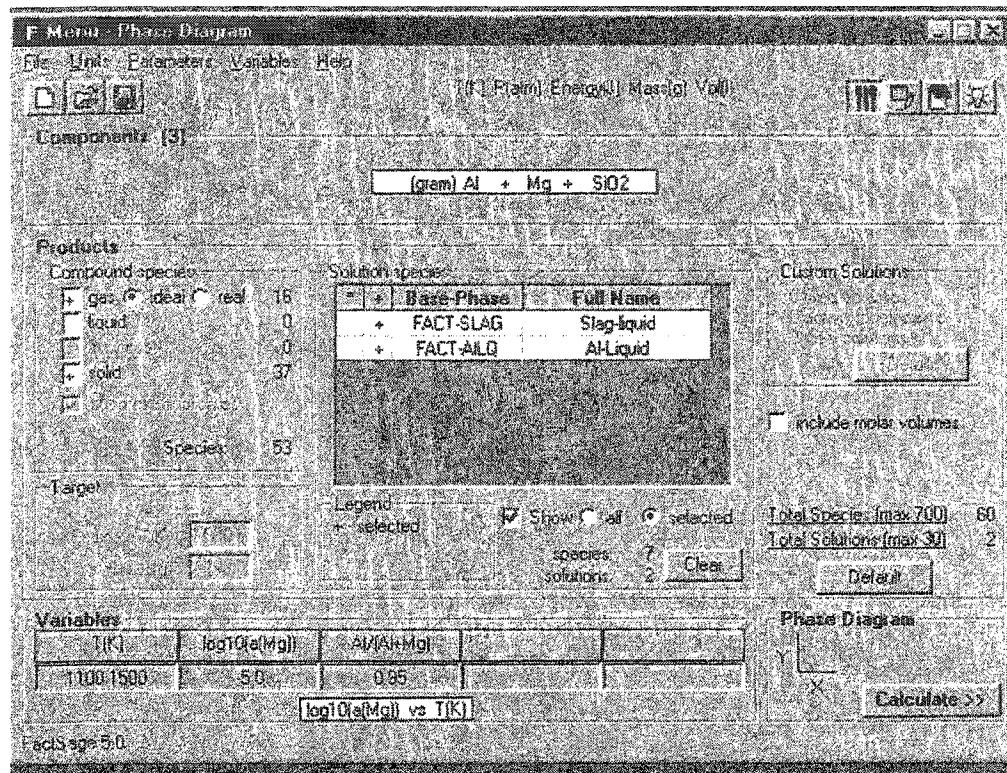
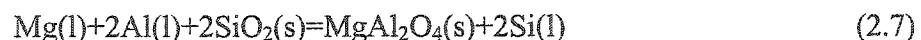


Fig.2-7 Design of the calculation of the diagram Al-Mg-SiO₂

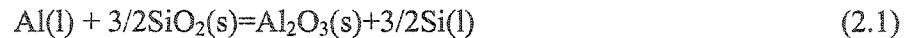
After calculation, the depletion of Mg in the corrosion process is shown in Fig. 2-8.

According to the depletion process of the Mg, as shown in Fig.2-8, an initial layer of spinel is expected to form at the refractory/molten aluminum interface, when the Mg concentration of latter is higher than C_{LAS}. The corresponding reaction (2.7) is given below.



This result is in accordance with the conclusion in previous works [15].

When the Mg content in the molten aluminum penetrating into the refractory is reduced to the C_{LAS}, corundum appears via the reaction (2.1) shown as following.



This becomes the main reaction in the corrosion process.

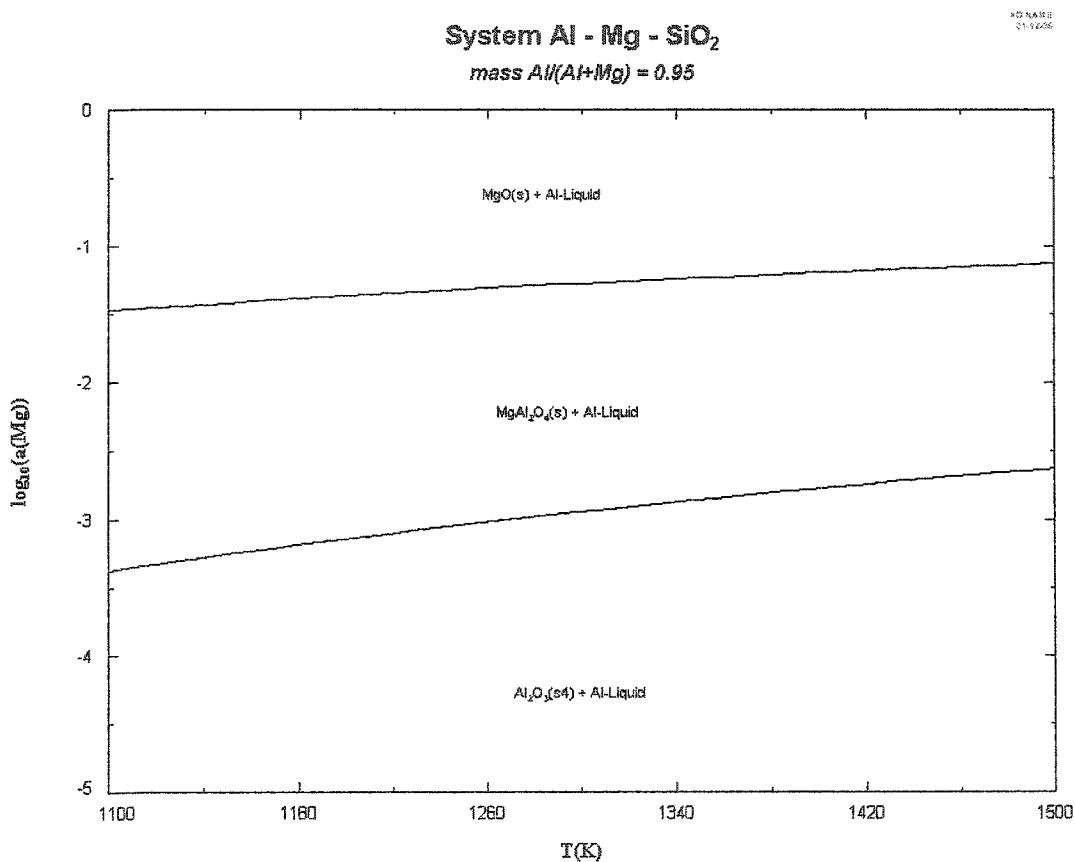
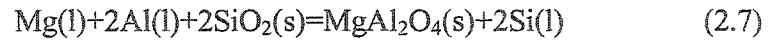


Fig.2-8 Depletion process of Mg in the corrosion process

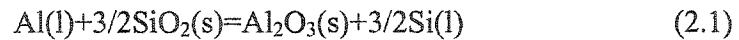
Based on the previous works, inward corundum growth should be considered to occur by oxido-reduction, irrespective of the temperature, the oxygen partial pressure and Mg content in the molten metal.

Therefore, after penetration of the bulk metal, the corrosion process of refractory material at or below the metal line can be described by the following steps:

- The formation of a spinel layer at the interface of molten aluminium / refractory material takes place by the reaction shown in reaction (2.7).



- The corundum formation starts when the Mg content in the molten aluminum is reduced to C_{LAS} .
- The continuous corrosion takes place mainly by silica reduction reaction, which is shown as following.



So, the schematic of a refractory submitted to an inward corundum growth can be shown as following, in Fig.2-9.

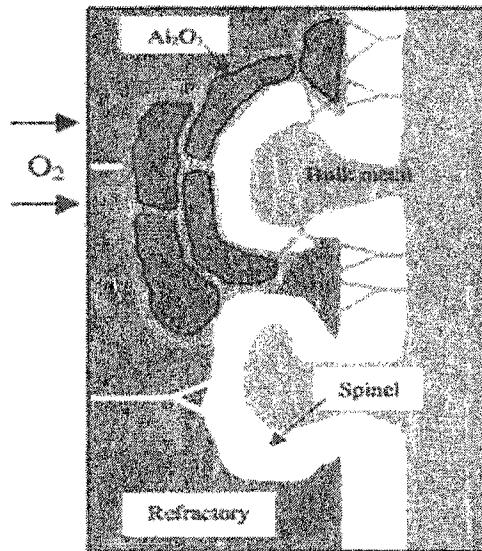
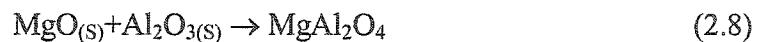


Fig.2-9 Schematic of a refractory subjected to an inward corundum growth [10]

- **Inward corundum growth following outward growth**

In the corrosion process, according to the DIMOX™ process, a top layer of magnesia should accompany the growth of the $\text{Al}_2\text{O}_3/\text{Al}$ composite, which is initiated at the metal line following the primary spinel formation. The composite is more likely to promote oxido-reduction according to the thermodynamics. The top magnesia -layer should first be converted into spinel before the metal contained in the composite can promote oxido-reduction. This conversion is believed to take place according to the following reaction:



- **Outward corundum growth following inward growth**

During the inward corundum growth, in the presence of large defects such as cracks in the refractory material, outward corundum growth that take place by direct metal oxidation inside the refractory, and can start at the refractory/atmosphere interface.

2.3 Understanding corrosion of refractories from a kinetics point of view

2.3.1 Basic principle of wetting

It is believed that before penetration and the chemical reaction between the refractories and hot liquid or slag, wetting to the refractories should happen first, and hence wetting is very important for corrosion of refractories.

Wettability can be defined as a property shared by a solid and liquid, which reflects the ability of the liquid to spread out on the solid in the presence of another surrounding gas or fluid. When considering attack by molten metals on the refractory materials, wetting between the two phases must occur. The phenomenon is shown in Fig.2-10.

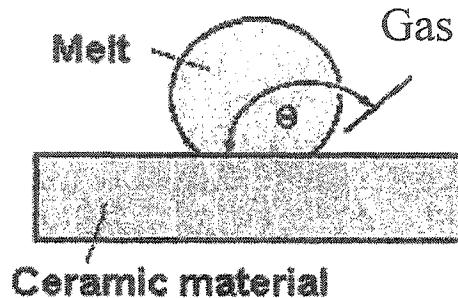


Fig.2-10 Wetting between melt and Ceramic material [16]

The wettability of the liquid can be ranked by wetting angle (θ) (see Fig.2-10), which is defined as the vertical angle made by the edge of a stationary body of a liquid with the flat surface of a solid [17].

It is known that for good wetting, the contact angle (θ) is less than 90° and for non-wetting, the angle is greater than 90° .

When wetting can occur between the molten alloy and the refractory material, under thermodynamic equilibrium and steady state conditions, the relation between the wetting angle and the surface tensions is given by the equation, which is so called Young's equation, shown as following.

$$\cos \theta = (\gamma_{sg} - \gamma_{sl}) / \gamma_{lg} \quad (\text{Eq.2.1})$$

where, γ_{sg} is the interfacial tension between the solid substrate (refractory) and gas, γ_{lg} is the interfacial tension between the liquid (metal) and gas, and γ_{sl} again is the interfacial tension between the solid substrate and the liquid [18].

2.3.2 Basic principle of penetration

Once wetting has occurred, the refractories are susceptible to be attacked and degraded by molten metal. The metal can attack the refractory aggregates and the matrix phases, on the surface of the material, but also attack the interior of the refractory structure by infiltration in the pores of the lining.

Usually, penetration without dissolution is not strictly corrosion and dissolution without penetration is superficial. In practice, the two phenomena occur simultaneously. A useful distinction when treating penetration on its own is to consider two aspects: physical penetration and chemical invasion [5].

Physical penetration can be visualised as the penetration of mercury in capillary tubes. According to Poiseuille's law, the volume rate in the capillary tubes can be expressed as following [19].

Poiseuille's Law

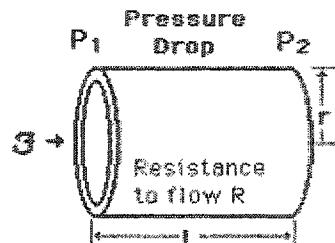


Fig.2-11 Capillary Tube

$$\frac{\text{Volume}}{\text{Flowrate}} = Q = \frac{P_1 - P_2}{R} = \frac{\pi(\text{Pressure difference})(\text{radius})^4}{8(\text{viscosity})(\text{length})} \quad (\text{Eq.2.2})$$

$$R = \frac{8\eta L}{\pi r^4} \quad \text{where } \eta = \text{viscosity}$$

For the liquid which can wet the surface of refractories, the capillary force is:

$$\Delta P = 2 \gamma_{lg} \cos\theta / r \quad (\text{Eq.2.3})$$

The rate of penetration, dL/dt can be expressed by the equation shown as following.

$$dL/dt = r \gamma_{lg} \cos\theta / 4\eta L \quad (\text{Eq.2.4})$$

where, "t" is time, "r" is the radius of the capillary tube, " γ_{lg} " is the interfacial tension between the penetrating liquid and the gas phase, η is the viscosity, L is penetration depth by liquid, and θ is the contact angle between the liquid and gas phase.

According to equation (5), "L" can be calculated out as following:

$$L = [(r \gamma_{lg} \cos\theta / 2\eta) t]^{1/2} \quad (\text{Eq.2.5})$$

So, the penetration depth in refractories materials is a function of pore size, metal surface tension and wetting angle, viscosity of the molten metal and time.

In porous refractories, corrosion-dissolution follows penetration (chemical invasion) into pores, but also in all openings: at the lining level, in open joints, gaps, and cracks; at brick level, in connected networks of voids. This indicates that the texture of refractories and the method of installation are very important [5].

2.3.3 Wetting and penetration of aluminum into refractories

The measured values of wetting angle θ , for molten aluminum with different refractory material surface is presented in TABLE.2-1. Based on these observations, it is pointed that molten aluminum can wet aluminosilicate refractories [22].

TABLE.2-1 Wetting angles of aluminium alloys to alumino-silicate material [22]

Conditions				Wetting angle		
Metal	Substrate	Time (min)	Atm.	800°C	1000°C	1200°C
Al	Al-silicate	> 60	Reducing	85	75	65
Al+1Mg	Al-silicate	> 60	Reducing	80	-	-
Al+5Mg	Al-silicate	> 60	Reducing	75	-	-

On the other hand, the aluminum can react with the silica content inside the refractories, so the wetting of the aluminum on refractories is assisted by chemical reactions.

Based on the experiment results, it is suggested that the rate of chemically assisted wetting, W , can be expressed as following [23].

$$W = k \exp(-Ea / RT) \quad (\text{Eq.2.6})$$

where,

k : a constant depending on the Gibbs free energy of the interfacial chemical reaction, the interfacial energy and the ability of the system to convert the energy released by the relevant interfacial reaction to the energy of the new surface created in the melt,

Ea : activation energy for the process of immersion,

R : gas constant, and

T : absolute temperature.

2.3.4 Incubation time existence prior to chemical reaction

According to many experiments on the corrosion of refractory material by molten aluminum, there is a period existing before the chemical reaction takes place between the molten aluminum and the refractories. This means the first step of the corrosion process is wetting or penetration to the refractory material by molten aluminium. This has been supported by many test results obtained in the previous research under static or dynamic conditions [23, 24, 25]. As an example, K. Prabriputaloong and M. R. Piggot's results are shown in Fig.2-12.

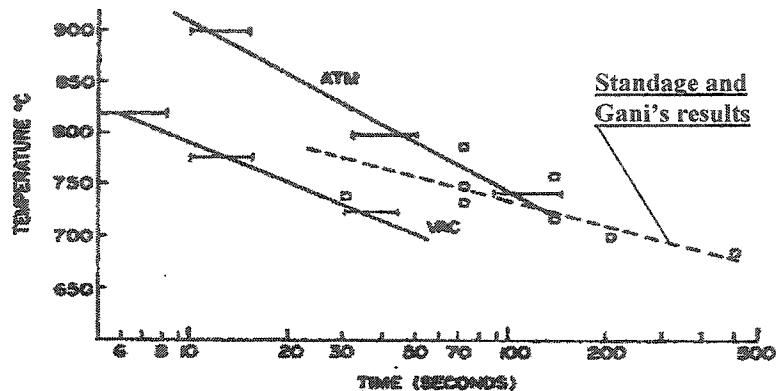


Fig. 2-12 Time until first observation of reaction product as a function of the temperature, for reaction in vacuum and in air, compared with results of Standage and Gani. Left ends of horizontal bars indicate no reaction products observed; right ends indicate first observation of Si [25]

2.3.5 Porosity effect on the corrosion of refractories

In theory, as discussed earlier, porosity has some negative influence on the corrosion or penetration, but after some corrosion test, some interesting and strange results had been obtained.

Bronyke's test [12] has shown that porosity of refractory material has no clear relation with the corrosion rate of silica containing refractories by molten aluminum.

R. Angers also pointed that the corrosion resistance of the tested material is higher notwithstanding its higher porosity content. Corrosion process independent with porosity has also been found in some other works [15, 17].

2.4 Controlling mechanism of corrosion of refractories by molten aluminum

2.4.1 Verification criteria of controlling mechanism

In theory, according to the mechanism of the corrosion process in molten aluminium, an interfacial layer exists between the molten aluminum and the refractory material.

According to the model of metal oxidation in air [18], a reaction model can be established for the penetration layer growing in molten aluminum (as shown in Fig.2-13).

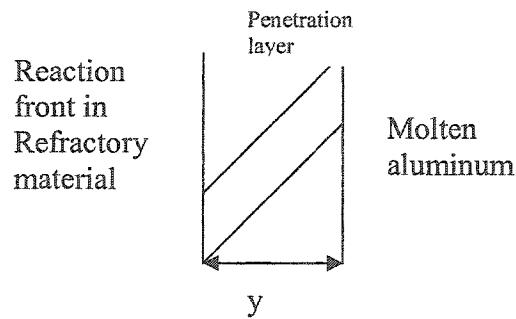


Fig.2-13 A reaction model for penetration process in molten aluminum

The rate of the penetration layer growth can be expressed by dy/dt .

When the chemical reaction is taking place stably, the rate of the chemical reaction should be equal to the diffusion rate of Al from the molten aluminum to the reaction front. The Al concentration in the molten aluminum is considered to be C_0 , and C at the reaction front (interface of the refractory and the interfacial layer), thus an equation can be obtained:

$$dy/dt = k_d(C_0 - C)/y \quad (\text{Eq.2.7})$$

where, k_d is a constant related to the diffusion coefficient.

The rate of the chemical reaction can also be expressed as following:

$$dy/dt = k_r C \quad (\text{Eq.2.8})$$

where, k_r is a constant related to chemical reaction rate.

When the corrosion process is stable, these two rates are equal. If C is deduced, a new equation can be obtained:

$$(dy/k_r) + (ydy/k_d) = C_0 dt \quad (\text{Eq.2.9})$$

When $t=0$, the value of 'y' is 0. After integrating and rearranging, Eq.2.9 becomes:

$$k_d y + k_r y^2/2 = k_d k_r C_0 t \quad (\text{Eq.2.10})$$

When the interfacial layer is very thin, the y^2 will be much smaller than y , so Eq.2.10 will become:

$$y = k_r C_0 t \quad (\text{Eq.2.11})$$

When the interfacial layer is very porous or has many cracks, $k_d \gg k_r$, this condition also leads to Eq.2.11. In this case, the general reaction is controlled by the chemical reaction process and the penetration depth is a linear function of time.

When the interfacial layer is very dense and it is not very thin, thus $k_d \ll k_r$, the equation Eq.2.10 is induced to Eq.2.12.

$$y^2 = 2 k_d C_0 t \quad (\text{Eq.2.12})$$

In this case, the corrosion process will be controlled by the diffusion process, which is commonly called $t^{1/2}$ kinetics.

Based on the analysis shown above, if the corrosion depth increases linearly with time, it is controlled by a chemical reaction process. On the other hand, if the corrosion depth increases linearly with the square root of time, it is considered controlled by a diffusion process.

2.4.2 Possible controlling mechanisms of corrosion process of refractories by molten aluminum

There are two possible controlling process for the chemical reaction between the refractories and the molten aluminium, the silica reduction process and Si diffusion process. Which one would be the controlling process for penetration? The answer to this question depends on the following parameters: the concentration of the silica in the

refractory materials, the temperature, the incubation time and the interfacial layer that formed by the chemical reaction.

There have been many research works to investigate the kinetics of the penetration process. Most of them were based on the test of immersing mullite or alumina –silicate refractories in molten aluminium. Based on the different test results, two hypothesis have been formulated by now: (1)--Si production controlling process and (2)--the diffusion controlling process.

G. William investigated the relationship between the incubation time and the penetration depth [26]. The samples used for the experiments were cut from a block of high purity commercial mullite. The reactive metal was pure aluminum (99.9%). In this test, flowing ultra-high purity argon was used as a cover gas over the melt.

The result of the test has shown that penetration depth increases linearly with the reaction time for all temperatures. After immersion test, the reaction layer thickness was found to increase linearly as the time increased for reaction temperature in the range of 900—1100°C. The results are shown in Fig.2-14.

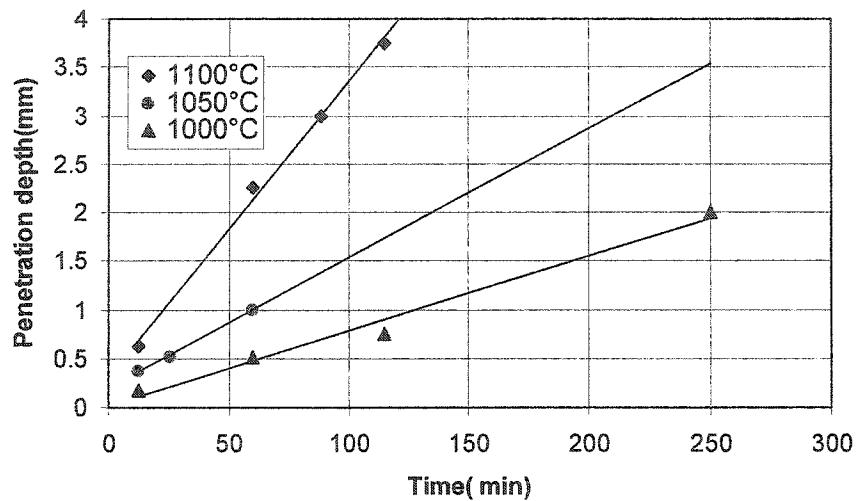


Fig.2-14 Aluminum penetration depth, as a function of time, for the reaction of aluminum and Ceraten mullite at 1000 °C, 1050 °C, 1100 °C [26]

Some other information can be obtained from this test results. The channels, which existed in the interfacial layer between the refractory and the liquid metal, allow for the macroscopic flow of molten aluminum to the reaction front, rather than atomic -scale diffusion through narrow grain boundaries. At a temperature $< 1150^{\circ}\text{C}$, the rate of diffusion away from the reaction front cannot be the rate-determining step, because significant Si build-up at the reaction front would slow or stop the reaction, and it does not happen below 1150°C as it does in high temperatures.

In these tests, the Si production and transport rate were also studied, as shown in Fig.2-15. The Si production rate is higher than Si transport rate at the temperature below 1150°C , while it is converse at the temperature above 1150°C .

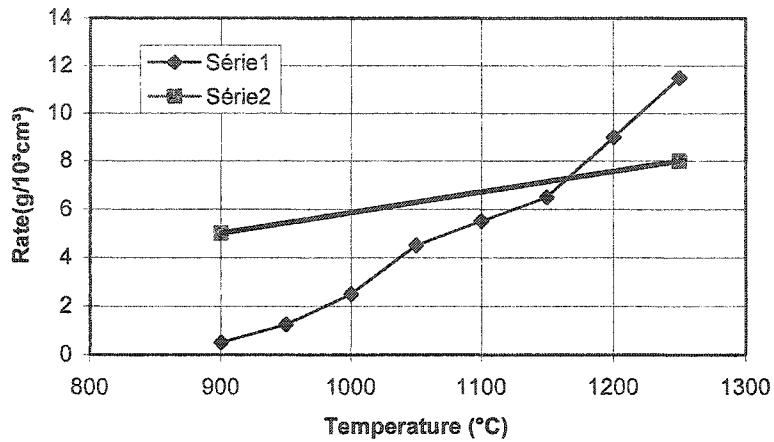


Fig.2-15 Si production /transportation rate as function of temperature [26]

Standdage and Gani also studied the kinetics of this reaction [23]. The fused silica rod was used for penetration in the molten alloys of pure aluminum at the temperature below 801.5°C , and the molten aluminum was exposed to air during the test. The test results are shown in Fig.2-16. The penetration depth is a linear function of the time, and penetration rate increases with test temperature.

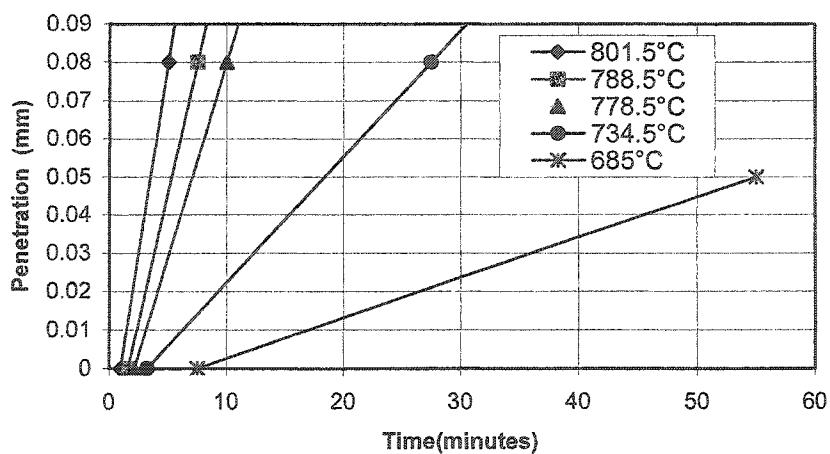


Fig.2-16 Penetration .vs. time for Al [23]

K.Dakabripuraloong [25] studied the depth .vs. time for bulk reaction at 800°C by lowering a SiO_2 rod into bath of molten Al kept at the desired temperature. The test result is shown in Fig.2-17. Their results also exhibit the linear relation between the penetration depth and the reaction time.

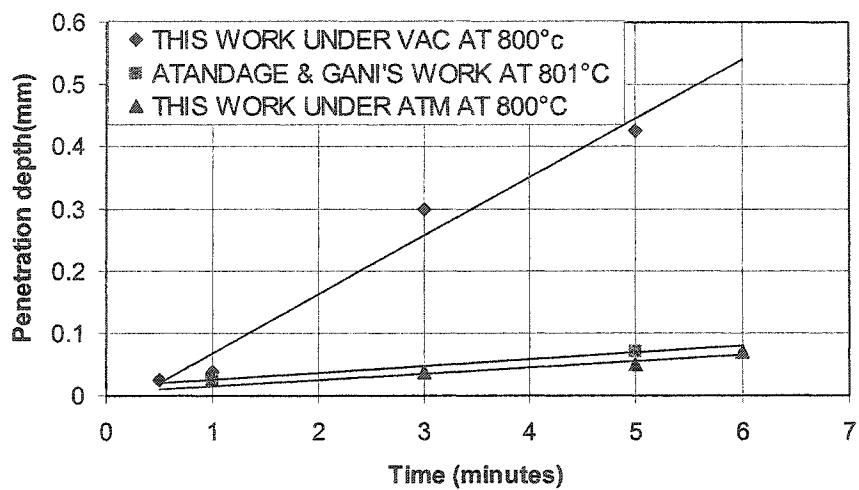


Fig.2-17 Depth of penetration vs. time for bulk reaction at 800 °C [25]

All above results showed that the penetration depth is a function of the reaction time, and that the penetration depth increases linearly with the increase of time.

In Bronyke's refractory cup test with a long processing period at the temperature of 870°C [12], the relations of the Si pick-up and the test time have been studied, as shown in Fig.2-18. It was declared in this research that the rate of reaction is controlled by the diffusion of the aluminum through the penetration zone.

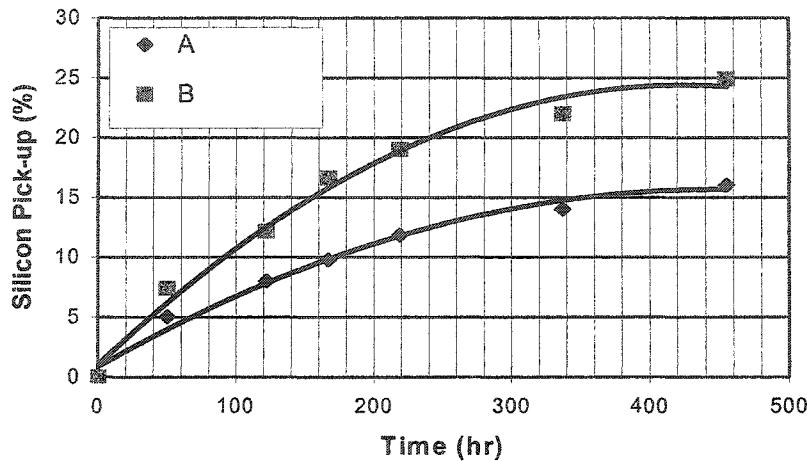


Fig.2-18 Effect of time on Si pick up(A: 35% SiO_2 , 64% Al_2O_3 , B: 54% SiO_2 , 45% Al_2O_3) [12]

In the experiment of Loehman [27], the effect of time on the penetration was studied by the reaction between mullite and molten aluminum at 1000°C during sessile drop experiment, as shown in Fig.2-19. The result also exhibited a $t^{1/2}$ kinetics in the penetration process.

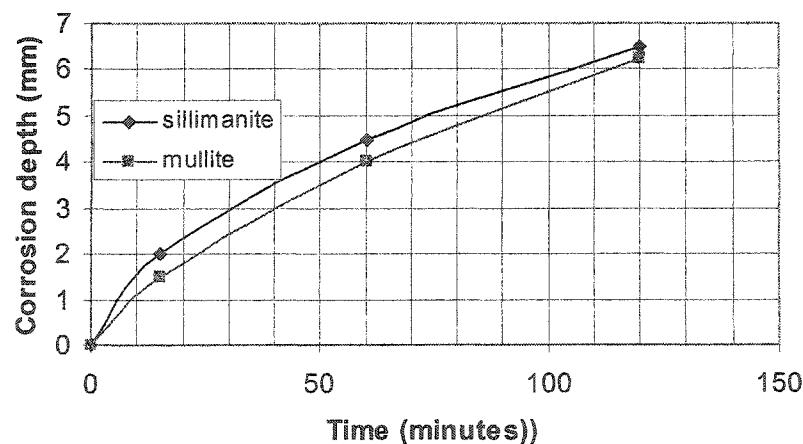


Fig.2-19 Growth of the composite reaction layer from Al penetration at 1000 °C into mullite and sillimanite [27]

On the other hand, some researchers [6] had found higher Si concentration at the reaction front inside the refractory material than in bulk metal. This also indicated that Si produced by chemical reaction can not diffuse fast into bulk metal through the metal channel, so the corrosion process may be controlled by Si diffusion process.

In general, there are two possible processes controlling the corrosion of refractory material, but which one is the real controlling process for the corrosion of refractory material by molten aluminum is unclear and further research input is required to clarify this issue.

2.5 Corrosion process of refractories by molten aluminum under dynamic condition

2.5.1 Experimental set-ups to create different dynamic conditions

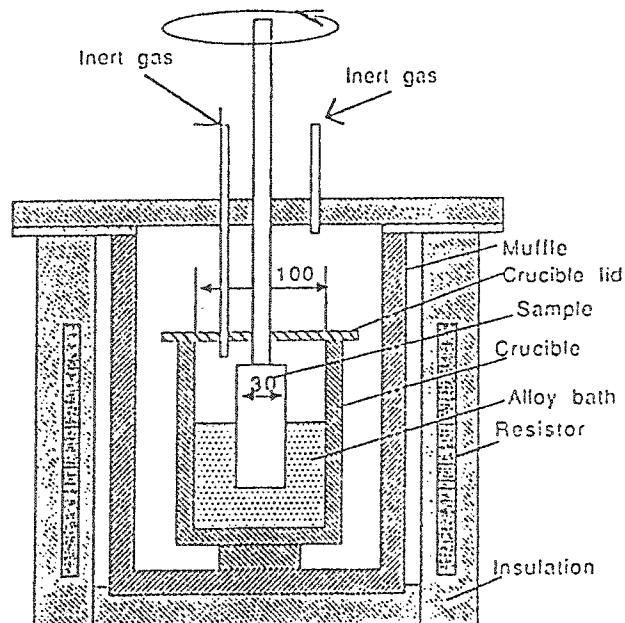


Fig.2-20 Principle of the test furnace [15]

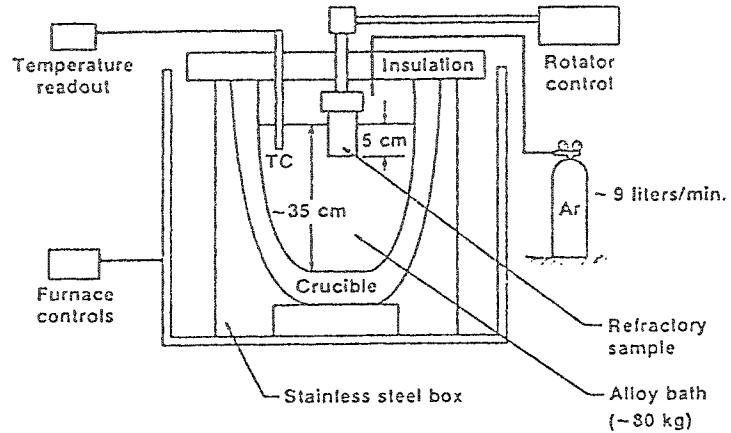


Fig.2-21 Schematic layout of the rotating cylinder apparatus [17]

Till now, compared with the corrosion test under static condition, insufficient research works have been carried out to understand the influence of dynamic condition on corrosion of refractories by molten aluminum. The experimental set-ups used are shown in Fig.2-20 and Fig.2-21 [14, 15, 17]. In general, according to the literature review, the main method to create dynamic conditions is to rotate the sample in the molten aluminum or alloy, as shown in Fig.2-22.

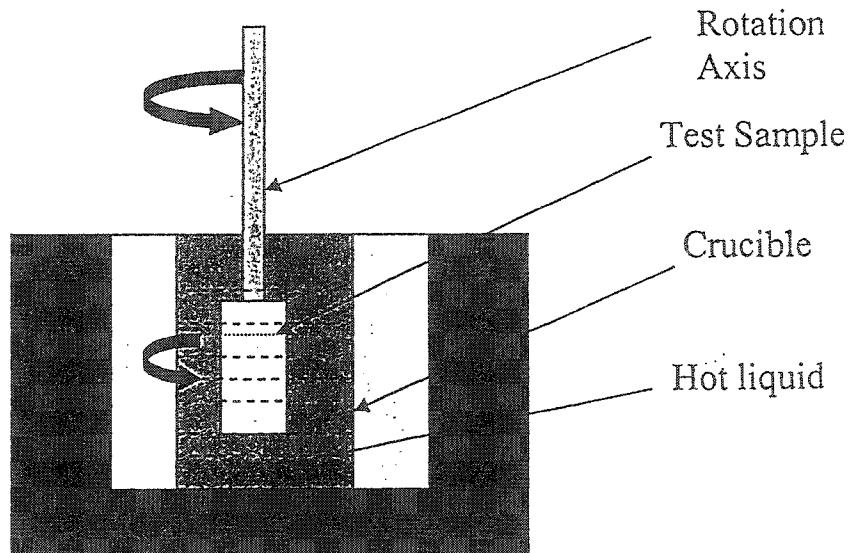


Fig.2-22 Main methods to create different dynamic condition

2.5.2 Effect of dynamic conditions on the corrosion process of refractory material by molten aluminum

In most cases, the dynamic conditions accelerate the corrosion of refractory material by molten aluminum. In R. Angers' test [14], the effect of dynamic condition is shown as in Fig.2-23.

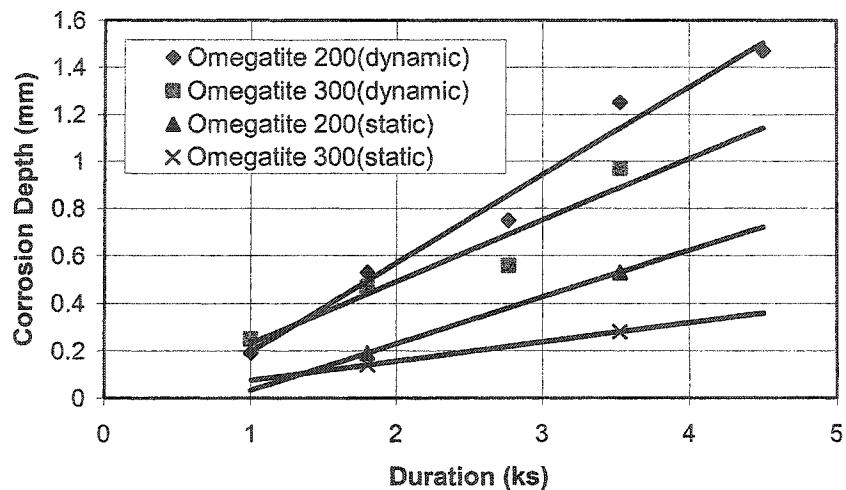


Fig.2-23 Difference between dynamic corrosion and static corrosion [14]

Mireille Fouletier and Dieter Gold [15] also designed an accelerated test for evaluation of refractory lifetime in contact with aluminum alloys by using a dynamic corrosion experimental set-up.

It seems that the dynamic condition do have some effects in accelerating the corrosion of refractory material by molten aluminum, but whether the effect is very significant to all the materials under corrosion need to be verified.

2.6 Influence of parameters on corrosion of refractory material by molten aluminum containing Mg

2.6.1 Effect of Mg on the corrosion process of molten aluminum

The surface energy and wettability is affected by liquid composition. In aluminium industry, molten aluminium often contains Mg. It is found that the Mg content can reduce the surface tension of the molten aluminum [28].

The corrosion process has also been studied in previous works, in which the refractory material is corroded by molten aluminum at high or low temperatures, with or without Mg. The corrosion test results have shown increase of corrosion in the presence of Mg at low temperature. [10].

2.6.2 Effect of Si on the corrosion process

Many research works on the effect of Si in the corrosion process have been reported. Unfortunately, the role of Si or the combined effect of Si and Mg is still not clear. For Si, this may be explained by the fact that this element has two opposite effects on corrosion: it unfavourably reduce the metal viscosity but favourably decreases the tendency of silica to be reduced since the metal is more concentrated in metallic Si [13].

According to the previous research [6, 11, 13], we can get the following conclusions:

- 1) Si is involved in the corrosion process of refractories by molten alunminum
- 2) Si lowers the surface tension and the density of molten aluminum.
- 3) Both Mg and Si lower the viscosity of molten aluminum.
- 4) The presence of Si and Mg improve the wettability of Al_2O_3 or MgAl_2O_4 by molten a luminum. This should facilitate the capillary penetration of the liquid metal into the refractory porosities and then increase the corrosion rate [6].

- 5) Simply adding Si cannot simulate the real situation produced by the chemical and /or physical changes due to the reduction of silica or other silicates presents in the refractory materials [6].

2.6.3 Influence of partial oxygen pressure on the corrosion process

The Mg depletion rate will influence the thickness of spinel, which is considered to be protective for refractory against the corrosion of molten aluminum. To verify the effect of oxygen partial pressure on the corrosion of refractory material, it is necessary to know the influence of oxygen partial pressure on the Mg stability in the aluminum.

This can be calculated using F*A*C*T software, and the result is shown in Fig.2-24.

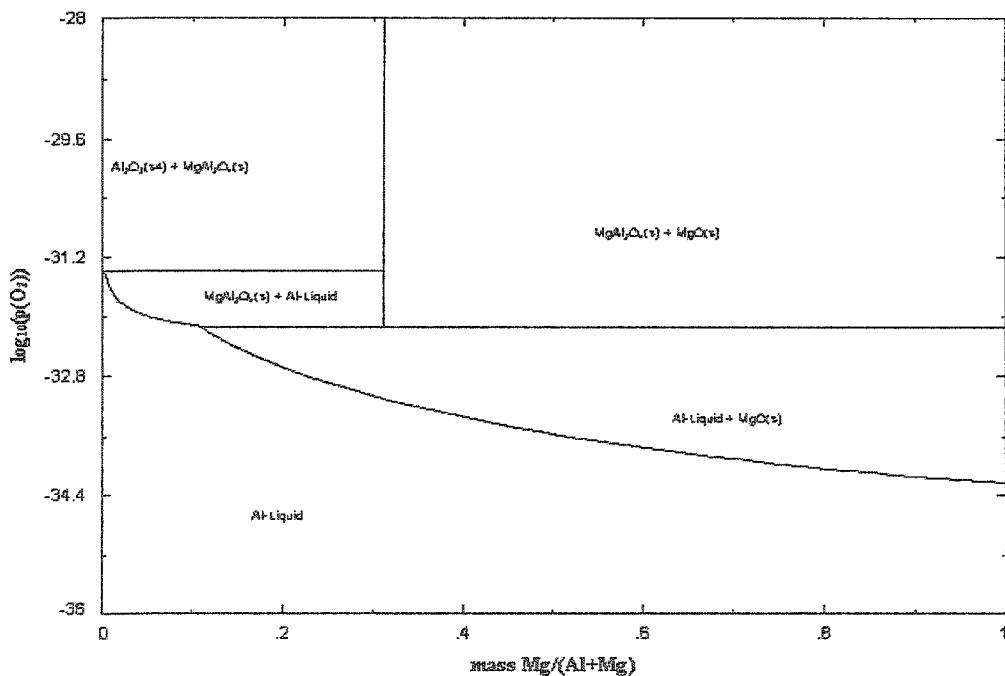


Fig.2-24 Stability diagram for the Al-Mg-O at 1100°C

The oxygen partial pressure also has some effect on the stability of alumina and silica. This influence can be predicted using the F*A*C*T software, as shown in Fig.2-25.

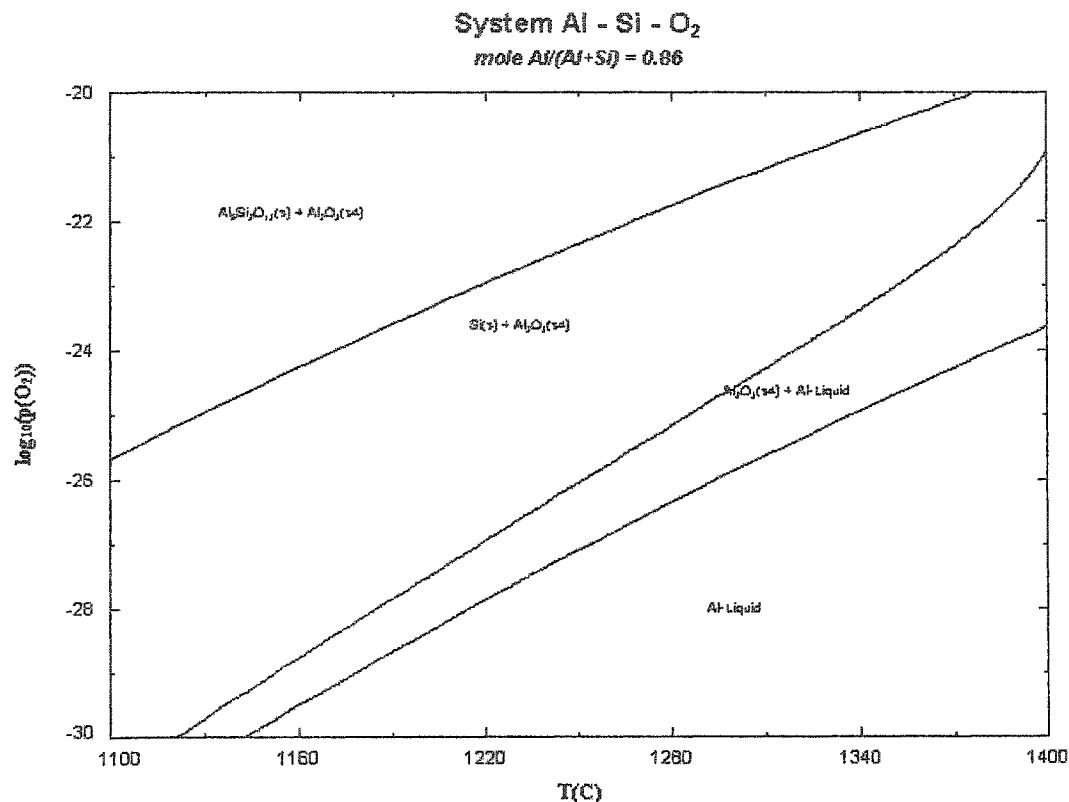


Fig.2-25 Effect of oxygen partial pressure on the relative stability of alumina and silica

According to Fig.2-24, the Mg solubility in molten aluminium is reduced at higher PO_2 . This could accelerate the depletion of Mg in the penetrating molten metal through the micro-channels inside the spinel. Thus the Mg concentration at equilibrium should be achieved after the spinel has grown up to a maximum thickness, which should be less at higher PO_2 than at lower PO_2 . A higher spinel thickness is expected to be favourable for protecting the refractory against silica reduction via reaction (2.1).

According to Fig.2-25, which shows the effect of oxygen partial pressure on the relative stability of silica, decreasing the oxygen partial pressure increases the stability of alumina as compared to silica so that reaction (2.1) becomes more favoured, promoting the corrosion in refractories.

So, increasing or decreasing the oxygen partial pressure has two opposite aspects effect on the corrosion of the refractory in molten aluminium. Increasing the oxygen partial pressure can lower the thickness of spinel formed at the interface of refractory and the molten aluminium, then the corrosion process should be more favoured. On the other hand, decreasing oxygen partial pressure leads to an increased stability of alumina as compared to silica, so that silica reduction should be more favoured. The influence of oxygen partial pressure can be illustrated by Fig.2-26.

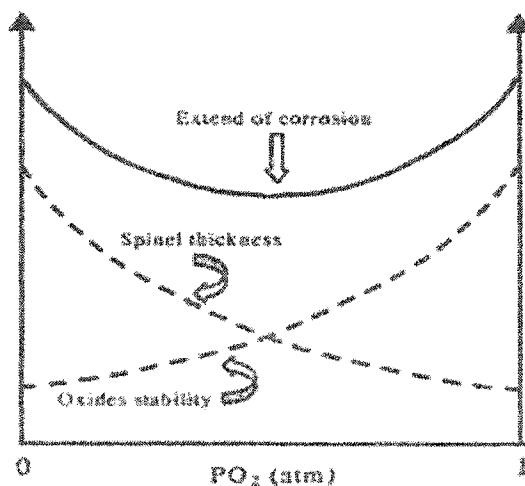


Fig.2-26 Effect of oxygen partial pressure on extend of corrosion of refractory material during inward corundum growth [10]

2.6.4 Effect of temperature on the penetration process

The corrosion rate varies with the temperature at which the refractories are tested. This can be described by the Arrhenius relation [20]:

$$\ln k = \ln Z - E/RT \quad (\text{Eq.2.11})$$

Where, k is reaction rate, Z is a constant, E is the activation energy, R is the gas constant, and T is the absolute temperature.

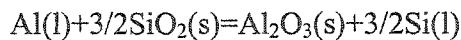
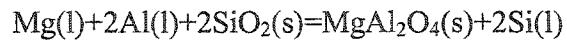
According to the Arrhenius relation, the reaction rate will increase with the increase of the temperature for reaction of refractories with molten aluminum, as previously shown in Fig.2-16.

On the other hand, the solubility of the Si in molten aluminum is a function of the temperature, and is 50% at 1100°C [26], 30% at 850°C [6], and only 1.5% at 570°C [26]. Higher Si solubility in the molten aluminum provides the possibility for more silica to be reduced and be released away from the refractory material, and then permits higher penetration depth.

According to the conclusion achieved by Fahrenholtz (see Fig.2-15), the Si production rate at the temperature above 1150°C is higher than the Si transportation rate, so diffusion should be the controlling process in this case. This phenomenon is in accordance with the explanation given for the effect of Mg on corrosion process (see section 2.6.1).

2.7 Summaries of literature review

- In molten aluminium, corrosion of refractory materials is often taking place by oxido-reduction and direct metal oxidation processes. Outward corundum growth is attributed to the direct metal oxidation process while inward corundum growth is attributed to the oxido-reduction process.
- The mechanism of degradation of refractory material is caused either by outward corundum growth, inward corundum growth, outward corundum growth following inward corundum growth, or inward corundum growth following outward corundum growth.
- For the corundum growth below the metal line, two reactions are responsible for the corrosion process of refractory material, which are shown as following.



- Mg effect on corrosion can be summarized as below:

- Mg can reduce the surface tension of molten aluminum;
- Increase of corrosion was observed in the presence of Mg at low temperatures

- Si effect on the corrosion can be listed as following.
 - Si is involved in the corrosion process of refractories by molten alumininum
 - Si can lower the surface tension and the density of the molten aluminum.
 - Both Mg and Si lower the viscosity of the molten aluminum.
 - The presence of Si and Mg improve the wettability of Al_2O_3 or MgAl_2O_4 by molten aluminum, this should facilitate the capillary penetration of the liquid metal into the refractory porosities, and then increase the corrosion rate.
 - Simply addition of Si cannot simulate the real situation produced by the chemical and /or physical changes due to the reduction of silica or other silicates presents in the refractory materials.
- Oxygen partial pressure has opposite effect on the Si reduction and spinel formation. Increasing the oxygen partial pressure can lower the thickness of spinel formed at the interface of refractory and the molten aluminum, then the corrosion process will be more favoured. On the other hand, decreasing oxygen partial pressure leads to an increased stability of alumina as compared to silica, so that silica reduction should be more favoured.
- Dynamic conditions lead to a higher diffusion rate of the Si produced during the silica reduction process and this accelerates the dissolution of the Si build-up at the reaction front. Higher rotation rate of the sample can lead to a higher diffusion rate and then to a higher silica reduction rate.
- Rotating the sample in the molten aluminum is the main method to create dynamic conditions. During dynamic corrosion tests, argon or nitrogen gas

should be used as protective gas to prevent corundum growth on the surface of the molten metal.

CHAPTER 3: INFLUENCE OF SILICA ON THE INCUBATION TIME PRIOR TO THE CHEMICAL REACTION

3.1 Introduction

According to the previous works, a period called "incubation time" exists prior to chemical reaction at the interface of refractory material and aluminum containing Mg alloy. This chapter presents the influence of the silica content in aluminosilicate material on the incubation time prior to chemical reaction in presence of Al -5wt% Mg.

3.2. Experimental procedure

3.2.1 Preparation of samples

For the incubation time study, seven types of samples containing 10%, 15%, 20%, 25%, 30%, 35%, 40% silica, were used. The samples were made from fume silica and alumina through mixing, drying, pressing and firing. The size distribution of silica and alumina powders used is shown in Fig. 3-1.

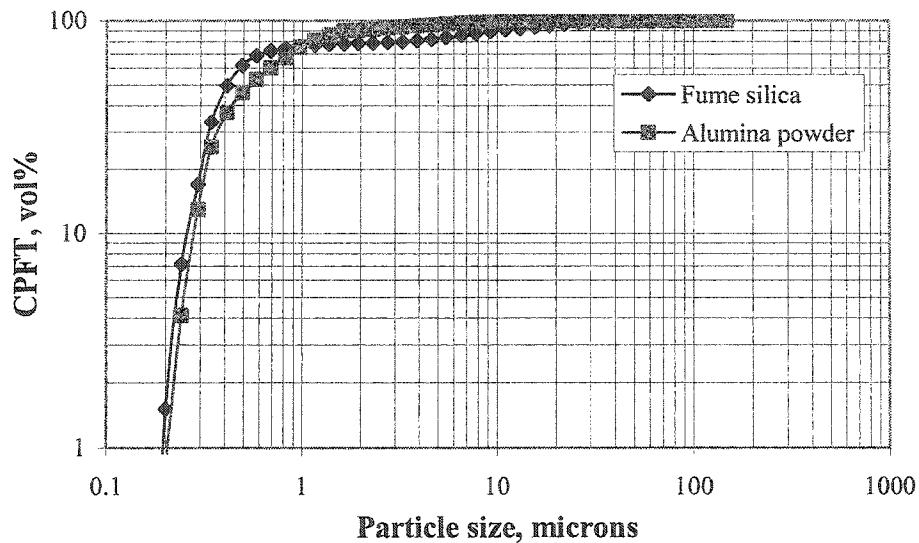


Fig.3-1 Particle size distribution of the powders used in the test

The details of the preparation steps can be listed as following.

- 1) Mixing: Mix containing 10% fume silica and 90% alumina powders were milled together at 80 rpm in alcohol medium to break the agglomerates and to get homogenous mixture. Same procedure was repeated for the other mixes containing 15%, 20%, 25%, 30%, 35%, 40% silica content.
- 2) Drying: The mixture was poured into a big cup and kept in atmosphere for 48 hrs for alcohol to evaporate from them.
- 3) Pressing: After 48 hrs, when the mixtures were totally dry and ready for pressing, they were pressed at 10000L.B.S into cylindrical samples with dimension of $\varnothing 19.25\text{mm} \times (17-19)\text{ mm}$, using a steel die. The press and die used for pressing are shown in Fig.3-2, Fig.3-3 and Fig.3-4.

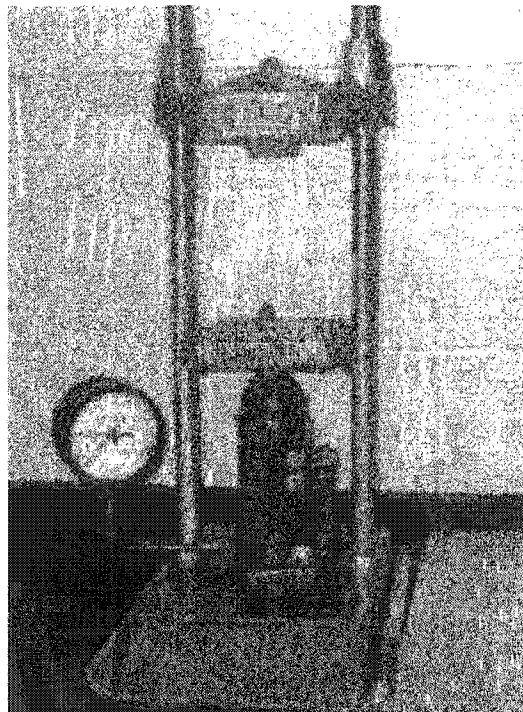


Fig. 3-2 Press used in the tests

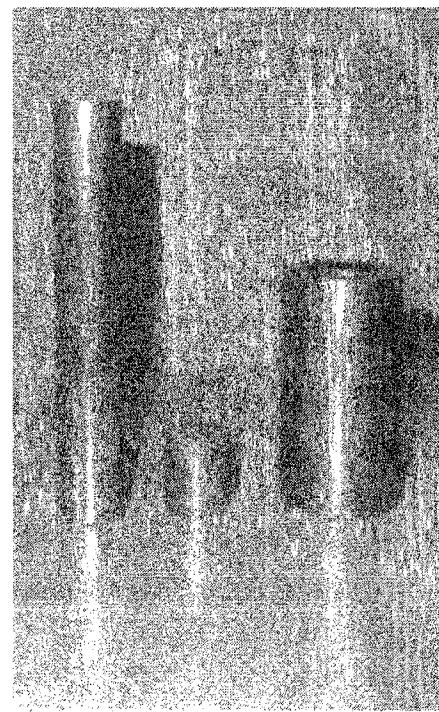


Fig.3-3 Die used for pressing

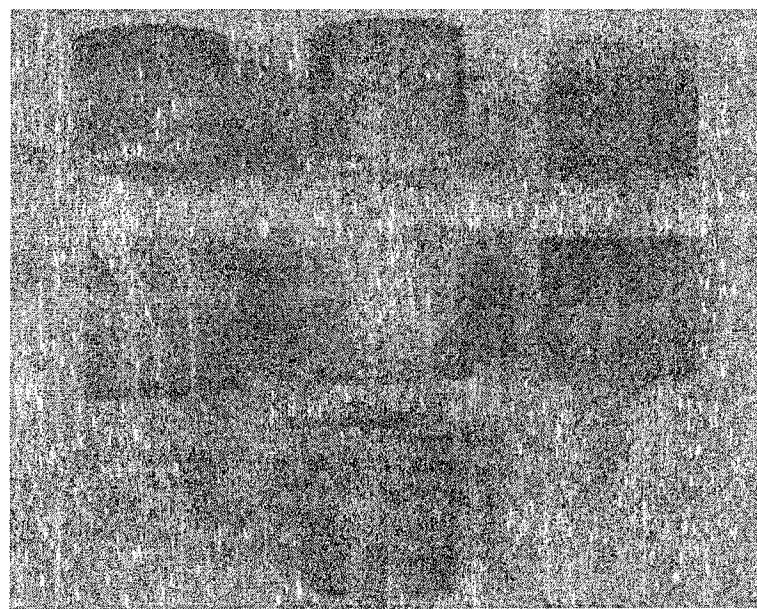


Fig.3-4 Samples after pressing

- 4) Firing: The samples were fired at the temperature of 1200 °C for 6 hours. The operating program of the furnace is shown in Fig. 3-5.
- 5) After firing, all the samples were withdrawn from the furnace. These samples were used for corrosion test.

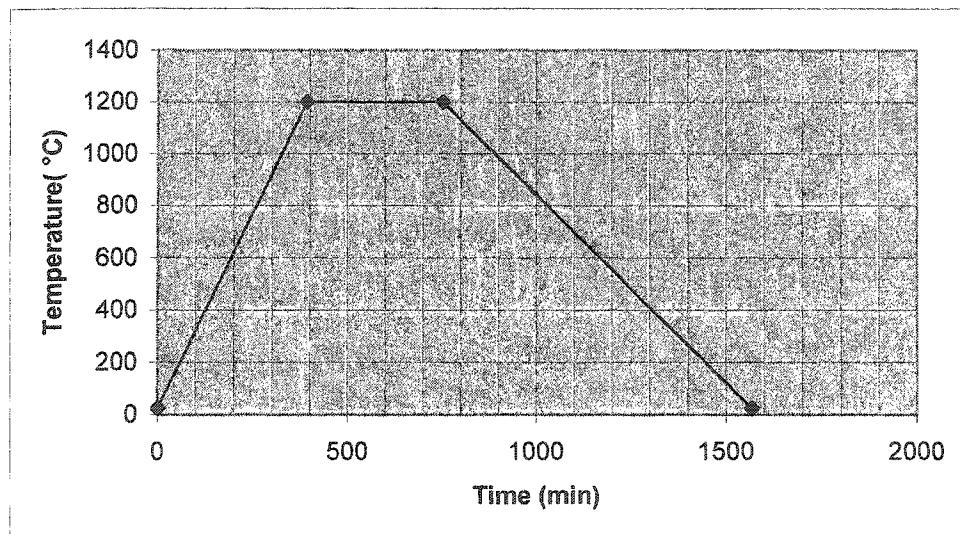


Fig.3-5 Operating profile of the furnace during firing

3.2.2 Description of the experiment process:

- **Experimental set-up**

The CIREP-standard Immersion Test set-up was used in this work and is shown in Fig.3-6 and Fig. 3-7.

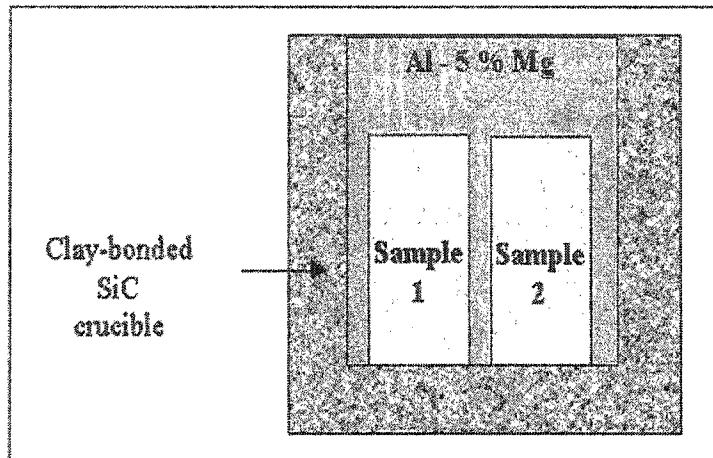


Fig. 3-6 CIREP-standard immersion test

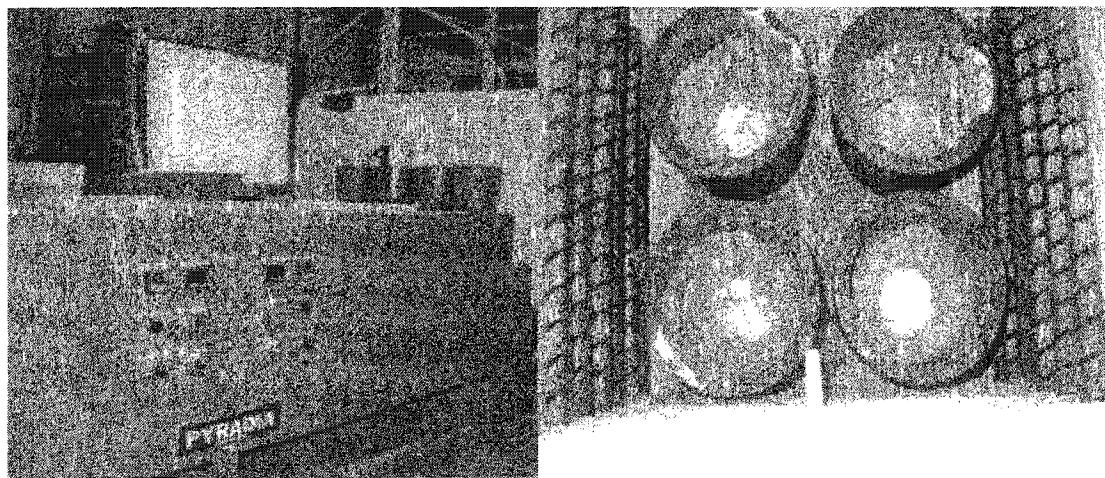


Fig.3-7 CIREP-standard immersion test set-up

- **Experiment procedure:**
- 1) Ten samples for each given type were put in the furnace and heated outside the crucibles, as shown in Fig.3-8.

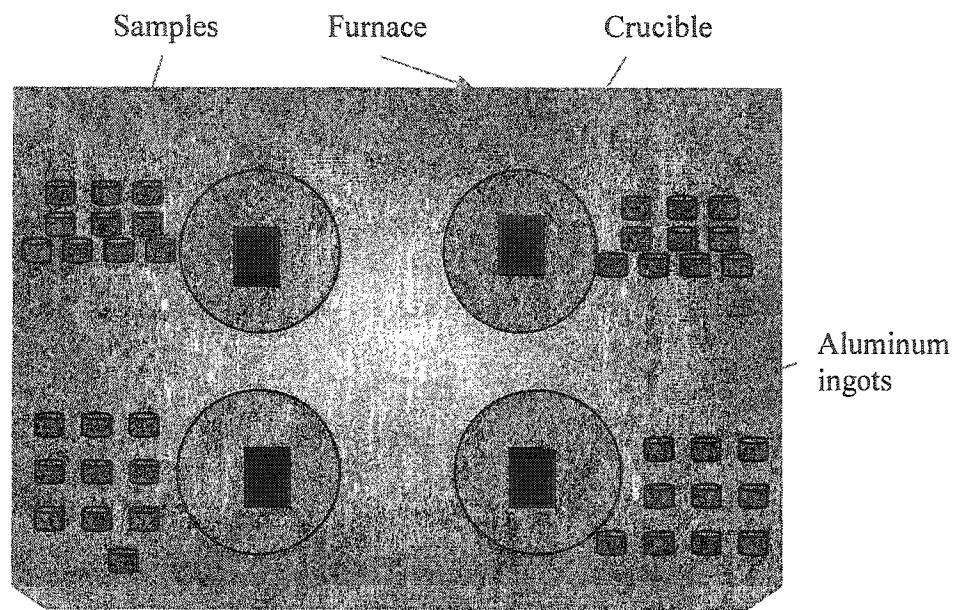


Fig.3-8 Samples and crucibles inside the furnace

- 2) About 1 kg of aluminum was put into the furnace.
- 3) The furnace was started and then run according to the operation profile shown in Fig.3-9.

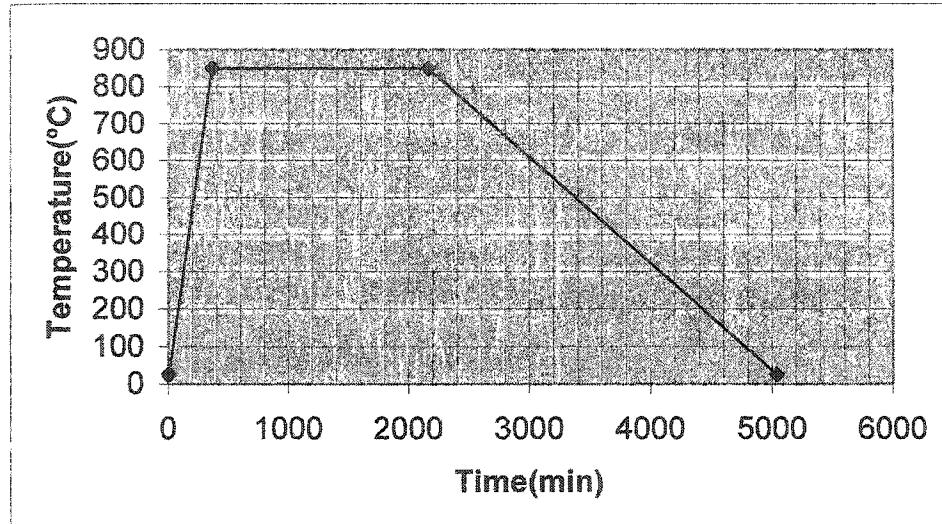


Fig.3-9 Operating curve of the furnace during test

- 4) Once the temperature reached 850°C, another 1 kg aluminum was put into the crucible. After complete melting of aluminum ingot, 5wt% Mg was put into the crucible.
- 5) The samples were introduced into the molten Al-5wt%Mg.
- 6) Withdrawing the sample from the crucible: Every 15 minutes, a sample was taken out from the metal bath for corrosion evaluation.
- 7) Cutting: The sample was cut from the middle line to verify the corrosion condition. The cut samples can be shown in Fig.3-10--3-13.
- 8) During the test, every 24 hrs, additional 40 g Mg were put into the molten alloy to supplement the Mg lost by evaporation.

3.3 Results and discussion

After corrosion test, the samples ever put into the molten aluminum were all taken out from the crucible and cut to verify the corrosion condition by the naked eye.

3.3.1 Criteria to verify corrosion

The verification criteria are based on the analysis of the corroded part of the samples.

According to previous works [29, 30], precise micro-structural examination revealed that the corroded part has black color. In this part, the structure is changed and higher concentration of Al, Mg and metallic Si can be found.

There is also a discolored part, where the original microstructure of sample is preserved, whereas a different morphology and contrast can be observed in the corroded region.

The discoloration of aluminosilicates after the immersion test in molten aluminum alloys may be attributed to the partial reduction of certain oxides, especially those easily reducible by aluminum or magnesium. It has been verified by some researcher [29] that the discoloration can be eliminated by heating a discolored sample in air at 1000°C for a few hours. The discoloration may occur via the reaction of some oxides with aluminum or magnesium vapors diffusing through the porosity network (prior to contact with aluminum or magnesium).

By the naked eye, the corrosion of aluminosilicate refractories is often recognizable by its black appearance. This criterion for verifying the corrosion condition of samples has been used in the test.

3.3.2 Results and discussion

The samples after different immersion period are shown in the following figures. The initiation of visible chemical corrosion was found in samples in the marked circle.

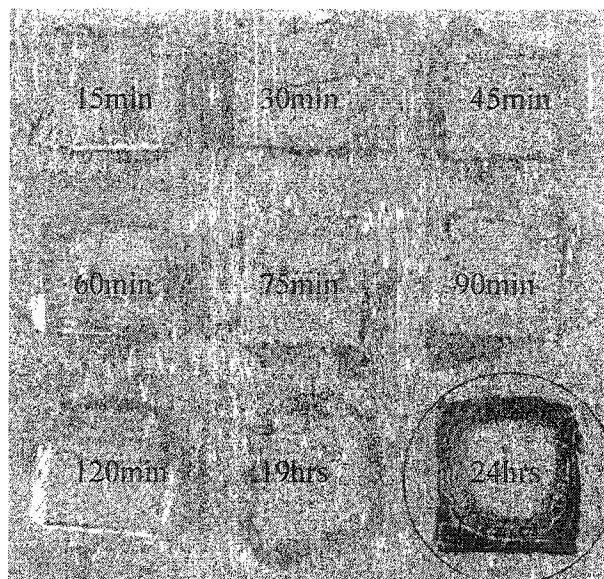


Fig.3-10 Samples containing 10% silica after different immersion periods

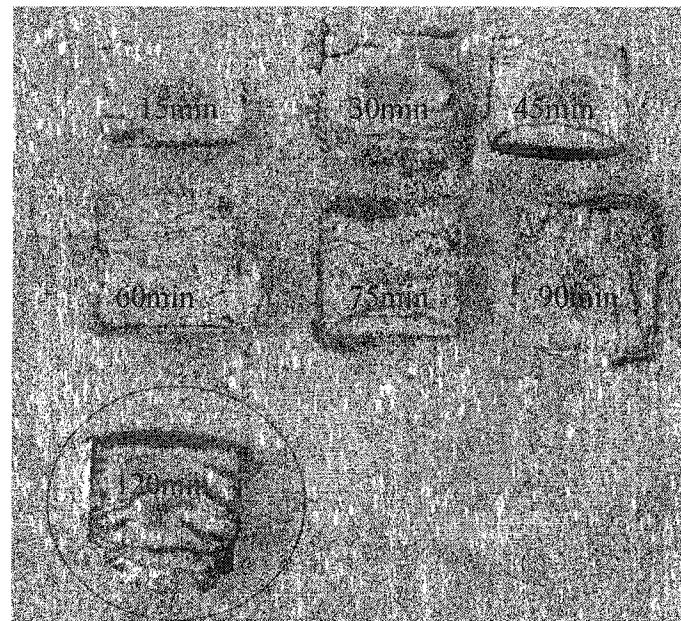


Fig.3-11 Samples containing 20% silica content after different immersion periods

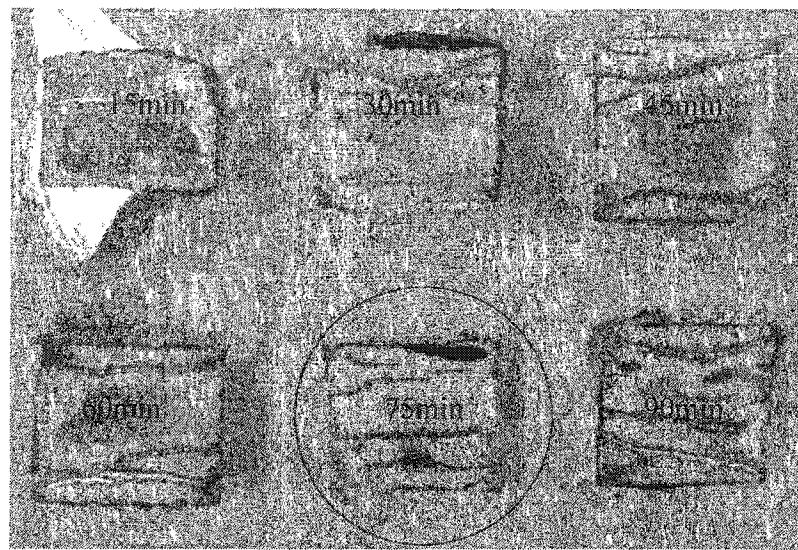


Fig.3-12 Samples containing 30% silica content after immersion different periods

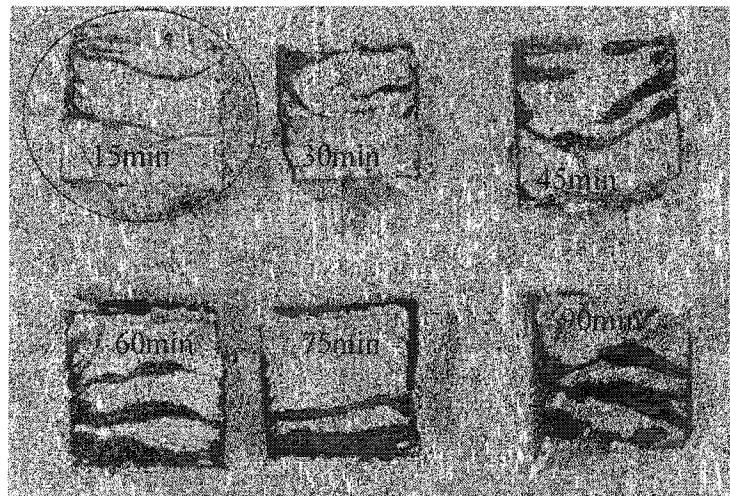


Fig.3-13 Samples containing 40% silica content after different immersion periods

Incubation time changes with increasing silica content inside the refractories is schematically shown in Fig.3-14.

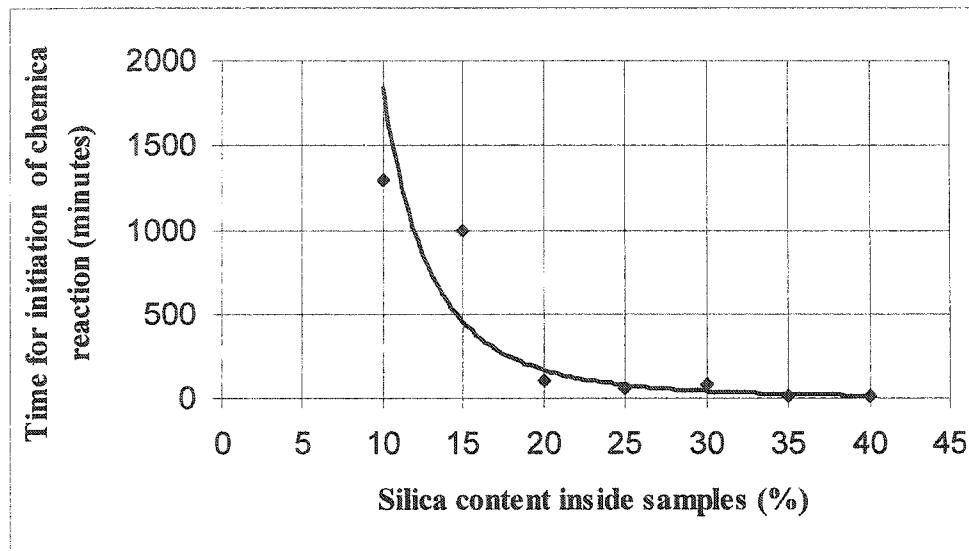


Fig. 3-14 Effect of silica content influence on the incubation time prior to chemical reaction

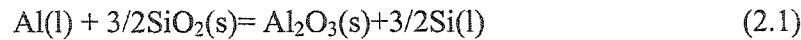
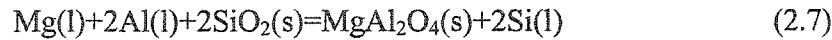
It should be pointed that, because of our observation technique, the incubation time shown in Fig.3-14 is not the incubation time in strict terms. The incubation time measured in this test includes not only the theoretical incubation time but also the period from beginning of chemical reaction till visual corrosion appearance. So, the measured incubation time includes two periods, the wetting period and the period from beginning of chemical reaction till visual corrosion appearance.

The incubation time measured in this test is influenced not only by the rate of chemical reaction assisted wetting, which has relations with the Free energy changes of the chemical reaction and temperature, as shown in Eq.2.6, but also influenced by the degree

of chemical reactions between the silica content and molten aluminum containing 5wt%Mg.

For different materials, the rate of chemical reaction assisted wetting is different, which causes the different incubation time existing before the chemical reaction initiates.

According to literature review in previous part, when aluminosilicate materials contact with molten aluminum containing Mg, the following two chemical reactions are concerned.



So, the degree of chemical reactions for different silica content samples may also be different.

According to Fig.3-14, for the higher silica content samples containing 25% to 40% silica, the influence of silica content on incubation time is weak, as compared with its influence in the higher alumina samples (10%, 15%, 20%silica content samples).

For the higher alumina content samples, the limited degree of chemical reaction may prevent the observation of corrosion, so the incubation time measured in the test is very long. For the higher silica content samples, the degree of chemical reaction is higher, which allows visual corroded part appear with a short period.

3.4 Conclusion of Chapter 3

Based on the test results and what is discussed above, the influence of silica content on incubation time is weak in higher silica content samples, as compared with its influence in lower silica content samples.

CHAPTER 4: SILICA INFLUENCE ON THE CORROSION PROCESS OF REFRactories BY MOLTEN ALUMINUM

4.1 Introduction

It is well known that molten aluminum and especially its alloys high in magnesium are corrosive to commercial refractories, necessitating replacement and repair in furnaces handling such alloys. Brondyke, in 1953, described the problem as penetration of alumina-silica refractories by aluminum with a reduction of silica and silicate bearing minerals to form corundum and elemental silicon [12]. This reaction is accompanied by an increase in volume of the penetrated zone, which results in stresses causing cracks and spalling. Moreover, serious contamination of metal by silicon can result, depending on the silica content of the refractory material. It is a general concept that more silica content inside the refractories will lead to more cracks inside the material when they contact with the molten aluminum containing 5 wt% Mg, allowing more molten alloy penetrate into the internal part, and then more corrosion will happen. But what is the influence degree of silica content impact on the corrosion process of refractory material by molten aluminum has not been clarified clearly. The research in this chapter will verify how the silica content influences the corrosion rate of refractory material by molten aluminum containing 5wt% Mg.

4.2 Experimental procedures

The experimental procedure related to the research in this part contains sample preparation, test procedures and measurement of the corroded samples after test.

4.2.1 Sample preparation

- **Composition designing:**

To study the silica content influence on the corrosion of refractories, three series of material containing 15%, 20%, 34% silica were used.

The size distribution inside the samples is designed according to the Andreason formulas, as given below.

$$\text{Andreason Formula: } \text{CPFT} = 100 * (D/D_{\max})^n \quad (\text{Eq.4.1})$$

where,

CPFT “Cumulative percent finer than”,

D Particle size

D_{\max} Largest particle size

n Distribution modulus (in this test, n=0.3)

After calculation and modification, the particle size distribution is designed as following.

TABLE.4-1 The composition for the 15% silica content samples

Grain size(mm)	Material	Volume(cm ³)	Density(g/cm ³)	Weight(g)	Weight (%)
0.045-0.075	Fine Alumina	14.21	3.9	55.419	18.03
0.02-0.045	Fine Alumina	18.52	3.25	60.19	19.58
0.005-0.02	Fine Alumina	22.89	3.17	72.5613	23.61
0.001-0.005	Fine Alumina	17	3.17	53.89	17.53
<0.001	Fine Alumina	5.78	3.17	18.3226	5.961
<0.001	Fume silica	21.36	2.2	46.99	15.29
Total		100		307.3729	100
	DARVAN				0.77%
	Sodium Citrate				0.15%

TABLE.4-2 The composition for the 20% silica content samples.

Grain size (mm)	Material	Volume (cm ³)	Density(g/cm ³)	Weight(g)	Weight (%)
0.045-0.075	Fine Alumina	14.21	3.9	55.419	18.33
0.02-0.045	Fine Alumina	18.52	3.25	60.19	19.91
0.005-0.02	Fine Alumina	22.89	3.17	72.5613	24
0.001-0.005	Fine Alumina	17	3.17	53.89	17.83
<0.001	Fume silica	27.38	2.2	60.236	19.93
Total		100		302.2963	100
	DARVAN				0.77%
	Sodium Citrate				0.15%

TABLE.4-3 The composition for the 34% silica content samples

Grain size (mm)	Material	Volume (cm ³)	Density(g/cm ³)	Weight(g)	Weight (%)
0.045-0.075	Fine Alumina	14.21	3.9	55.419	19.39
0.02-0.045	Fine Alumina	18.52	3.25	60.19	21.06
0.005-0.02	Fine Alumina	22.89	3.17	72.5613	25.39
<0.001	Fume silica	39.14	2.2	97.636	34.16
Total		100		285.8063	100
	DARVAN				0.77%
	Sodium Citrate				0.15%

- **Mixing of these compositions:**

The ingredients as shown in TABLES 4.1to 4.3 were weighed as per composition and mixed for 15 minutes with 16-17% water, to achieve good flowability.

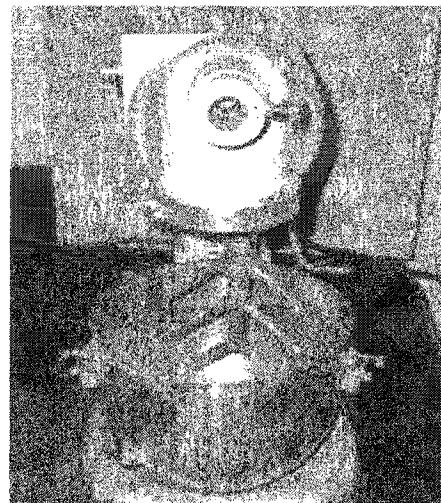


Fig.4-1 Mixing machine used in the test

- **Casting samples:**

After mixing, the mixture was put into the molds on the vibration table shown in Fig.4-2, and then vibrated for 5 minutes at a fixed frequency.

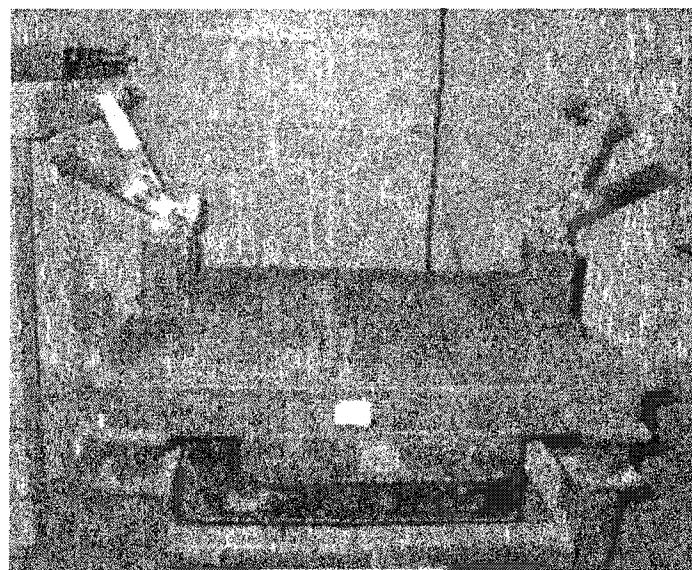


Fig.4-2 Vibration table used for casting samples

- **Curing castables**

After casting, the castables were cured in molds for 24 hrs at room temperature 25°C.

- **Drying samples**

After curing, the samples were demolded, and put into the drier at a temperature of 110°C.

- **Firing samples**

After drying, the samples were put into the furnace, and all of them were fired at a temperature of 1200°C for 6hrs. The operation profile of the furnace for firing is shown in Fig.4-3.

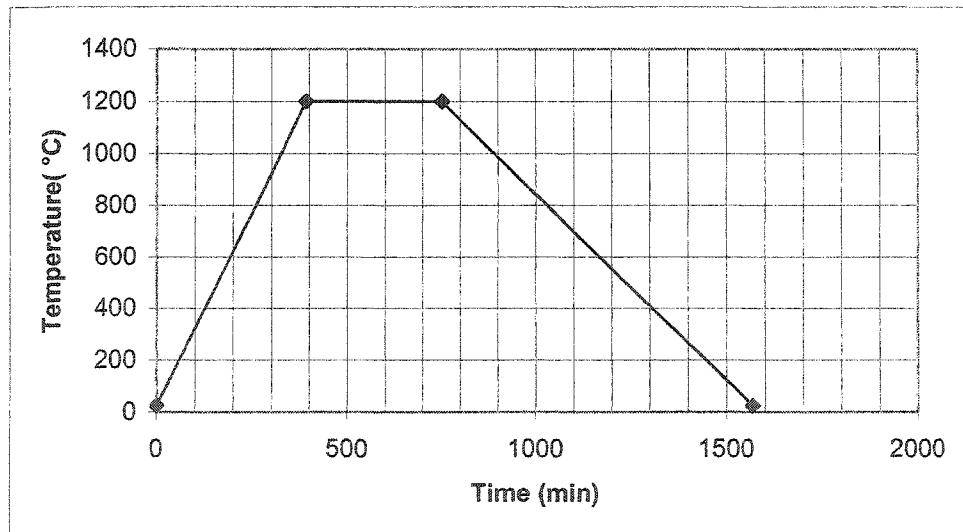


Fig.4-3 Operation profile for the furnace during corrosion test

After fired and cooled, the samples can be taken out from the furnace, and then cut into samples with dimension of 1*1*2 inches, waiting for corrosion test.

Porosity measurement

Two or three samples were taken from each serie for porosity measurement.

4.2.2 Corrosion test experimental set-up

The experimental set-up used is as same as in the corrosion test to verify the influence of silica content on the incubation time, which is shown in Fig.3-6 and Fig.3-7.

4.2.3 Corrosion test procedure

- Corrosion test procedures
- The samples were put into three crucibles along 1 kg aluminium for each crucible. And then the three crucibles are put into the same furnace at the same time, as shown in Fig.4-4.

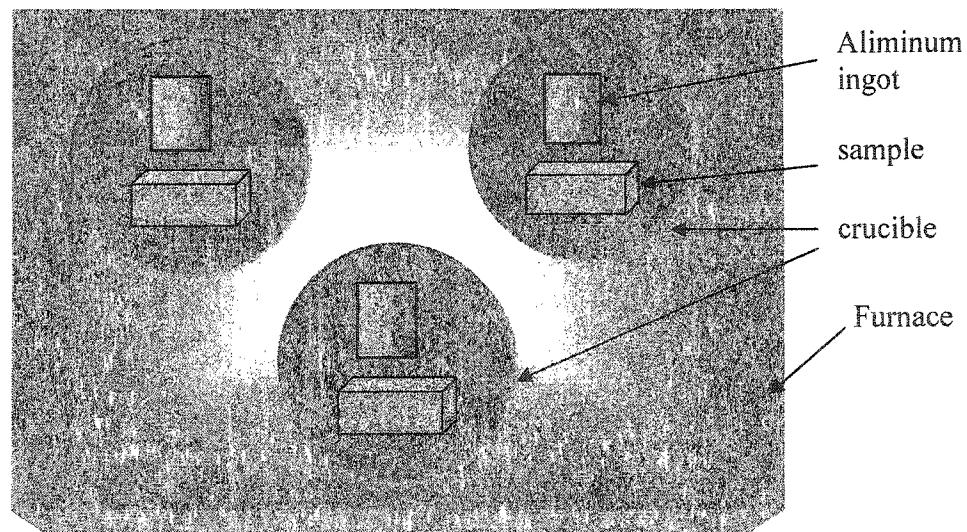


Fig.4-4 Arrangement of samples and crucibles in the furnace in the corrosion test

- Then the furnace was started. The operation profile for the furnace is designed as shown in Fig.4-5.

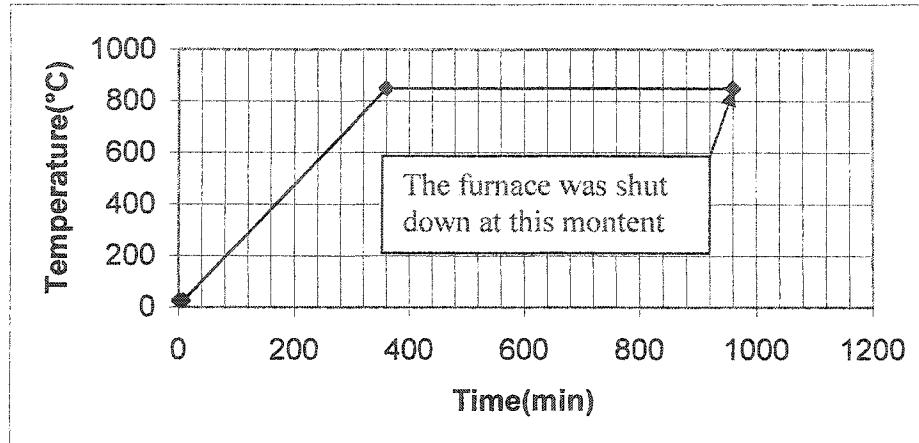


Fig.4-5 Operation profile of the furnace for corrosion test

- After the aluminum was totally melted, another 1 kg aluminum was also put into each crucible.
- When the aluminum added into the furnace was in molten state, the 5wt% Mg was added into the crucible.
- After 8hrs since the addition of the Mg, the samples were taken out from the furnace. After cooling in air, all the samples were cut from the middle line.
- **Measurement and Calculation of Corrosion Area of Each Series Samples by a Computer Program**

The computer program is called Image-Plus. The method to measure the corrosion area is described as follows.

- Open the Image-Plus program in the computer, and then open the image of the corroded area obtained by digital camera.
- Select the “measurement” tool in the program and then adjust the ruler in this program.

- Select “area calculation” tool, and then mark the boundary of the corroded area (the black area on the surface of the image), as shown in Fig.4-6. After that the calculation for the corroded area can be processed automatically. At the same time, perimeter of the section of sample can also be measured in this program.

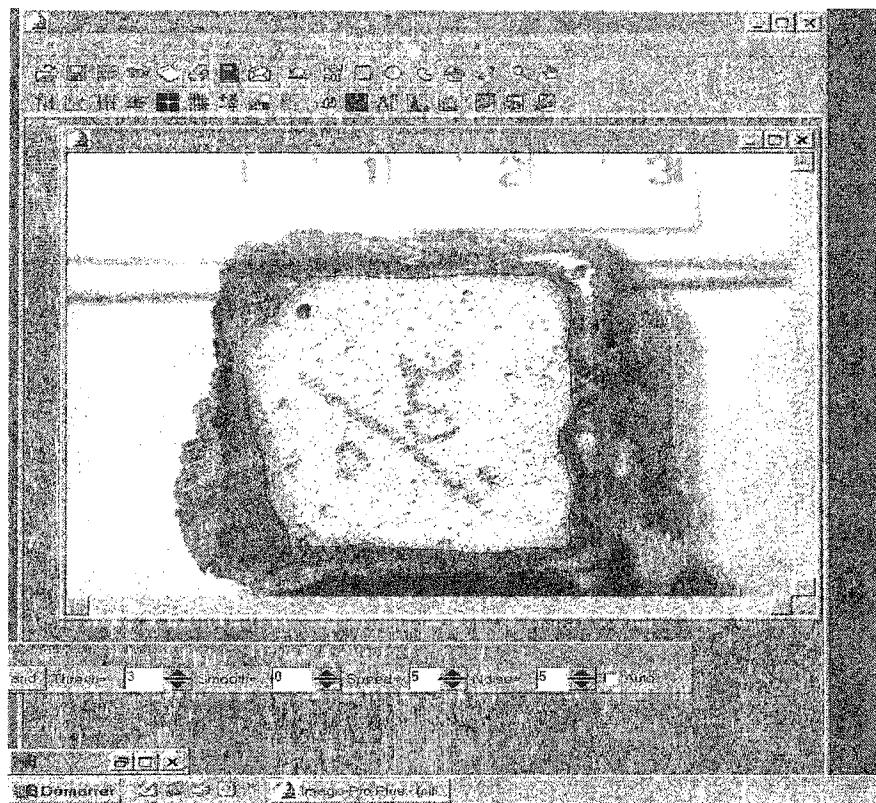


Fig.4-6 Measurement of irregular area by computer

4.3. Results and discussion

The value of porosity is 20.3%, 23.7%, 29.1% for 15%, 20%, and 34% silica content materials, respectively.

The samples corroded after corrosion test at 850°C are shown in Fig.4-7. The corroded or penetrated area is calculated by method described as above by using computer program Image-Plus.

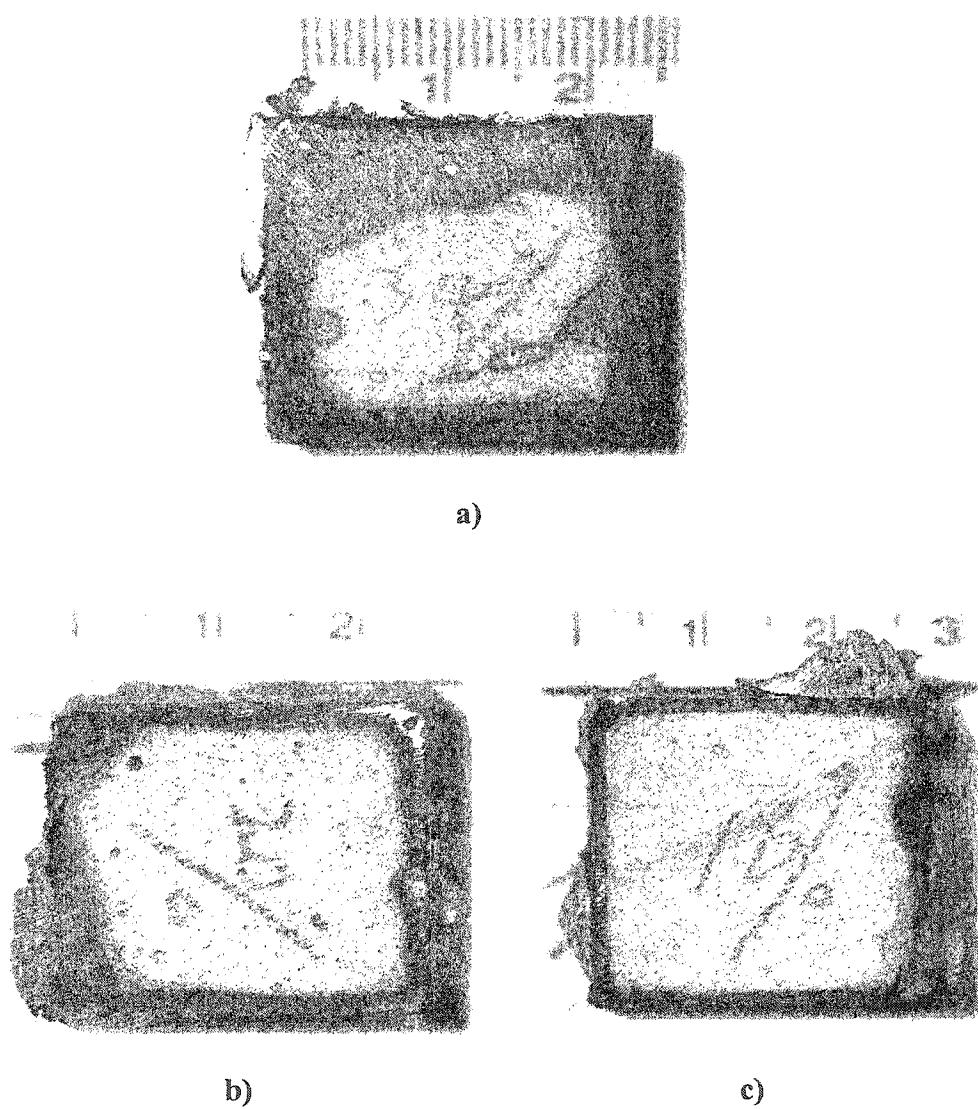


Fig.4-7 Samples with a) 34% silica, b) 20% silica, c) 15% silica after corrosion test in molten Al-5%Mg alloy at 850°C

After the measurement of the perimeter and the area of the corroded part for each sample, the corrosion depth was calculated by the following formula.

$$\text{Corrosion Depth} = \text{corrosion area} / \text{perimeter of section} \quad (\text{Eq.4.2})$$

After calculation, the relationship between corrosion depth and silica content inside refractories can be schematically shown in Fig.4-8.

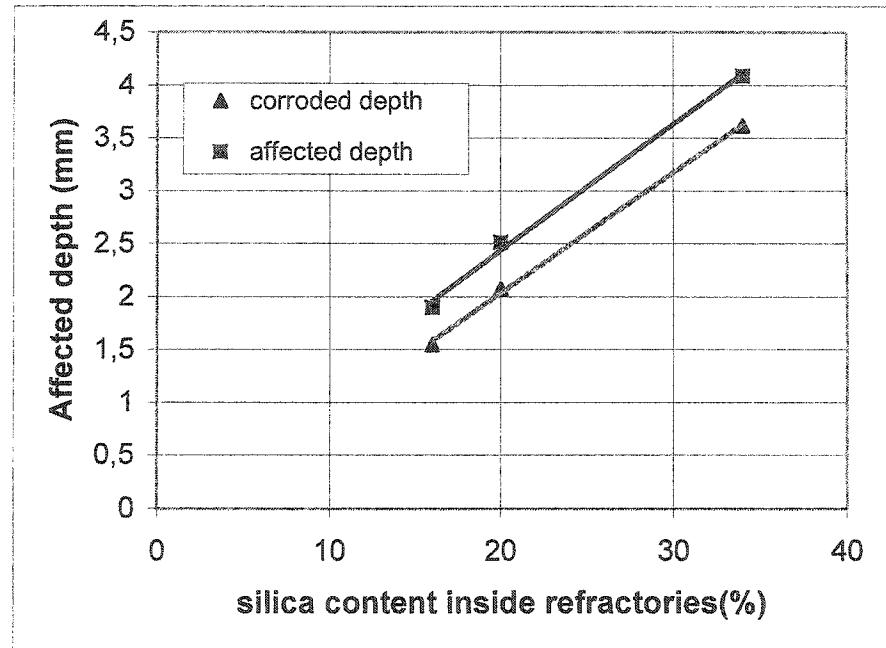


Fig.4-8 Influence of silica content inside the refractories on corrosion

The above results indicate both affected depth and corrosion depth increase linearly with the increasing of silica content inside the samples. These results are in good agreement with previous research results by studying on the corrosion of aluminosilicate materials attacked by 7075 aluminum alloy [31], which are shown in Fig.4-9.

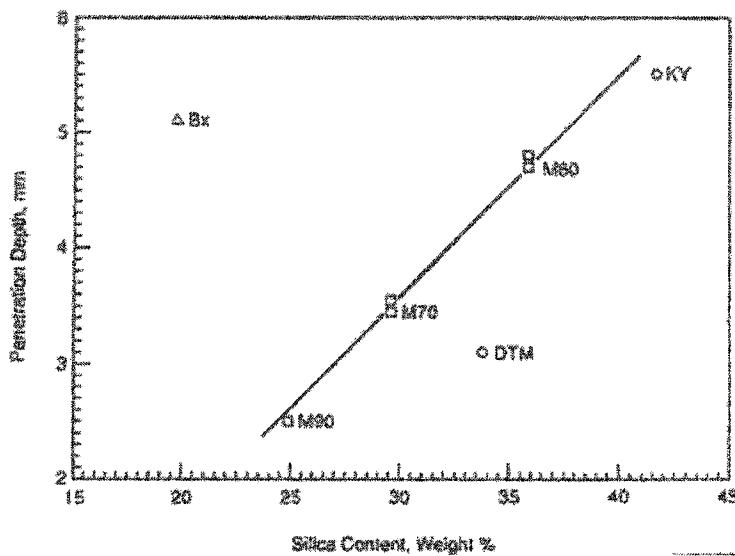
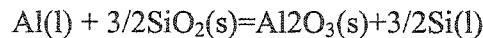
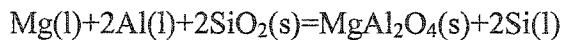


Fig.4-9 Effect of silica content on the corrosion of silica content refractories [31]

It is accepted that when silica-containing material contacts with molten aluminum containing Mg, following two reactions are considered.



These two reactions are accompanied by volume decrease. In theory, more silica leads to more chemical reaction and more volume decrease. According to the results calculated by F*A*C*T program, which is shown in Fig.4-10, the amount of volume decrease should have a linear relation with the silica content inside the refractory material when it contacts with the molten aluminum containing 5wt% Mg.

On the other hand, it should be noted that, both affected depth and corrosion depth have good linear relation with silica content inside material. This indicates that affected depth also has a linear relation with corrosion depth.

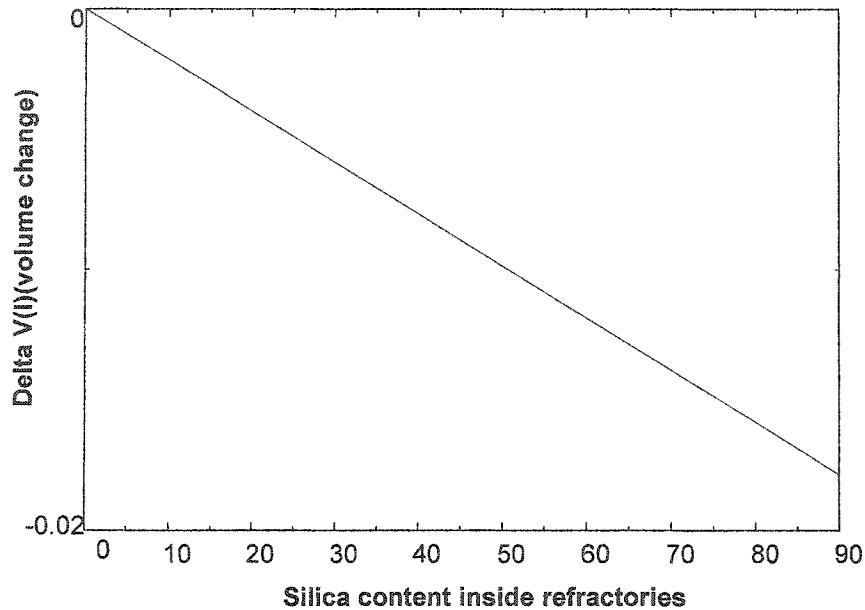


Fig.4-10 Relation of volume change and silica content inside the refractories at 850 °C

The linear relation between corrosion and silica content also indicates that silica content may be the more critical factor, as compared with porosity. Actually, this view can also find support from previous test results concerning porosity effect on the corrosion of refractory material by molten aluminum. More than one researcher pointed out that the porosity of samples has almost no clear relation with the corrosion depth of samples when they contact with the molten aluminum [12] [15] [17].

This phenomenon can be explained as following: by comparing the influence of silica content on the corrosion process and the influence of silica content on the incubation time prior to the chemical reaction, it is very clear that different silica content inside the material mainly cause different degree of chemical reaction rather than much incubation time difference. So, the penetration of refractory by molten alloy is continuously influenced by the chemical reaction between the silica inside the refractory material and

the aluminum containing 5% Magnesium. This reaction leads to continuously crack formation inside the refractory material, allowing macroscopic molten aluminum alloy continuously penetrate into the internal part of the material. The penetration through cracks is much more severe than the pure penetration through porosity, the significant effect of cracks formation on penetration may have covered the effect of different porosity on penetration, while the difference in penetration caused by porosity difference can be ignored as compared with macroscopic penetration of molten alloy through cracks.

In general, the results in previous works and the test results here showed that the penetration/corrosion of refractory material by molten aluminum is mainly caused by the chemical reaction between the silica inside and the molten aluminum often containing 5wt% magnesium. Silica content is the critical factor for penetration/corrosion of refractories by molten aluminum. Affected depth /corrosion depth increases linearly with increasing of silica content inside samples. Continuous crack formation may be the main cause of continuous penetration and corrosion.

4.4 Conclusion of the chapter 4

- Silica content has a more significant effect on the chemical reaction, as compared with its effect on the incubation time prior to the chemical reaction between the silica inside and the molten aluminum containing 5wt% Mg.
- Both affected depth and corrosion depth increase linearly with the increasing of silica content inside the refractory material when they contact with the molten aluminum containing 5wt% Mg, despite the samples had different porosity. This also means the relationship between corrosion depth and affected depth is linear in the corrosion process.

CHAPTER 5: CONTROLLING MECHANISM OF CORROSION OF REFRACTORIES BY MOLTEN ALUMINUM-----CORROSION DEPTH VS. TIME

5.1 Introduction

When a refractory material is corroded by the molten aluminum containing 5wt% Mg, the chemical reaction will happen at the interface of the melt and the material, and cracks inside the material is caused by reaction $\text{Al(l)} + \text{SiO}_2(\text{s}) \rightarrow \text{Al}_2\text{O}_3(\text{s}) + \text{Si(l)}$ ($\Delta V < 0$). The crack formation allows more molten aluminum alloy to penetrate to the chemical reaction front.

Some researchers pointed that, according to Le Chatlier's principle, if the silicon concentration near the chemical reaction front reaches saturation, the reaction will cease, because the silicon precipitate covers the reaction front [26]. At the same time, the product of the chemical reaction, Si, can diffuse through the metal channel because of the silicon concentration difference between reaction front and bulk metal. So if the chemical reaction rate is higher than the Si diffusion rate, the corrosion is controlled by diffusion process; if the chemical reaction rate is lower, the corrosion is controlled by chemical reaction process. The question here is which one is the real controlling process under given condition. Unfortunately, there is no definitely answer so far. On the other hand, despite which is the controlling process, chemical reaction rate and silicon diffusion rate through the metal channel will achieve a balance at last.

5.2 Experimental procedures

5.2.1 Sample preparation

In this research, to study the corrosion kinetics of refractories by molten aluminium under static condition, two kinds of material are used, one is made from commercial castable material SP, and the other is made from a precast brick SF. The preparation for these two series of samples is described as following in detail.

- **SP series samples preparation process**
 - First, suitable amount of castable material was dry mixed in a mixing machine for 5 minutes.
 - After dry- mixing, 5.5wt% water was added into the mixture and wet mixed for 10 minutes is needed for mixing. During mixing, the metal mold used for casting was made ready on the vibration table.
 - When the mixture containing 5.5% additional water became suitable for casting, the mixing was stopped and the mixture was taken out from the mixing machine (as shown in **Fig.4-1**) and filled into the mold on the vibration table (as shown in **Fig.4-2**).
 - After being vibrated on the vibration table at the frequency of 60/s for 5 minutes, the mold containing castable was moved away from the vibration table.
 - After curing at room temperature for 24 hrs, they were put into the drier at 110°C for 24 hrs.
 - After the samples were totally dried, they were fired at 1200°C for 6 hrs. The operation profile designed for firing is shown in **Fig. 4-2**.

- After that, the samples were machined into smaller samples with dimension of $1 \times 1 \times 2$ inches, ready for test.

According to the instruction provided by the manufacturer, the material is a high alumina castable having high strength and non-wetting to molten aluminum at normal operating temperatures.

The typical test data, properties and chemical analysis for this material can be shown in following tables.

TAB.5-1 Typical test data of SP material

Maximum recommended temperature °C	1704°C
Material required kg/m ³	2595
Water required to temper wt%	5.0%
Setting characteristics	Hydraulics
Minimum time before firing	24hrs
Average storage life	3 months

TAB.5-2 Physical properties of the SP material

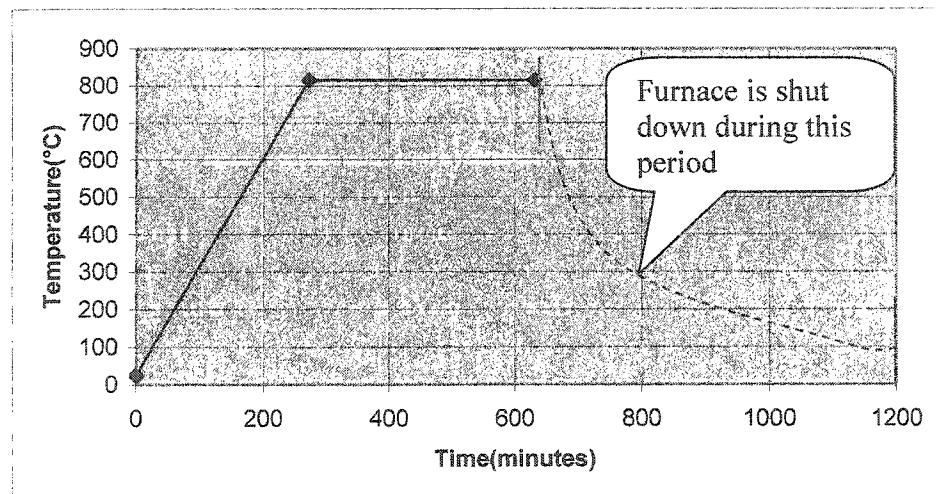
Tested after firing at test temperature, and cooling					Test at temperature	
Test temperature (°F)	Bulk Density (1b/ft ³)	Total linear changes(%)	CMOR (1b/in ²)	Cold crushing strength (1b/in ²)	Thermal conduct	HMOR (1b/in ²)
230	163	-0.1	1800	11500	10.6	
1500	162	-0.2	2200	13000	11.3	4650
2000		0.02	3000	13500	12.3	4050
2500		0.0	3000	13500		1200

TAB.5-3 Chemical composition analysis of SP material

CHEMICALS	FORMULA	WT% dried basis
Silica	SiO ₂	30.26
Alumina	Al ₂ O ₃	57.29
Iron Oxide	Fe ₂ O ₃	0.84
Calcium Oxide	CaO	1.42
Magnesia	MgO	0.07
Alkali	Na ₂ O+K ₂ O	0.09
Titanium Oxide	TiO ₂	1.43
Zirconium Oxide	ZrO ₂	3.29
L.O.I		1.99

- SF Samples preparation

The pre-cast bricks are fired at the temperature of 815°C in the furnace, the operation program designed for the firing is shown as following, in Fig.5-1.

*Fig.5-1 Operation profile of furnace firing the SF precast samples*

When the firing is finished, the brick is taken out from the furnace and cut into the samples with dimension of $1 \times 1 \times 2$ inches, then the samples are ready for test.

The chemical composition of the SF material can be shown in following tables.

TAB.5-4 Chemical composition of the SF material

CHEMICALS	FORMULA	WT%
Silica	SiO_2	83.5-85.5
Alumina	Al_2O_3	11.5-12.5
Iron Oxide	Fe_2O_3	<0.1
Others		4.0

5.2.2 Experimental set-up

The experimental set up for the research in this chapter is the same shown in Fig.3-6, Fig.3-7.

5.2.3 Corrosion Test Procedure

- First, the samples for test were put into three crucibles, and then 1 kg metal aluminum was added into each crucible. After that, the three crucibles were put into the furnace at the same time. An additional lid for each crucible was used as cover to avoid corundum growth.
- The operation program designed for this furnace is as same as shown in Fig.4-4.
- When the 1kg metal aluminum ingot in each crucible was melted totally, another 1 kg aluminum ingot was put into each crucible in the furnace.
- After all the aluminum ingots were totally melted into liquid, 5wt% Mg was added into each crucible, and was stirred uniformly.

- During the corrosion test, every 24 hrs since the addition of Mg, about 40 g Mg was added into the molten aluminum to supplement the loss of Mg.
- After different corrosion period since the addition of Mg into the crucible, a sample was taken out from the furnace, cooled and cut. The test was stopped when all the samples were taken from the furnace.
- Corrosion depth measurement

The method for measurement of corrosion depth for each sample has been described in Chapter 2. After measurement of corrosion depth for each sample, the relationship between corrosion time and depth was found.

5.3 Discussion of the test results

5.3.1 Test results

The corroded SP samples after corrosion test for 21, 34, 47, 62, 72, 79 hrs can be shown in Fig.5-2. The corroded SF samples after test are shown in Fig.5-3.

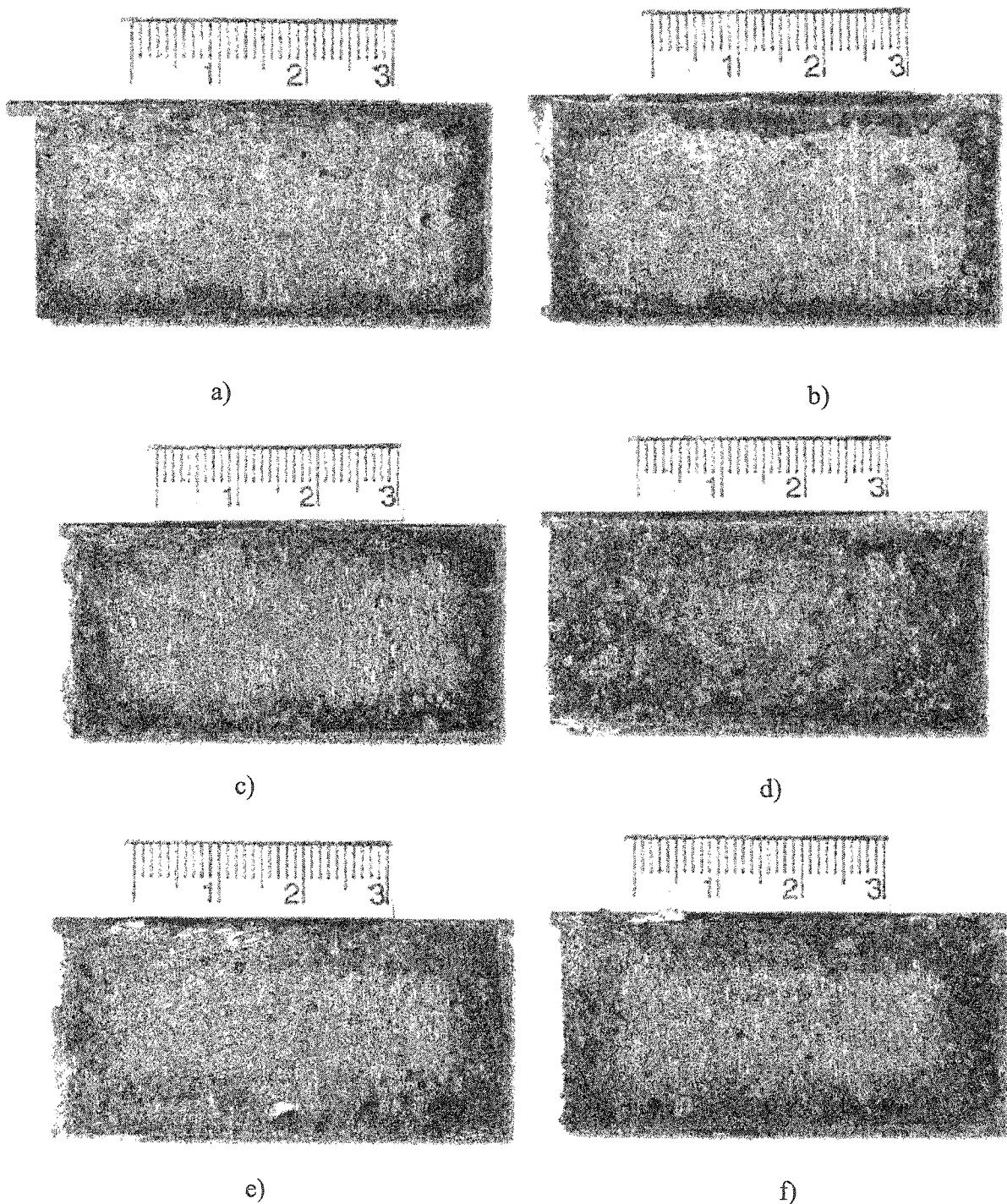
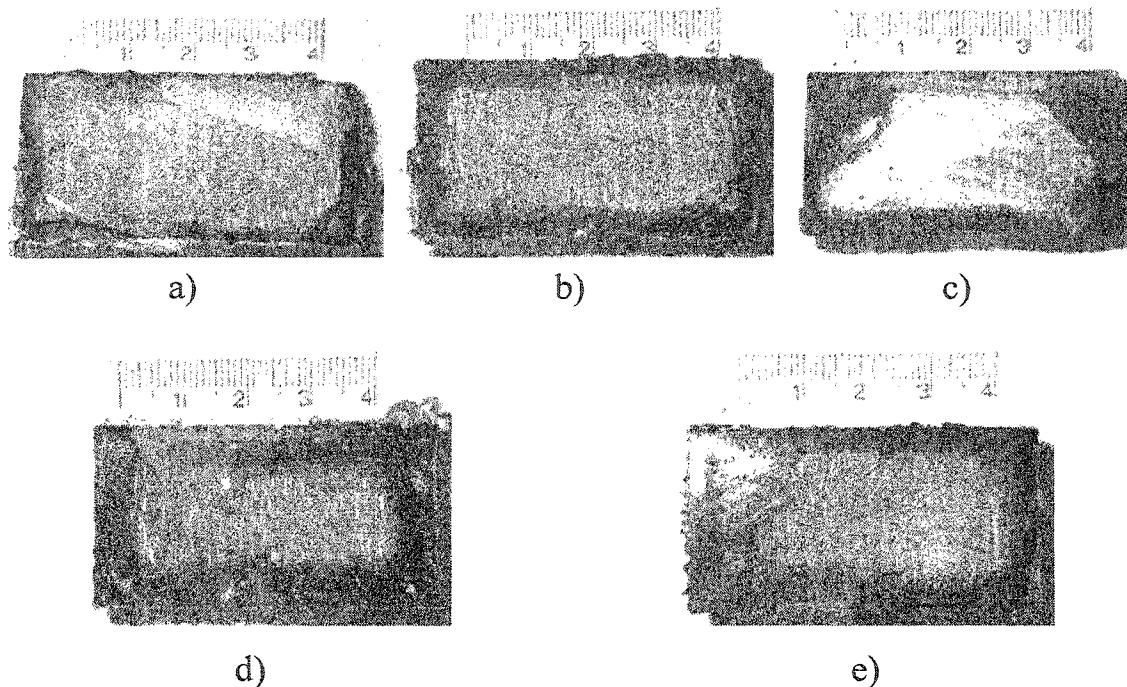


Fig.5-2 Corroded SP samples after different test period corrosion

a) 24hrs, b) 31hrs, c) 47hrs, d) 62hrs, e) 72hrs, f) 79hrs at the temperature of 850° C



*Fig.5-3 Corroded SF samples after different test period corrosion
a) 12hrs, b) 24hrs, c) 48hrs, d) 60hrs, e) 72hrs*

According to experience, the affected depth of aluminum in the refractories can be considered zero before the addition of Mg into the molten aluminum, because of the protective layer of alumina on the surface of the samples.

Based on the corrosion depth measurements for samples shown in Fig.5-2 and Fig.5-3, the relation between corrosion depth and time was obtained as shown in Fig.5-4 and Fig 5-5.

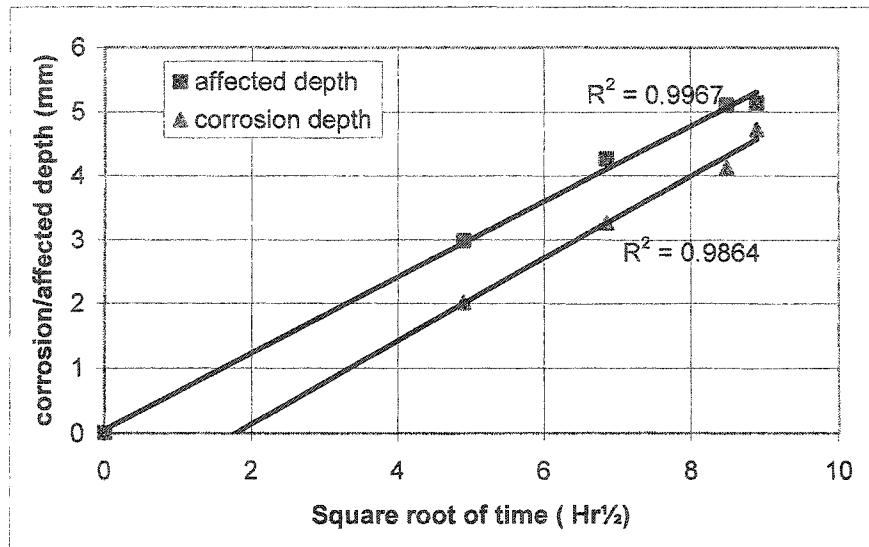


Fig.5-4 Relationship between affected depth, corroded depth of SP material and square root of time

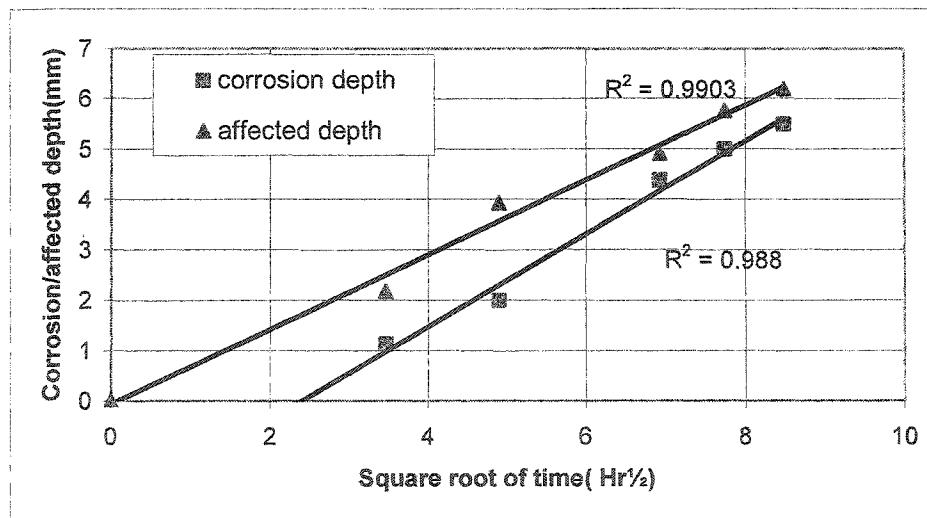


Fig. 5-5 The relation between the corrosion depth of SF samples and square root of time

The relationship of corrosion/penetration depth with time, rather than with square root of time, is shown in Fig.5-6 and Fig.5-7.

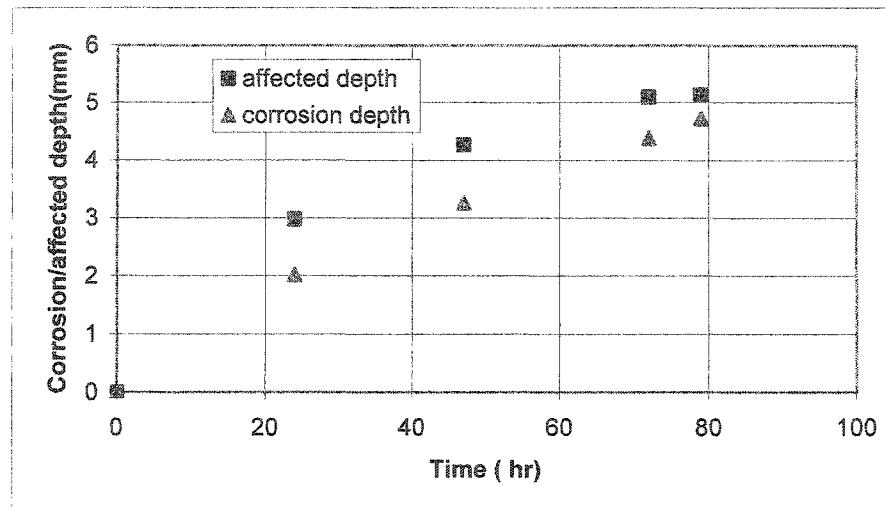


Fig.5-6 Affected depth .vs. time for SP samples

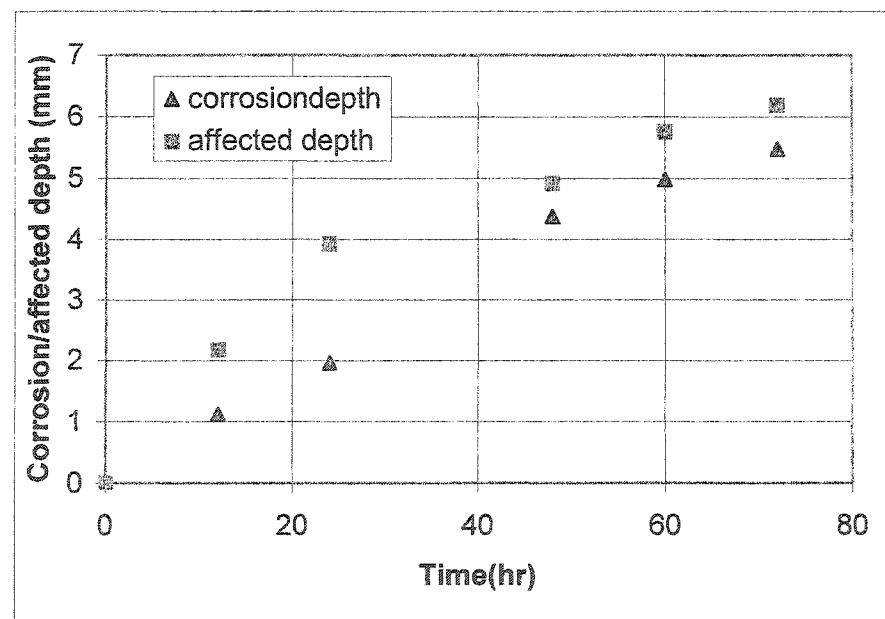


Fig.5-7 Affected depth .vs. time for SF samples

5.3.2 Discussion of test results

- **Controlling mechanism of corrosion process of refractories by molten aluminum**

It is known that, when refractory material contacts with the molten alloy, the molten alloy wets and penetrates into the material, and then reacts with the silica inside the refractories at the reaction front. According to corrosion mechanism of refractories in molten aluminium, the corrosion below the metal line is mostly caused by redox reaction between the silica and molten aluminum, and this reaction is accompanied by a volume decrease which should allow further metal penetration in the refractory, and according to the previous works [11], a metal channel was found inside the refractories after corrosion test. Higher silicon concentration in the metal channel was also found as compared with in the bulk metal. This indicates that the silicon produced during corrosion may not completely and rapidly diffuse through the metal channel of corroded refractory.

This also indicate that the silicon diffusion rate from reaction front to the bulk metal through metal channel is lower than the silicon production rate by redox reaction between molten aluminium and silica inside refractories, and hence, the corrosion process may be controlled by the diffusion process.

According the test results in this research, which is shown in Figs. 5-4, 5-5, 5-6 and 5-7, the growth of corroded depth inside refractory material has a linear relation with square root of immersion period of samples in molten aluminum. According to the discussion in literature review, this kind of relation indicates the corrosion of refractory material, such as SP or SF material, by molten aluminum, is controlled by diffusion process.

In Figs.5-4 to 5-7, linear relation of penetration depth .vs. $t^{1/2}$ is more apparent; as compared with corrode depth. But in fact, if the relation between penetration and $t^{1/2}$ is linear, the relation between corroded depth and $t^{1/2}$ should also be linear, because of

linear relationship between corrosion area and penetration area, which has been discussed in Chapter 4.

In summary, it can be concluded that the corrosion process is controlled by diffusion process.

- **Discoloration and corrosion rate**

During the whole corrosion process, the discoloration depth (as shown in Fig.5-8), deceases with time, as shown in Fig.5-9 and 5-10.

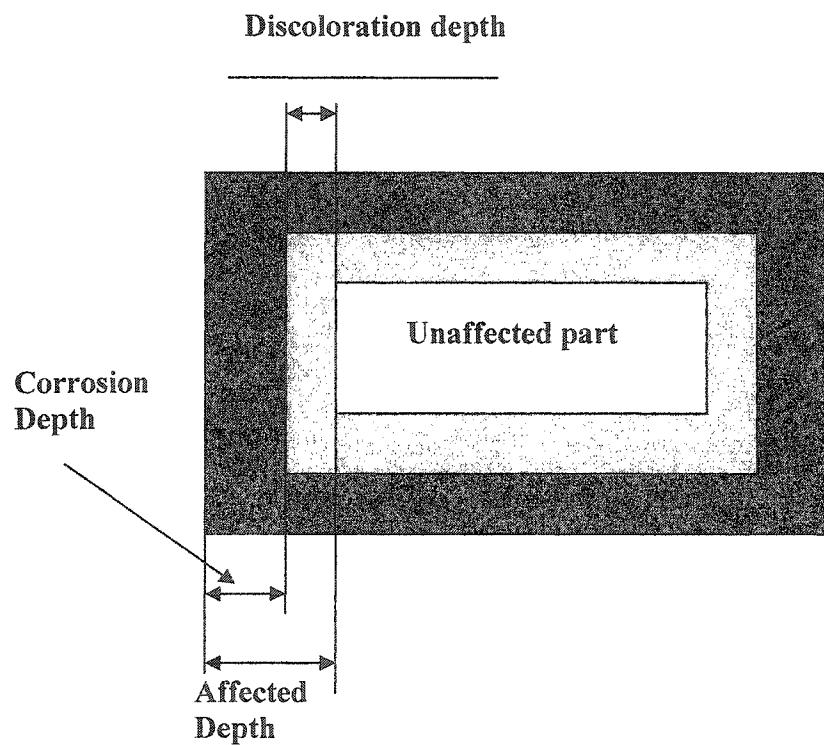


Fig.5-8 Schematic of the sample with penetrated/corroded area

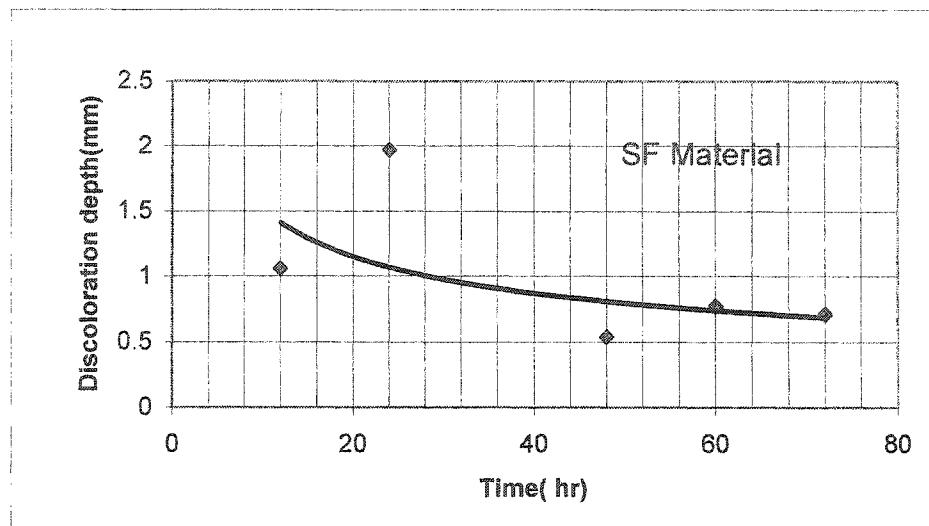


Fig.5-9 Discoloration depth .vs. time (SF material)

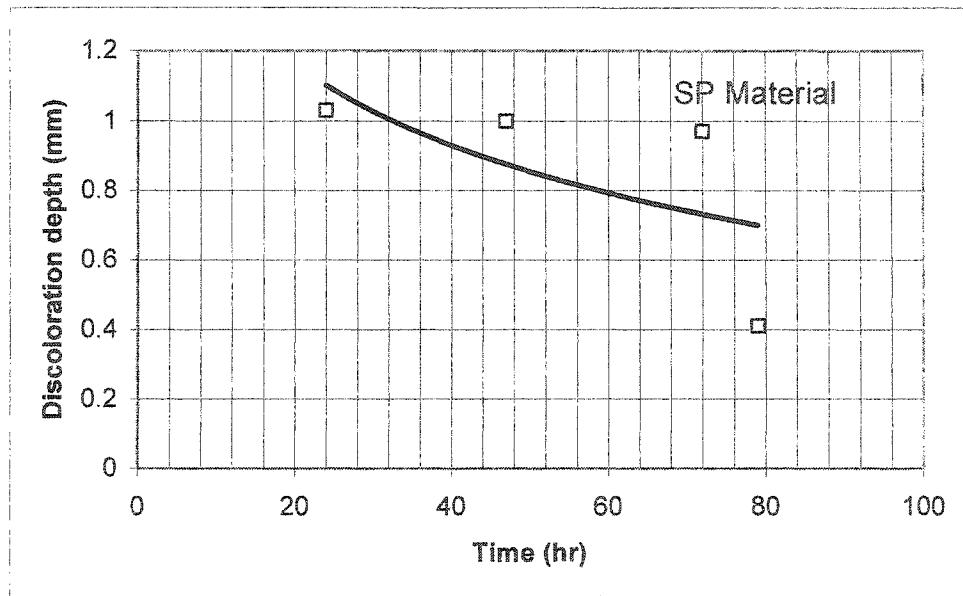


Fig.5-10 Discoloration .vs. time (SP material)

According to the previous results, Eqs.5.1 to 5.3 can be written:

$$\text{Corrosion depth} = Kc * t^{1/2} - A \quad (A>0, Kc>0) \quad (\text{Eq.5.1})$$

Where, A (>0) is a constant related to the incubation time prior to the chemical reaction.

$$\text{Affected depth} = Kp * t^{1/2} \quad (Kp>0) \quad (\text{Eq.5.2})$$

$$\text{So,} \quad \text{discoloration depth} = A + (Kp - Kc)t^{1/2}. \quad (\text{Eq.5.3})$$

Since the discoloration depth is decreasing with time, $(Kp - Kc) < 0$. It means the value of Kp is lower than the value of Kc , so the corrosion kinetics of refractory material by molten Al-5wt% Mg is higher than the affection kinetics.

5.4 Conclusion of chapter 5

Based on the above results and discussion, the following conclusions can be obtained.

- Affected depth and corrosion depth most likely increase linearly with the square root of time. This kind of relation shows that the affection and corrosion of refractories by molten aluminum is controlled by diffusion process of silicon from reaction front to bulk metal.
- In this study, from the two tested material, the corrosion kinetics of refractory material by molten aluminum is higher than affection kinetics.

CHAPTER 6: INFLUENCE OF DYNAMIC CONDITION ON CORROSION PROCESS OF REFRACTORY MATERIAL BY MOLTEN ALUMINUM

6.1 Introduction

In service, aluminosilicate refractory material in aluminum industry are often subjected to some dynamic conditions. Till now there is little information found in the literature about the influence of melt convection on the penetration rate in aluminosilicate refractories.

On the other hand, to predict the lifetime of a refractory material and to optimise the position inside the triangle of cost of refractory, quality of the final product, productivity of the installation, test which can accelerate the failure mechanism of the refractory material subjected to molten aluminum alloy is needed. The acceleration of lifetime reduction phenomenon must not modify the principle of its action. For example, the increase of temperature may be efficient in accelerating a chemical attack, but may as well activate chemical reactions negligible at realistic temperature and thus lead to improper conclusions. So, in this case, dynamic corrosion test may be a good selection to achieve this goal if it does have an influence on the corrosion process.

The objective of the present work is just to verify whether dynamic condition has some influence on corrosion process, especially on the kinetics of corrosion of the refractories by molten aluminum containing 5wt% Mg. During this research, a test set-up was established to generate different dynamic conditions. At the same time, static corrosion

test were also processed by using the same experimental set-up, in order to compare static corrosion with dynamic corrosion.

6.2 Principle and method of the dynamic test

According to the literature review, dynamic conditions can be generated by rotating the sample which is partially immersed in the molten aluminum, so the corrosion test in this chapter was conducted in a furnace with a sample rotated by a motor placed on the top of the furnace.

During the test, it is very important to avoid the oxidation of molten Al-5wt%Mg alloy. This phenomenon can not only influence the corrosion of samples in the molten aluminium but also cause a safety problem of the experimental set-up, because the corundum formed by direct oxidization can adhere to the rotating sample toughly. Therefore, the rotating finger test must take place under very low oxygen partial pressure, and this can be achieved by purging Nitrogen or Argon gas into crucible directly by using three alumina tubes, as shown in Fig.6-1.

The tests for this research were conducted at the temperature of 850°C, over a period of 24 hours or more, at the rotation speed from 0-200rpm. The samples used for the research had to be machined to cylinder shape (60mm diameter, 400mm long), as shown in Fig.6-2. Because of the big dimensions, the sample used in the test could not be taken from the common bricks, but had to be made from castable material.

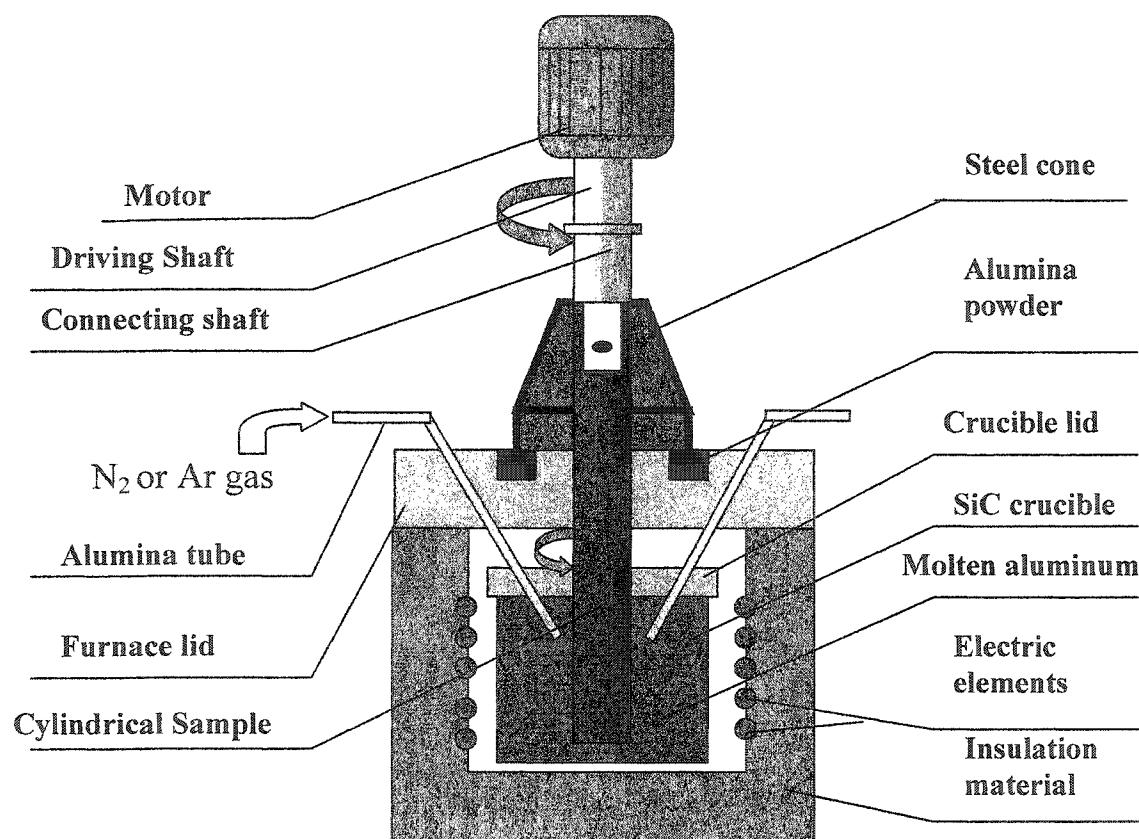


Fig.6-1 Experimental setup for dynamic corrosion test

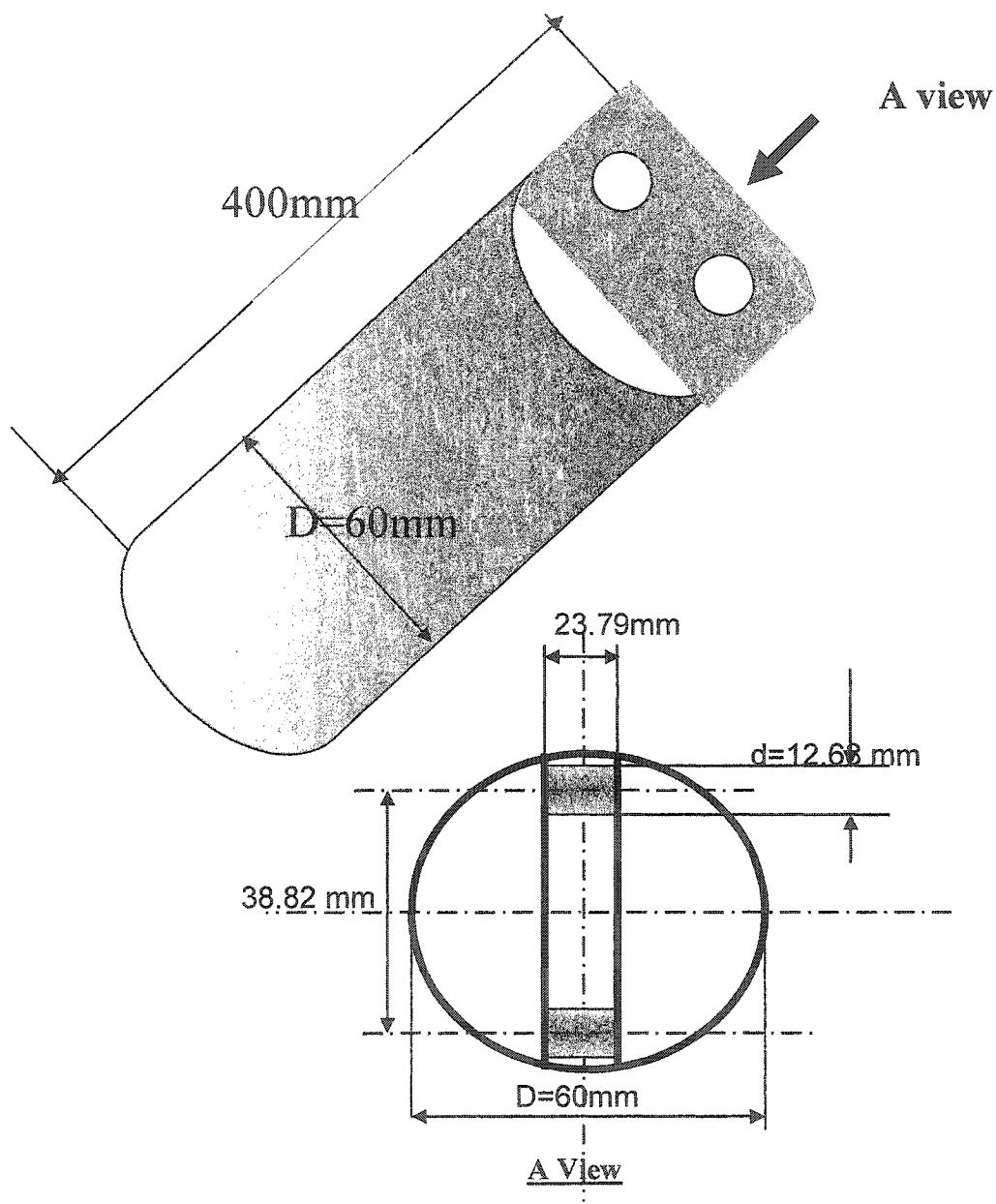


Fig.6-2 Dimension of sample used in the dynamic /static corrosion test

6.3 Experimental Procedure

6.3.1 Sample preparation

The sample preparation process for this research is almost as same as the SP samples' preparation process which has been described in Chapter 5, except for some differences shown:

- In this work, the mold used for casting was a cylinder shape with a diameter of 60mm.
- After firing at a temperature of 1200°C, the big cylinder castable was machined to the sample with the dimensions shown in Fig.6-2.

The samples used for this research were made from SP material and NA material. The chemical composition and properties of SP material has been described in the Chapter 5. NA material is a kind of low moisture aluminum resistant castables. The chemical composition and properties of the NA material is given in the following Tables 6.1 and 6.2.

TABLE 6-1 Chemical analysis of the NA castable

NAME	FORMULA	CONTENT (%)
Silica	SiO ₂	23.6
Alumina	Al ₂ O ₃	60
Iron Oxide	Fe ₂ O ₃	0.9
Titanium Oxide	TiO ₂	1.5
Calcium Oxide	CaO	1.1
Alkalies	Na ₂ O+ K ₂ O	0.2

TABLE 6-2 Physical properties of the samples

(Note: The above data came from product instruction provided by the manufacturer)

6.3.2 Test procedure

The crucible was first put into the furnace as shown in Fig.6-1. After that, 2 kg aluminium ingots were put into the crucible. Then, the big cylindrical sample for the test

was partially immersed into the crucible, and all arrangements were also made ready, as shown in **Fig.6-1**.

When the 2 kg aluminum ingots were totally melted, another 2 kg aluminum ingot was added. After the furnace was heated to 850°C, and all the aluminum ingots were totally melted, 5wt% Mg were added into the molten aluminum, and made uniform in molten alloy by stirring. After that, motor was started to rotate the sample, at the speed of 200rpm or 400rpm. At the same time, the protective gas such as nitrogen or argon gas was purged into crucible directly.

During the test, Mg was added according to the CIREP standard immersion test procedure.

After the samples were corroded for 24 or 48 hrs, the samples were taken out from the furnace and cooled at room temperature, in air.

To compare static corrosion with dynamic corrosion, corrosion tests under static condition had also been carried out on this experiment set-up under same conditions but without rotation.

6.3 Test results and discussion

After dynamic or static corrosion test on the same experimental set-up shown in **Fig.6-1**, the corroded samples were cut from the middle line to verify the corrosion condition for each sample, which are shown in following figures.

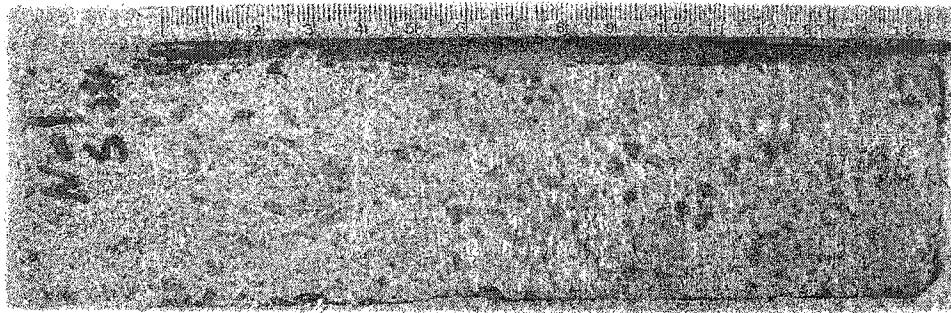


Fig.6-3 Corroded NA sample under static condition

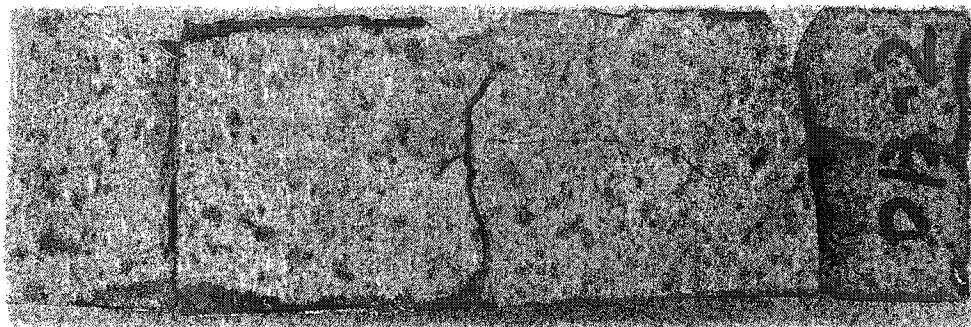
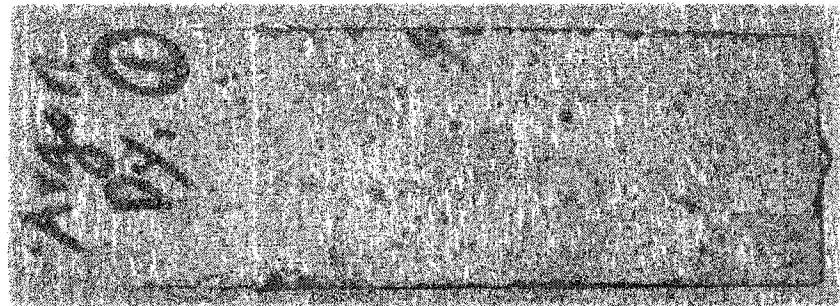


Fig.6-4 Corroded NA sample under dynamic condition

According to Fig.6-3 and Fig.6-4, the corrosion depth of the sample under static condition is less than that under dynamic conditions. This means dynamic condition has some influence on the corrosion, and it can accelerate the corrosion of refractory material by molten aluminum containing 5wt% Mg.

For the samples made from SP material, which contains non-wetting additives, the samples were not corroded significantly, and no apparent difference was observed between the samples corroded under dynamic conditions and static condition.

The corroded samples made from SP material after the test are shown in Figs.6-5, to 6-8. For these samples, maybe the good resistance of this kind of material prevented corrosion to occur in both corrosion tests.



*Fig.6-5 SP sample after Dynamic corrosion test under Ar
(850° C, 3.34 r.p.s.)*

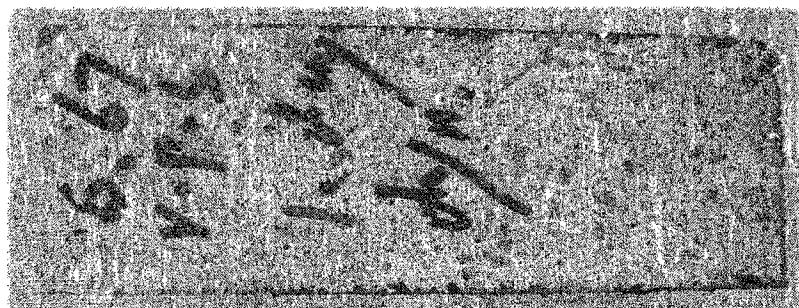


*Fig.6-6 SP sample after Dynamic corrosion test under Ar
(850° C, 6.67 r.p.s.)*

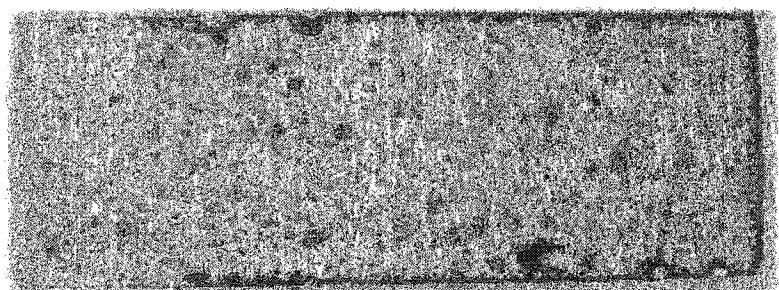


Fig.6-7 SP sample after Dynamic corrosion under N₂ (850° C, 3.34 r.p.s.)

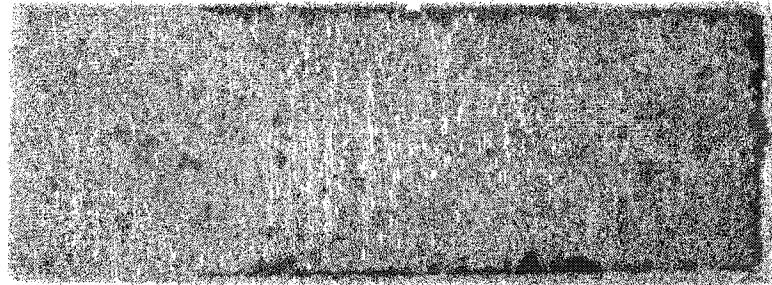


Fig.6-8 SP material after Static corrosion test under N_2 (850° C)

The effect of protective gas on the corrosion aspects of materials was studied, using Nitrogen gas or Argon gas. It is shown that for SP material, the corrosion under nitrogen gas is more severe than under argon gas at the temperature of 850°C. The corroded samples are shown in Fig.6-9 and Fig.6-10.

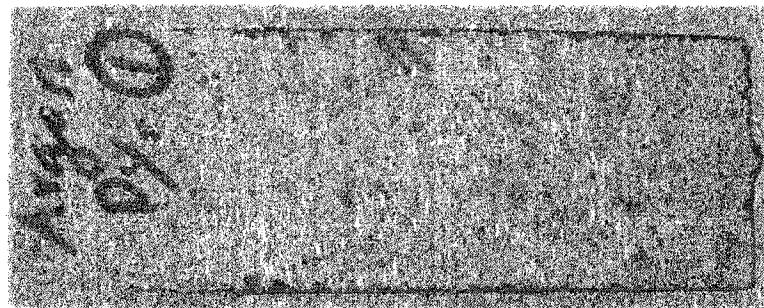


Fig.6-9 SP samples after Dynamic corrosion under Ar (850 ° C, 3.34r.p.s.)

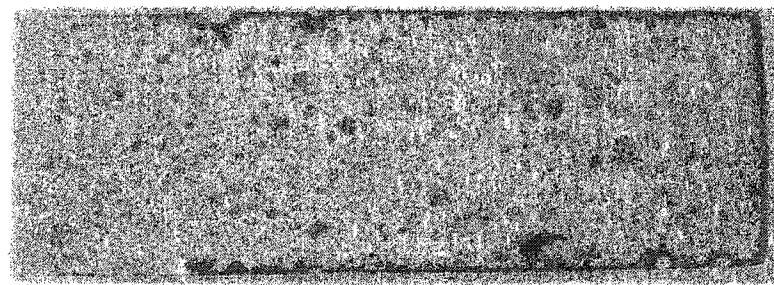


Fig.6-10 SP samples after Dynamic corrosion under N_2 (850 ° C, 3.34r.p.s.)

When the refractory material is subjected to a dynamic corrosion, liquid flow can influence the corrosion in two aspects: the first is the mechanical effect, and the second is the effect on silicon diffusion process.

The mechanical effects of liquid flow can be listed as following:

- It favors the renewal of aggressive species such as Mg and the elimination of the reaction products, mainly silicon;
- It produces erosion effects, carrying away the loosely bound refractory particles;
- It can influence the morphology of the precipitated spinel. Under stagnant conditions, the spinel can prevent pores from opening, which would permit aluminum penetration in the material. On the other hand, when the metal is vigorously stirred, the precipitated oxide is swept along with the flowing metal, when the bonding material is eliminated, enabling generalized attack of the material.

As discussed in Chapter 5, silicon diffusion is the controlling process for corrosion of refractory material by molten aluminum. The growth of corrosion depth inside the refractory can be analyzed as following: In Fig.6-11, the silicon can diffuse from the reaction front (where silicon concentration is C_s) to the refractory material /bulk metal interface (where the silicon concentration is C_m) through metal channels, and then into the bulk metal (where the silicon concentration is C_o) through the diffusion layer on the interface.

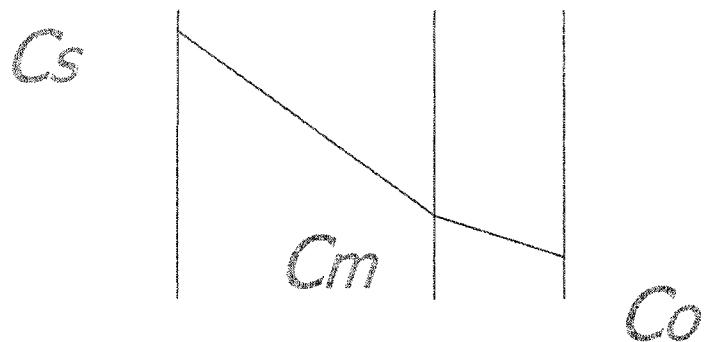


Fig.6-11 Schematic of silicon diffusion from reaction front to bulk metal

where,

C_s the silicon concentration at the reaction front

C_m silicon concentration at the interface of refractory material and liquid

C_o silicon concentration in bulk metal

$$\frac{dL}{dt} = D \frac{C_s - C_m}{L} \quad (\text{Eq.6.1})$$

$$\frac{dL}{dt} = D \frac{C_m - C_o}{\delta} \quad (\text{Eq.6.2})$$

where, $D = D_d/C_s$,

L the penetration depth of the refractory material by molten aluminum;

t time ;

D_d silicon diffusion coefficient;

δ thickness of diffusion layer.

From (Eq.6.2), it can be derived: $C_m = C_o + \frac{\delta}{D} \times \frac{dL}{dt}$ (Eq.6.3)

If (Eq.6.3) is introduced into (Eq.6.1), the following equations will be derived out.

$$\frac{dL}{dt} = D \frac{C_s - C_o - \frac{\delta}{D} \times \frac{dL}{dt}}{L}$$

And then this equation can be changed as following:

$$(L + \delta) \frac{dL}{dt} = D(C_s - C_o) \quad (Eq.6.4)$$

$$\frac{1}{2}(L + \delta)^2 = D(C_s - C_o)t + K_1 \quad (Eq.6.5)$$

Where K_1 is a constant, which can be derived from the boundary condition.

When $t=0$, L is zero also, so, $K_1 = \frac{1}{2}\delta^2$. Introducing this into equation (6.5), the

following equation can be obtained.

$$L = \sqrt{2D(C_s - C_o)t + \delta^2} - \delta \quad (Eq.6.6)$$

When the corrosion period is fixed, the value of "t" in equation (6.6) is a constant, the change of "L" with the "δ" can be shown by Equation (6.7)

$$\frac{dL}{d\delta} = \frac{\delta}{\sqrt{2D(C_s - C_o)t + \delta^2}} - 1 \quad (Eq.6.7)$$

According to (Eq.6.7), the value of $\frac{dL}{d\delta}$ is always a negative value, so when δ decrease, corrosion depth within a fixed period, L , will increase.

Some researchers had found that the forced convection can accelerate the corrosion of refractories, if the corrosion process is controlled by diffusion process [32] [33][34][35].

In such a case, the value of "Sh" can be expressed as following:

$$Sh = 0.0791(Re \cdot d)^{0.7} Sc^{0.356} \quad (Eq.6.7)$$

$$So, \delta = 12.6d(Re \cdot d)^{-0.7} Sc^{-0.356} \quad (Eq.6.8)$$

where,

Sh Sherwood number;

Re Reynolds number;

d Diameter of cylinder sample;

Sc Schmidt number.

The value of 0.7 is a constant only for cylinder shape sample.

So, the liquid flow should influence the corrosion rate of refractories by changing the diffusion layer thickness.

According to the analysis described above, dynamic condition should have some influence on corrosion of refractory material by molten Al-5%wt. Mg, by influencing the diffusion layer or impacting the mechanical effect on refractories.

In this test, by using NA sample under dynamic and static conditions, the difference has been found. It means that the dynamic conditions do have some effect on corrosion rate by influencing the diffusion layer or by removing the protective layer formed on the surface, so it can be concluded that dynamic condition can make the corrosion more severe than static condition.

But for SP material, little difference was found by the naked eye. A possible explanation is that this kind of refractory material is very difficult to be corroded within the limited period under test conditions. Less reaction in fact happened between the molten aluminum and the refractory material. So for this material, liquid flow effect on corrosion is not so clear, even after corroded for about 24hrs testing at 850°C.

So, according to the test results, the dynamic conditions can accelerate the corrosion process, but the degree of influence on different material is different.

On the other hand, from Fig.6-9 and Fig.6-10, it is seen that the corrosion under Nitrogen gas is more severe than under argon gas. This test result is in agreement with previous research results obtained by others [36].

The increase in corrosion of aluminosilicate refractories in the presence of alkalis and a reducing atmosphere could be related to the fact that the interfacial alumina deposit formed by reduction reaction reacts in the presence of Na_2O to form a sodium aluminate, particularly NaAlO_2 . The formation kinetics of latter increases in a reducing atmosphere in the presence of Nitrogen by the action of aluminum nitride according to the following reactions:



The density of sodium monoaluminate is 2.69g/cm^3 , as compared to 3.96g/cm^3 . Thus, sodium aluminate formation from alumina deposit should be accompanied by an increase in volume which would favour penetration by aluminum and thus corrosion of refractory.

6.4 Conclusion of Chapter 6

- The reformed experiment set-up can make dynamic corrosion test proceed safely and successfully. During the corrosion test, no apparent corundum growth took place at the interface of molten metal and gas.
- Dynamic conditions have different effects on different materials. In the case of a low cement castable NA material, more severe corrosion was observed under

dynamic conditions compared to static conditions. But for the SP material, no significant difference was found between static and dynamic corrosion.

- For SP material, the corrosion under nitrogen gas is more severe than under argon gas at the temperature of 850°C.

CHAPTER 7: GENERAL CONCLUSIONS

Based on the test results and discussion described in previous chapters, the following general conclusions can be obtained.

- The incubation time prior to chemical reactions decreases with increasing the amount of silica in the samples. However, influence of silica on higher silica content samples is weak, as compared with its influence on lower silica content samples.
- Silica content inside refractories has a more significant influence on the chemical reactions or chemical corrosion. Both affected depth and corrosion depth increases linearly with the increasing of silica content in aluminosilicate refractory material during immersion test in molten aluminum at 850°C.
- Under static conditions, corrosion of refractories is governed by a diffusion process.
- The reformed experiment set-up can make the dynamic corrosion test proceed safely and successfully, since no apparent corundum growth took place on the surface of the molten aluminum.
- In the case of a low cement castable NA material, more severe corrosion was observed under dynamic conditions compared to static conditions. But for the SP material, no significant difference was found between static corrosion and

dynamic corrosion. Thus, the dynamic condition has a different effect on different materials.

- For SP material, the corrosion under nitrogen gas is more severe than that under argon gas at the temperature of 850°C.

REFERENCE

1. ALAN G. FURNESS, "The Importance of Refractory Materials in Aluminum Production", Proceedings of International Symposium on Refractories", ED. Zhong Xiangchong, Lu Jiaquan, Yan Xingjian 1988, pp539-548.
2. G. EDWARD GRADDY, JR. and DOUGLAS.A.WEIRAUCH, JR. "Refractories Used for Aluminum Processing" UNTER'93 CONGRESS, 1993, pp489-493.
3. A. K. Chatterjee, "Refractories for Non-Ferrous Industries" The Refractories Engineer, Sep. 2000, pp2-9.
4. S. QUESNEL, C. ALLAIRE and S. AFSHAR, "Criteria for Choosing Refractories in Aluminum Holding and Melting Furnace", Light Metals, Ed. Barry Welsh, TMS, 1998, pp1391-1402.
5. J. G. LINDSAY, W. T. BAKKER, and E. W. DEWING, "Chemical resistance of refractories to Al and Al-Mg alloys", Journal of the American Ceramic Society, vol. 47, no.2, 1964, pp90-94.
6. S. AFSHAR and C. ALLAIRE, "The Corrosion of Refractories by Molten Aluminum," JOM, May, 1996, pp23-27.
7. C. ALLAIRE and M. GUERMAZI, "The Corrosion of Furnace Refractories by Molten Aluminum" Aluminum Transactions, vol. 1, no.1, 1999, pp163-170.

8. WWW.REFRAL.POLYMTL.CA , "Corrosion test on refractories for aluminum treatment furnace".
9. MICHEL A. RIGAUD, RICHARD A. LANDY, Pneumatic Steelmaking, vol.III, 1996.
10. C. ALLAIRE, "Mechanisms of Corundum Growth in Refractories Exposed to Al-Mg Alloys" Aluminum Transactions, vol.3, Nov.1,2000.
11. "Non Ferrous Metal Industry", Refractories Handbook, Japan, pp423-429,1998.
12. K, J. BRONDYKE, "Effect of Molten Aluminum on Alumina -Silica Refractories", Journal of the American Ceramic Society, vol. 36, no.5,1953, pp163-174.
13. MOHAMED GUERMAZI and C. ALLAIRE, "Effect of Temperature, Atmosphere, Alloy Composition and Cryolite on the Corrosion Resistance "CIREP-CRNF Report No.27,1998.
- 14 C. ANGERS, R. TREMBLAY, L. DESROSIERS and D. DUBE, "Interactions between dense alumina silica ceramics and molten aluminum" Journal of the Canada Ceramic Society, vol.66, No.1 Feb.1997, pp64-71.
- 15 MIREILLE FOULETIER, and DIETER GOLD, "Selective, accelerated test for evaluation of refractory lifetime in aluminum", UNITER '91 pp36-38
- 16 CRCT, "F*A*C*T Course Notes". Sept.2001.

- 17 D. A. WEIRAUCH and G.E.GRADDY,JR., "Wetting and corrosion in the Al-Mg-Si-O System" Proceeding of International Symposium on advances in Refractories for the Metallurgical Industries, Ed. M.A.J.Rigaud, Pergamon Press, New York, 1988, pp.251-226.
- 18 HTTP://WWW.RANEWS.INFO/FEAT_ART/FEATURE%20MAY%202001.PDF, "Refractory material technology".
- 19 <HTTP://WWW.A-M.DE/ENGLISCH/LEXIKON/BENETZUNGSWINKELBILD1.HTM>, "Wetting angle".
- 20 LIANG YINGJIAO, Physical chemistry (Chinese), 1983.
- 21 <HTTP://HYPERPHYSICS.PHYASTR.GSU.EDU/HBASE/PPOIS.HTML>, "Poiseuille's law".
- 22 OLE-J. SILJAN and CHRISTIAN SCHONING, "Refractories for molten aluminium contact part II: influence of pore size on aluminium penetration", UNITECR'01, pp551-570.
- 23 VARUXAN M. KERVORKIJAN, MATJAZ TORKAR, and BORIVOJ SUSTARSIC, "Modelling of the reactive immersion of ceramic particles into molten aluminum alloys", Composite Science and Technology, 59, 1999, 1503-1511.
- 24 A. E. STANDAGE and MARY S. GANI, "Reaction between vitreous silica and molten aluminum" J.Am.Cermamic.Soc.vol.52, no.2, 1967, pp101-105.

- 25 PRABRIPUTALOONG, K. and PIGGOTT, M. R, "Reduction of SiO_2 by Molten Al" J.Am.Ceramic.Soc.74.1991, 2781-2685.
- 26 WILLIAM G. FAHRENHOLTZ, "Kinetics of ceramic-metal composite formation by reactive metal penetration" J.Am.Soc.,81(10)2533-41,1998.
- 27 R. E. LOEHMAN, K.G.EWSUK, a nd A.P.TOMSIA, "Synthesis of Al_2O_3 – Al composites by reactive metal penetration", J. Am. Ceram. Soc. 79(1), 1996, pp27-32.
- 28 CLAUDE. ALLAIRE, Metallurgy of aluminium part I , 2001.
- 29 ALLAHVERDI, M., AFSHAR, S. and ALLAIRE, C., "Additives and the Corrosion Resistance of Aluminosilicate Refractories in Molten Al-5 Mg", JOM, pp. 30-34, February 1998.
- 30 AFSHAR, S. and ALLAIRE, C., "Furnaces: Improving Low Cement Castables by Non-Wetting Additive", JOM, pp. 24-27, August 2001.
- 31 H. OB'RIEN and M. AKINC, "Reduction in aluminum alloy attack on aluminosilicate refractories by addition of rare earth oxides", Journal of the American Ceramic Society, vol. 73, No.3, 1990, pp 491-495.
- 32 R. COOPER, J. R. and W. D. KINGERY, "Molecular diffusion natural convection and forced convection studies of Sapphire dissolution in Calcium aluminium silicate", Journal of the American ceramic society Vol.47, No.1,1964, pp37-41.

- 33 CHEN ZHAOYOU, WU XUEZHEN and YE FANGBO, "Dissolution kinetics of MgO-CaO and magnesitechrome refractories in secondary steel slag", vol.13, No.4, p475.
- 34 CHEN ZHAOYOU, "Dissolution kinetics of solids and its application to refractories" Silicate Academics, Vol.11, No.4, 1983, p498.
- 35 D. R. POIRIER and G. H. GEIGER, Transport Phenomena in Materials Processing, ED., Publication of TMS,1994.
- 36 CLAUDE ALLAIRE and PAUL DESCLAUX, "Effect of alkalis and of a reducing atmosphere on the corrosion of refractories by molten aluminum", Journal of the American Ceramic Society, vol. 74, no.11, Nov.1991, pp2781-85.